24

COMPUTATIONAL AND MODELLING ASPECTS OF MARINE RISER ANALYSIS

R. PHAAL

B.Sc. (Mechanical Engineering)
University of Cape Town

September 1987

Submitted to the University of Cape Town
in partial fulfilment for the degree of
Master of Science in Engineering

DECLARATION

I, Robert Phaal, submit this thesis in partial fulfilment of the requirements for the degree of Master of Science in Engineering. I claim that this is my original work and that it has not been submitted in this or in a similar form for a degree at any University.

Signed ....

Date ....2/9/87........

ABSTRACT

In recent years much interest has been shown in the design of offshore structures. Flexible members such as marine risers and mooring cables are critical components in such structures. These systems are characterised by nonlinear geometry and loading. In the formulation of an algorithm to model such systems, simplifying assumptions must often be made. This thesis attempts firstly to give an overview of the literature available in this field.

The testing of a riser model is important to ensure that it may be used with confidence. There are several sources of error inherent in a model of this nature. Modelling errors are those caused by the simplifying assumptions made in developing the mathematical statement of the model. Numerical errors include those due to the approximation method and the finite accuracy of the computing machine. Finally, there is a level of randomness in the design parameters, which results in a lack of confidence and an uncertainty in the response obtained from a deterministic model.

This thesis attempts to qualify, if not quantify, the sources of error innate to the modelling of flexible offshore structures; in particular, marine risers. Extensive use has been made of a sophisticated, commercially available finite element program, ABAQUS. Three commonly occuring riser configurations have been modelled successfully with ABAQUS. These are the standard, the catenary, and the hanging riser configurations (see figure 1.1).

A geometrically linearised finite element riser model has also been developed and tested. The linearised model is shown to be applicable to problems where the maximum model deflection is less than approximately 10% of the riser length.

A Probabilistic Finite Element Method (PFEM) has been implemented in order to investigate one source of uncertainty in the problem: that of the hydrodynamic loading. The method is shown to have limitations expressed by coefficient of variation bounds for the random parameters. The C_d data available in the literature is within these bounds, while the C_m data is not. These bounds are shown to be problem dependent, and the PFEM to be more applicable to the modelling of the uncertainties associated with the analysis of drag dominated problems such as mooring cables.

ACKNOWLEDGEMENTS

I would like to express my gratitude to:

Dr. H.T. Pearce of the Dept. of Mechanical Engineering, University of Cape Town, for his guidance and constructive criticism.

The Applied Mechanics Research Unit (AMRU); the Dept. of Mechanical Engineering, University of Cape Town; and the Council for Scientific and Industrial Research (CSIR) for their financial support.

CONTENTS

LIST OF FIGURES

NOMENCLATURE

General

t	time	[s]
x,y	global coordinates	[m]
$\underline{\bullet}$	a vector or a matrix. Generally matrices are upper case, and vectors lower.	
$\bar{\bullet}$	the mean value of $\bullet$	
$\$(\bullet)$	sign of $\bullet$	
$\delta\bullet$	small increment of $\bullet$	
$\frac{\delta^n \bullet}{\delta *^n}$	n^{th} partial derivative of $\bullet$ with respect to $*$	

Subscripts

$\bullet_o$	$\bullet$ at the riser outer diameter
$\bullet_i$	$\bullet$ at the riser inner diameter
$\bullet_r$	$\bullet$ of the riser
$\bullet_x$	$\bullet$ in the x direction
$\bullet_w$	$\bullet$ of the wave
$\bullet_c$	$\bullet$ of the current
$\bullet_{i,j}$	i and j^{th} component of $\bullet$

Vectors and matrices

$\underline{a}$	acceleration	[m/s^2]
$\underline{d}$	displacement	[m]
$\underline{f}$	force	[N]
$\underline{v}$	velocity	[m/s]
$\underline{C}$	damping	[Ns/m]
$\underline{K}$	stiffness	[N/m]
$\underline{M}$	mass	[kg]

Fluid parameters

p..................pressure.......................... N/m^2

C_d.................drag coefficient

C_m.................mass coefficient

KC.................Keulegan-Carpenter number

H..................sea height......................... m

R_e.................Reynolds number

..................density............................ kg/m^3

Riser parameters

d..................diameter.......................... m

m..................mass/unit length................... kg/m

x..................lateral displacement.............. m

A..................area.............................. m^2

E..................Youngs modulus.................... N/m^2

I..................second moment of inertia.......... m^4

T_e.................effective tension................. N

W_e.................weight per unit length............ kg/m

..................angle of riser to normal.......... rad

Finite element parameters

h..................element length.................... m

u, ...elemental degrees of freedom

Probabalistic parameters

b..................random parameter

q..................dimension of random parameter vector

Cov(.).............Covariance of

E ....expectation of

Var( ).............variance of

GLOSSARY

coefficient of variation....... cov = σ/μ, the ratio of the standard deviation to the mean value, a measure of dispersion.

Keulegan-Carpenter number... KC, represents the relative importance of the drag over the inertial forces of a structure.

Monte-Carlo Simultaion......... A simulation technique where a number of simulations are performed using statistically chosen parameters.

Reynolds number.... R_e, represents the ratio of the inertial to the viscous forces in a fluid.

INTRODUCTION

There is an ever increasing demand for energy and mineral derived products. As the cost of harnessing these resources rises, it is becoming necessary and feasible to mine the more inaccessable mineral deposits, including those found in deep ocean regions. For such regions, a flexible riser system is the most feasible mining scheme. Schematic diagrams of various riser configurations may be seen in figure 1.1.

Marine risers may perform the following functions: Mooring of the offshore facility; conveyance of drilling-mud and crude oil; pumping of the treated oil back down to the well-head for transmission to a nearby export facility; and as a communications and power link.

The marine riser is a critical structural and operational link between the ocean floor and an offshore facility. The riser is a very slender, flexible pipe, seemingly simple in form, but with complex mechanics and loading. Closed form solutions to the problem exist only for very simple cases, and hence the engineer must usually resort to a numerical solution. Codes such as DnV and B31 do exist, but their applicability to extreme situations is uncertain [1,2].

Much research and design work has been done in the field, with recent work done by Bernitsas et al. [3,4,5,6], Bergan et al. [7], Chung et al. [8,9,10,11], Sparks et al. [12-14], and others. Many aspects remain inconclusive, and many problems unresolved. This is particularly true of very deep water risers (up to 6000 m), where the modelling and numerical problems are severe.

Researchers [7,15] report numerical instabilities in the nonlinear transient analysis using standard finite elements.

The loading and geometry of the riser are highly nonlinear. The axially stiff nature of the long pipe, coupled with its bending flexibility, leads to the ill-conditioning of the system of equations, with the associated numerical difficulties.

There are several sources of error in the modelling of a sys-tem such as the marine riser. Modelling errors are those caused by the simplifying assumptions made in developing the mathematical statement of the model. A model represents the real situation imperfectly. Numerical errors include those due to the approximation method and the finite accuracy of the computing machine. Finally, there is a level of randomness in the design parameters, which results in a lack of confidence and an uncertainty in the response obtained from a deterministic model. It is important to note that these three effects are interrelated, and cannot be analysed in isolation.

The objectives of this study are to increase the understanding of the mechanics and computational aspects of the problem, and to investigate the applicability of a commercially available finite element program, ABAQUS, to the problem. An attempt will be made to qualify, if not quantify, the sources of error in the modelling process. The applicability of the probabalistic finite element method [16, 17] in evaluating the statistical response characteristics of a linearised riser model, RISER, will be investigated.

Section 1 introduces the reader to the literature concerning marine risers, and deals with various issues that arise in the modelling of marine risers. Section 2 describes the marine riser models implemented with ABAQUS, a commercially available finite element program. Sections 3 to 5 deal with the numerical aspects of marine riser modelling, specifically with ABAQUS. Section 6 describes the development of the geometrically linearised model, RISER. Sections 7 and 8 introduce the Probabalistic Finite Element Method, and apply it to the linearised model, with respect to the uncertainties associated with the hydrodynamic coefficients.

This study is justified by the large costs involved in offshore mining. These costs include exploration, production and the costs of operation suspension or failure of the riser system. A riser failure may cause damage to both life and the environment. The offshore mineral potential in South Africa is being developed, and the results of this study might find local application.

1. LITERATURE SURVEY

The literature concerning marine risers and related fields, such as fluid-structure interaction and the study of wave phenomena, is extensive. Key papers relating to risers include those by Bernitsas et al. [3,4,5,6], Chung et al. [8, 9,10,11], McNamara et al. [15,18], Sparks [12,13,14], Chakrabarti et al. [19], Kirk [20], Young et al. [21], Patel et al. [22], Spanos et al. [23-25], and others (for a full list, see references).

Theoretical research into the field of tensioned strings and beams began with the work undertaken by Carrier and Woinowsky-Krieger in the 1940's [26]; and into the problem of the fluid-structure interaction by Morison in 1950 [27]. Since then the models developed have increased in complexity and scope, resulting in the present state of knowledge as expressed by the papers mentioned above.

Many problems still remain unresolved, particularly as the requirements of the mining systems are refined and extended. As deeper and deeper ocean regions are exploited, optimal design is desired. This may only be achieved if a better understanding of the mechanics, computational and modelling aspects of marine riser systems is attained.

There are aspects presented in the literature which are not fully understood, and about which there is much contention. The literature survey conducted in this section, as well as in sections 3 and 4, will attempt to highlight these aspects, as well as to give the reader an overview of the field.

1.1 MARINE RISER SYSTEMS

Generically, the marine riser is a simple structure, consisting of a pipe connecting the ocean floor to the offshore facility, which may be an oil rig or a ship. Bearing in mind the specific design requirements of a site, many structural and functional design details may be necessary.

Three basic riser configurations have been chosen, and these may be seen in figure 1.1. These configurations are the most frequently occuring ones, and are well documented in the literature [4,6,7,8,15,22-25,28-33]. The three basic riser configurations are the "standard" riser, the "catenary" riser and the "hanging" riser.

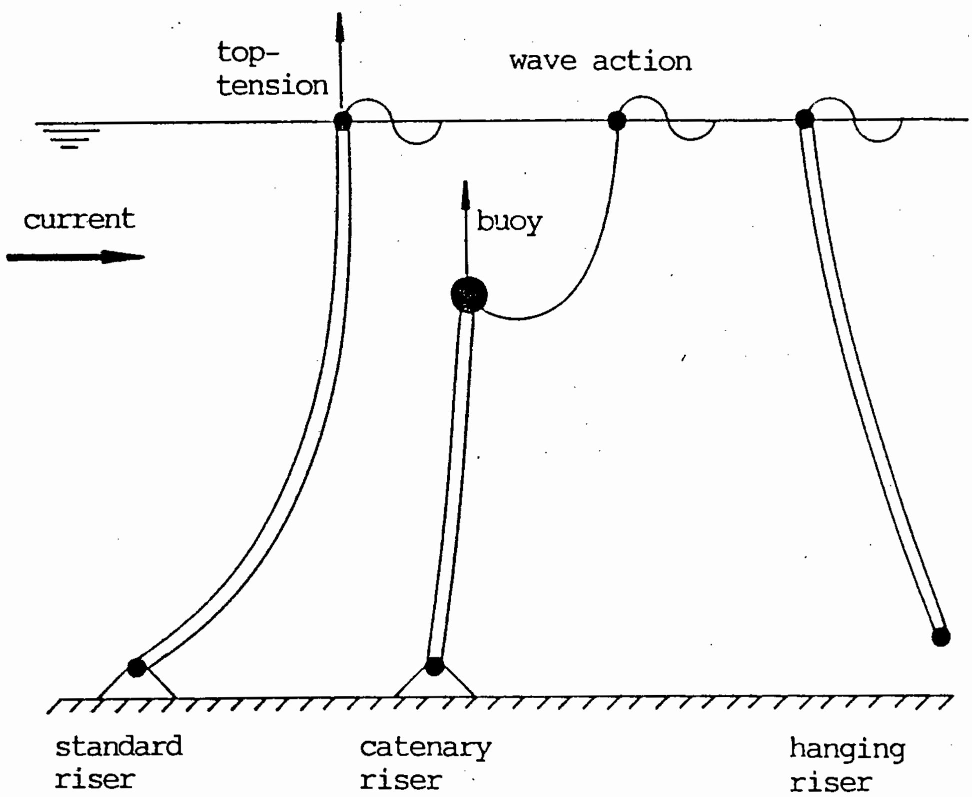

fig. 1.1 - Riser configurations of interest

The standard riser shown in figure 1.1 is the most basic form, and simply connects the well head to the floating facility. Understanding the mechanics of this configuration gives insight into most of the problems facing all underwater pipe analysis, such as pipe laying, riser installation and disconnection. This configuration is suitable for depths of up to 1000 metres [34], but is usually found in shallower water.

The catenary configuration shown in figure 1.1 consists of a fairly rigid lower section supported by a buoyancy module. A compliant upper section joins this to the floating facility, as most of the ocean's energy is concentrated in the upper wave-active, or splash-zone regions [13,35]. This sort of riser system is most suited to shallower water (up to 150 metres [7,15,33]).

During severe storms, the riser might have to be disconnected, or "hung-off", as shown in figure 1.1, which causes expensive operational down-time. There are two disconnection modes, planned and emergency [33]. The hanging configuration is also used for the mining of very deep-water manganese nodules, at depths of up to 6000 metres [8]. The riser hangs a few metres above the sea floor, connected loosely to a mining vehicle that collects the nodules.

In order to appreciate the subtleties of riser design, it is necessary to be aware of the requirements of a marine riser system. The riser may perform the following functions: mooring of the offshore facility; pumping of the crude oil, the treated oil and the drilling-mud; and as a cummunications and power link.

Optimal riser system design involves satisfying the above requirements as well as considering such factors as the system design life, which is usually decided by the projected life of the field [35]. An optimal system will also be designed for minimum down time, which requires design for extreme conditions such as storms.

The maintenance and operational control of the functioning riser system must also be carefully considered, which involves the design and integration of many sub-structures and sub-systems, such as accurate weather prediction. Denison et al. [36] deal with deep water marine riser management. Other researchers that consider these design aspects include Wybro et al. [35], Natvig [32] and Wolfram et al. [37].

The basic riser design may be complicated by features such as tensioning cables, kill and choke lines, collars, buoyancy and weight modules, articulations, multiple tubes, and material and geometric properties that vary along the riser. These factors are important when considering specific risers, but vary from system to system. The techniques for modelling these details must be dealt with separately, bearing in mind that these features often only affect the details of the design, and not the overall response of the system.

The design procedure would normally begin with the analysis and design of the basic structure, the results of which would be used for the detailed design. The overall response may be checked if necessary with the details included in the model, although this may prove to be expensive.

Existing riser systems can be modified if they have undesirable natural frequencies and/or mode shapes. Bernitsas et al. [3] deal with this problem using a nonlinear inverse perturbation method. The frequency response characteristics of the riser may be adjusted by adding mass or buoyancy modules to it, changing the drilling-mud density, changing the riser geometry, or altering the riser tension, on site.

1.2 LOADING EFFECTS ON RISER RESPONSE AND DESIGN

The riser is subjected to the effects of a varying and often harsh environment. A number of different processes give rise to loads on the thus causing fluctuating stress conditions.

Loading effects include: Wave and current effects, including vortex-shedding; wind-wave and wind-floating-structure interaction; end conditions, including reaction forces, applied tensioning and moored vessel motion; internal fluid effects including pressure, weight, friction and Coriolis forces; weight and buoyancy forces; centrifugal forces; concentrated loads, owing to ties and contact; thermal loads; residual stresses; impact loading due to mooring.

1.2.1 Tension effects

Sparks et al. [14] define the 'typical riser as one which uses tension principally to resist lateral forces'. Sparks et al. find the curvature of the riser to be very close to that of a cable everywhere except in zones near supports (within 20m), where bending effects become significant [7,13,15]. The structural stiffness of the riser arises primarily from the tension, and to a lesser extent from the resistance to bending.

It is important to note that it is the "effective" tension that is of importance in calculations, and not the actual tension. Sparks [13] defines effective tension as the 'total force in the riser, including contained fluids, less the force in the displaced fluid column'. The effective tension is defined mathematically in equation 6.3, section 6.

It is this 'commonly misunderstood' [38] term that is used in marine riser calculations. The term has no real meaning in terms of measurable tension, but is an algebraic expression that appears in the governing equations. It is, however, this effective tension that decides whether the riser will buckle or not. A riser may buckle due to the action of internal fluid pressure even though it is in positive tension [4,6]. The wall friction does modify the internal distribution of forces between pipe walls and internal fluid, but does not change the total column force, and thus does not change the effective tension [14].

The two most important parameters in a riser design, in terms of on-site monitoring of the riser, are the riser tension and the angular deflection at the bottom of the riser if ball-jointed, or the bending stress if not [23-25,32,35, 37].

There is an optimal riser top-tension that minimises the combined effects of riser stress, buckling and fatigue [35]. Experience gained in modelling risers with ABAQUS and RISER, in sections 2 and 6, indicates a marked dependence of the top-tension on the riser weight and length for a given static deflection. There is usually a facility, with the aid of a slip joint, to vary the riser top-tension on site [32].

Young et al. [21] maintain that increasing the riser tension has the effect of reducing the response amplitudes and thus the dynamic stresses, but that the static stresses are increased. Sparks [14], however, asserts that tensioning increases the response velocities. This has the effect of increasing the hydrodynamic drag forces, which depend on the square of the relative fluid velocity. The dynamic stresses thus increase.

Techniques for modifying the effective riser tension include the addition of buoyancy or weight modules, and the adjustment of the riser top-tension. As the floating vessel heaves up and down, the riser follows. The tension near the top of the riser thus fluctuates and the riser may experience compression on the way down, and increased tension on the way up. The parts of the riser in compression, or reduced tension, become less stiff, and may be prone to buckling [21].

If a slip-joint is present at the top of the riser, the chance of buckling is reduced. Weight modules are usually distributed in the upper regions of the riser, and buoyancy modules in the lower, to reduce the compression effects. Added weight near the top of the riser has a beneficial effect on the moment experienced by the riser near its base [13,14].

The linear weight of the riser causes the axial tension to decrease with depth, and contributes to the lateral load component on all segments of the riser that are not vertical, as described by equation 6.3, section 6. Buoyancy modules reduce the decrease of axial tension with depth, the riser's maximum bottom angle, and the lateral component of the riser's linear weight [13,14].

Patel et al. [22] show that even for small top vessel offsets, the lateral load intensity owing to self-weight is comparable to the hydrodynamic loading caused by the current.

Sparks et al. assert that the buoyancy modules must be continuous for this last advantage to be effected. Bernitsas [6] maintains that the required riser top-tension is reduced by concentrated buoyancy from modules, and not the continuous riser buoyancy, and therefore small modules are more effective than large or continuous ones. Sparks et al. indicate the disadvantage of increased drag created by buoyancy modules.

1.2.2 End conditions

The maximum bending stress in the riser occurs near the ends [24], and this value may be effectively monitored and limited by imposing a maximum permitted angle at the bottom ball-joint. Physically this angle is limited to less than about 30°, owing to the cost of a large-angle ball-joint [37]. Other authors limit the maximum stop-angle at the bottom ball-joint to between 5° and 10°, which may be monitored and maintained by adjusting the top-tension [24].

The ball-joint may be modelled as a linear or nonlinear reactive moment, as a constant friction force joint, or just with a maximum stop-angle imposed [32]. At the surface, slip-joints are commonly used, but ball-joints may also be employed, which reduce the bending moments. Spanos et al. [24] find that the maximum bottom angle is quite insensitive to the current profile, but depends strongly on the top-tension and the amplitude and period of the waves.

The marine riser experiences the imposed motion of the floating facility. The vessel has six degrees of freedom, but if a ball and a slip-joint are present, only surge and sway are important [24]. The vessel may be fully floating or tethered, in which case bilinear theory may be necessary [22,39].

Wolfram et al. [37] assert that the floating vessel controls the short period motion of the system, that is, the riser does not influence the short period motion of the vessel. The vessel motion at the top of the riser can be assumed to be that of a free vessel with no external forces. This has been verified by experimental model tests [37].

1.2.3 Wave and current effects on loading

For preliminary design based on regular waves, Wolfram et al. [37] assume that the vessel oscillates at a slightly different dominant frequency than that imposed by the waves on the riser. This accounts for the fact that the vessel responds more to the longer period waves in a wave train, and also that the riser and vessel are generally out of phase with one another.

Over a long enough period of time, all possible phase relationships will be experienced. Since out-of-phase motions generally give the highest forces, an upper bound is obtained [37]. Nielsen et al. [40] indicate that the stiffness of a large diameter pipe, such as a riser, will have a measurable effect upon the motion of the floating vessel in some of its modes.

Besides driving the floating vessel, there are other wave induced effects that are of importance. The parts of the riser that are in the wave zone will experience a fluctuating buoyancy force [22,27]. Usually the effects of wave steepness and slamming are neglected, but it is best not to site sensitive members in the splash zone [27]. The slamming effects may be severe when the dimension of the member is near to that of the wavelength.

Current-induced effects are important. The static problem is dominated by vertical variations of the current. There are annual, seasonal and geographical current variations. The density, viscosity and velocity profile of the current may vary significantly with depth, and internal waves may occur at temperature inversion interfaces [8-11].

The vessel is usually offset due to current and slow-drift effects. The lower riser stresses are strongly dependent on vessel offset [35].

The current, and hence forces acting on the riser, usually vary in both magnitude and direction down the pipe, and thus a three-dimensional analysis should be undertaken, although a two-dimensional analysis might be adequate for most design purposes [9].

Chung et al. [8,9] and Jain et al. [54] report complex whirling in the three-dimensional analysis, where there is bending-torsion coupling, and Chung et al. maintain that the prediction of the response is hindered by a 'dearth' of subsea current data, and that the response is very sensitive to the choice of environmental and external force models. Different models may give responses differing by a factor of as much as two.

1.2.4 Other loading effects

The effect of internal fluids must be considered. Only a fraction of the weight of the drilling-mud is supported by the riser, the vertical component being supported by the mud column. Internal discontinuities should be avoided, as the internal fluid pressure acts against them, and they lead to stress concentrations [6].

Wybro et al. [35] maintain that the internal fluid pressure does not affect the riser dynamics, as it does not influence the riser wall stresses, since it produces a triaxial hydrostatic stress state. Most authors emphasize the importance of the effect of the hydrostatic pressure on the effective tension. This dependence is shown in equation 6.3, section 6.

Experience with ABAQUS and RISER, in sections 2 and 6 indicates the importance of the effective tension on the riser response characteristics.

Torsion effects, including torsion-bending coupling are usually neglected, although in three-dimensional models this should not be done [6,41].

Many of the loading considerations mentioned at the beginning of this section are neglected, as they might not be important in a preliminary analysis of a riser system. If important, though, these effects may be included in a specific design. The reader is referred to section 6, where the simplifying assumptions for a simple riser model are made.

Some authors neglect the dependency of the hydrodynamic loads, and the lateral component of the riser weight and buoyancy, on the deformation of the riser [28,34,41-43]. Bernitsas et al. [4,6] indicate that this assumption may result in drastic reductions in deflection slopes and bending stresses, particularly near the bottom ball-joint. The vertical component of the fluid forces should not be neglected either [4,6], as is often done [22,38].

Bernitsas shows that the lateral and extensional motion of the riser are coupled by the curvature of the pipe, and for large deflections, the de-coupling of these effects is not possible. Kim et al. [44] maintain that the geometric non-linearities are not important, even for moderately large deflections where a heave compensation system is used, because the dynamic tension is caused primarily by the stretching of the riser, and for at least the first four or five transverse natural modes the tension's spatial variation is small. This is only true if a heave compensator is in operation, as is usually the case.

1.2.5 Material and failure assumptions

Various different material assumptions have been used in the literature. Most authors assume an homogeneous, isotropic, linearly elastic material, with large displacement, and small strain theory, although McNamara et al. [15] have implemented, in ABAQUS, the facility for a fully anisotropic material.

McIver et al. [38] assert that the displacements of the riser are small relative to its length, and that the deformations are sufficiently small so as to allow for the elastic assumptions to be valid. Walker [45] has assumed an elastic-perfect-plastic model. Hibbitt et al. [46] have facilities in ABAQUS for plastic modelling.

The choice of the failure criterion used in a design may play a role in the type of analysis undertaken. Failure criteria include cost, danger, yield, buckling, fatigue and catastrophic failure. Wybro et al. [35] maintain that the low frequency vessel motions induced by wind-gust, and the slow-drift forces caused by wave action, have a significant effect on maximum riser stress and fatigue life.

On the other hand, Wolfram et al. [37] assert that fatigue need not be considered for most designs, because if a riser system is designed for yield in the hundred-year storm, the structure will usually have a fatigue life in excess of 20 - 30 years. Wolfram et al. admit that fatigue considerations are important for details of the structure.

1.3 DRAG AND MORISON'S EQUATION

One of the most contentious issues in the field of fluid-structure interaction, and specifically in the case of highly flexible structures such as marine risers, is the applicability of the Morison equation in describing the fluid-loading acting on the structure.

In 1950, Morison et al. [27] postulated that the fluid force on a stationary body is composed of two parts: an inertial (or virtual mass) component, which is proportional to the horizontal component of acceleration of the fluid particles; and a drag component, which is proportional to the square of the fluid velocity. The inertial component includes the added-mass of the entrapped fluid.

A wave theory is required in order to calculate the fluid velocity and acceleration.

Thus the total force may be written:

$F = F_i + F_d$

Where F_i = the inertial force component,
F_d = the drag force component.
(See Nomenclature for definition of other symbols)

$$F_i = C_m . \mu_o . A_o . a$$

$$F_d = \tfrac{1}{2} C_d . \mu_o . d_o . \$(v) . (v)^2$$

The above coefficients may be found in tables for different geometries, but these figures should be used with caution. For a flexible member, or an accelerating fluid field, lift forces also arise, which are described by the lift coefficient, C_l. This effect can give rise to the phenomena of vortex-induced oscillations, and the reader is referred to section 1.5 for details.

The Morison equation is suitable for slender members (d/lam $\leq .2$, where d is the diameter of the pipe, and lam the sea wavelength). Diffraction effects dominate the process outside of the slender range. The drag force is proportional to the member diameter, while the inertial force is proportional to the square of the diameter, and thus for large pipes, the inertial forces dominate [27].

1.3.1 Application of Morison's equation

A major problem in the application of the Morison equation in practical terms, is the nonlinear dependence on the square of the relative velocity. Nonlinear systems of equations are difficult to handle, often requiring sophisticated numerical techniques.

The standard Morison equation has been extended to apply to highly flexible structures such as marine risers. The fluid velocity and acceleration, relative to the structure, must be evaluated and used in place of the global fluid velocity, as in the case of fairly rigid structures [18,32,47,48].

Some applications, such as problems in the frequency domain and spectral analysis, require linearised versions of Morison's equation. The standard method of linearising Morison's equation is to assume that a linearised drag coefficient exists, C_d^*, which relates the drag force to the fluid velocity in a linear fashion. The error resulting from this assumption is then minimised in a least squares sense [27]. The equivalent drag coefficient may be expressed as:

$$C_d^* = C_d \sqrt{8/\pi}\, \sigma_v$$

where σ_v is the standard deviation of the wave-particle velocities for random waves, usually assumed Gaussian [27].

This linearisation process is equivalent to equating the energy dissipated by the two systems over a cycle [49]. Hall et al. [49] assert that the linearised version of Morison's equation is conservative, but fairly accurate. Shyam Sunder et al. [48] agree that the error is conservative for low velocities, but maintain that it is non-conservative for the higher frequencies, and that the uncertainties depend predominantly on the importance of the drag term.

Shyam Sunder et al. also maintain that the linearised version underestimates the high frequency force components associated with resonance, which are very important for the fatigue analysis of the system. Bernitsas et al. [5,6] assert that nonlinear components in a system have a stiffening effect, which is non-conservative. Kim et al. [44] indicate that "jump" phenomena, associated with hardened systems such as risers, occur. That is, sudden decreases in amplitude may occur with small increases in frequency of excitation.

Spanos et al. [23] report that the linearised equation gives results that agree within 15% of the nonlinear version, at 100 times the saving in computer costs, although Patel et al. [22] maintain that comparisons are not easily made between the two methods, and that linearisation should be used with care.

Sparks et al. [12-14] consider the velocity squared dependence of the drag beneficial, in that, although the drag forces are large, the resonance effects are well damped, and only contribute about 10% of the total dynamic tension. Thus, resonant effects are significantly damped out in severe sea-states.

King and Ramberg [50] demonstrated that the oscillations of circular cylinders are largely independent of angle of attack, and that for inclined members the component of the fluid velocity normal to the pipe, or the projected area of the pipe may be used in the calculations [27,48].

1.3.2 Morison coefficients

There are large uncertainties associated with the use of the coefficients in the Morison equation. Hogben [48] says: 'Although data on fluid loading is plentiful, there are many serious uncertainties and gaps in the knowledge', and Dawson [41]: 'There has been more than thirty years of debate' on this issue. The mechanisms of the fluid-structure interaction are not very well understood, and most of the models used to describe this phenomenon are empirically based.

Experiments in this field are notoriously difficult to conduct, and the results vary a great deal. Chakrabarti et al. [19] criticise wave-tank tests, as only a limited range of Reynolds numbers may be used. Most tests use mechanical oscillation of the model, rather than varying the fluid state. This has the advantage of accurate control, but the similarity to reality is questionable.

Wolfram et al. [37] point out the importance of matching the wave spectrum in experiments to that which occurs in the sea. It is difficult to match both significant wave height and energy spectrum. Model wave generators are not usually capable of producing waves in the high frequency region of the spectrum, and it is difficult to obtain realistic wave groupings.

The Morison coefficients are dependent on wave depth, wave frequency, Reynolds number (R_e), Keulegan-Carpenter number (KC), structural geometry, surface roughness and marine growth, the magnitude and direction of the current, and the randomness of the above effects [41]. There is also a dependence on whether or not vortex-induced oscillations are present.

The literature [51-53] reports increases of between 200% and 300% in the in-line drag forces during vortex "lock-on". The reader is referred to section 1.5, on vortex-induced oscillations.

Shyam Sunder et al. [48] maintain that the roughness of the pipe increases C_d dramatically, but not much data is available on this. The increased mass and added-mass arising from marine growth is not as significant as the direct increase in loading due to the greater drag resulting from this growth [48].

The literature indicates a strong dependence of the Morison coefficients on the Reynolds and Keulegan-Carpenter numbers [32,41,48,54,19]. Chakrabarti et al. [19] assert that KC is more important than R_e.

KC and R_e vary during the cycle of a wave. The water velocity varies with sea depth owing to the current profile and wave action, as does the sea density. The dynamic viscosity is highly stratified, with variations of up to 200%, owing to the temperature variation, which gives an R_e at the surface of the sea of up to 7 times greater than at the bottom [8-11].

There are also internal waves near thermal inversions below the surface of the sea, which complicate the R_e and KC dependence of the Morison coefficients. The environmental influences, and thus the Morison coefficients, are fairly constant below 9000 ft. [8-11].

These effects should strictly be included in any model used, however the cost of doing so is prohibitive. Usually average values are used. Values of $C_m = 2$ and $C_d = 1.4$ are recommended as upper bounds by Shyam Sunder et al. [49], and these values are in agreement with the values reported by Hogben et al. in their review of the field [55]. The correct average values to use are not clear, and the values quoted in Hogben's paper vary from 0 to 2.75 for the drag coefficient, and from 0 to 5 for the mass coefficient. Errors of more than 50% are common.

Wilson [55] showed that there was a marked dependence of the drag coefficient on whether or not current and phase effects were included in the analysis. C_d doubled from .32 to .60 if current and wave effects were included, and increased to 2.75 if phase corrections were made. The mass coefficients did not vary by as much.

Horton et al. [56] find that using average coefficient values over the wave cycle is not suitable for intermediate wave periods. Dawson [41] asserts that the average coefficient values give better results than time varying coefficients. Dawson attributes this to the decreased dependence of the coefficients on the flow parameters as a result of the near-circular particle motion and the large kinematic gradients in deep waters, where risers are usually found. He finds that the variable coefficients overpredict the drag forces, which is conservative.

Dawson [41] finds that there is more certainty in the use of Morison's coefficients in smaller waves, where the inertial coefficient dominates. In this case, Dawson suggests choosing a suitable C_m, and then optimising C_d. The drag effects increase rapidly with wave height. They comprise 1% of the total force for a 5 inch wave, and 90% for a 20 inch wave. Unfortunately, most risers must be designed for waves much larger than this.

1.3.3 Alternative approachs to that of Morison's equation

Horton et al. [56] maintain that Morison's approach to the problem is inadequate, as the method was derived for the simple, one-dimensional case. Horton et al. have developed an alternative approach using an inertial-pressure concept, which they illustrate with a one degree-of-freedom model.

In this method, Horton et al. take into account the diffractional, temporal and three-dimensional effects. In its simplest form, Horton's model reduces to Morison's equation, but in its full form it includes more fluid-interaction terms, and will eventually allow for the full modelling of currents, dispersion and diffraction [56].

Chung [57] has developed a hydrodynamic loading model based on a velocity-potential method. This model also reduces to the Morison equation.

1.4 WAVE AND CURRENT CONSIDERATIONS IN MARINE RISER ANALYSIS

'Ocean waves are complex phenomena, the most recognisable feature of which is their randomness in time and space' - Sigbjörsson [58]. The description of a sea-state for analysis purposes should strictly include stochastic effects, however, simplified deterministic models are often used.

Shyam Sunder et al. [48] observe that aerial photographs show complex but well organised wave patterns. Storm sea-states may be less well organised, but no photographic evidence is available to support this. Shyam Sunder et al. report that some wave growth is due to sea-wind interaction, and 60% to 70% due to nonlinear wave-wave interaction. The mechanisms of this process are not understood properly, the models are imperfect, and often work must be based on sparse empirical data.

Surface waves (gravity waves) are driven by gravity, trying to restore the fluid to an equilibrium condition [27]. Deterministic wave theories are derived from classical continuum mechanics considerations, and must satisfy Laplace's equation and the prescribed boundary conditions, such as no fluid crossing the boundaries, and zero guage pressure at the surface.

Linear (Airy) and nonlinear (Stokes, Gerstner) wave theories exist. The linearised equations are not applicable to large waves, storm or breaking waves, or shallow water; that is, for waves where the kinetic energy of the wave is high [27].

Two parameters are usually used to describe a random sea-state. These are: the significant wave height, h_s, which usually has a Weibull distribution [48]; and the mean zero crossing period, T_o. There is an uncertainty in the relationship between these two parameters that stems from a lack of data, and therefore a deterministic relationship is usually assumed [48].

1.4.1 Normal and storm sea-states

Normal sea-states should be dealt with in a stochastic fashion, but extreme cases, such as tidal waves, may be treated deterministically, as their occurrence is exceptional. They have a long wave length, and may be considered as time-dependant currents [27].

In the case of storms, where the storm dimensions are large compared to the other dimensions in the problem, the contributions of the different parts of the storm are assumed to be the infinite sum of randomly phased waves. A Gaussian distribution may be assumed, and this has been empirically supported.

The effect of a distant storm is different. A storm produces a broad frequency band of waves, but the longer waves travel faster and reach the destination sooner, while the others disperse. The spectrum is narrow-banded, and the distance acts as a "filter". This narrow-banded spectrum is best described by a Rayleigh distribution [27].

1.4.2 Wave energy spectra

The choice of what wave energy spectrum to choose for an analysis is important. Spidsöe et al. [59] indicate that the standard wave spectra that are found in the literature were developed for specific locations, and their applicability to other sites depends on the similarity between the sea-states of those sites.

The significant wave height, h_s, and mean zero crossing period, T_o, of a particular site might not be accurately modelled by existing wave spectra, so that a poor model reliability level may result. Spidsöe et al. [59] compare the ISSC (of the same type as the Pierson-Moskowitz and the Bretschneider), the JONSWAP (Joint North Sea Wave Project), and the Darbyshire-Scott spectra in their applicability to the Norwegian offshore conditions.

The ISSC spectrum applies to deep water conditions, the JONSWAP applies to fetch limited areas and homogeneous wind fields such as the North Sea, and the Darbyshire-Scott applies to extreme storm conditions. For severe sea-states, Spidsöe et al. report ±20% errors using the JONSWAP and D-S spectra. They report severe errors of 100% to 200% for moderate sea-states with all the spectra, and warn that care must be taken in the fatigue analysis of a system, as most fatigue damage occurs in moderate conditions. Shyam Sunder et al. [48], on the other hand, report that the spectral representation is good for light sea-states, and poor for heavy sea-states.

Some commonly used spectra in the literature are the Pierson-Moskowitz (P-M), which is used by Shyam Sunder et al. [48], Kao [42] and Chung et al. [8-11], and the Davenport, used by Wybro et al. [35], which is suitable for storms. Spanos [23] develops three algorithms for simulating time series compatible with a given power spectrum called autoregressive, autoregressive moving average, and moving average methods.

1.4.3 Wave theories

The most commonly used wave theory is the linear (Airy) wave theory, used by Natvig [32], Patel et al. [22], and Rajabi et al. [51]. Linear theory is necessary when the frequency domain is used, or superposition is required, as is sometimes required for random sea-state generation [47,48]. Mc-Iver et al. [38] maintain that the application of linearity in these cases is not without ambiguity, and assert that different wave conditions may not be just linearly super-imposed, and that there are difficulties in synthesising irregular waves in a meaningful fashion.

Other commonly used wave theories are the Stokes nonlinear wave models. Wybro et al. [35] use Stokes' fifth order theory, and Dareing et al. [28] the first order version. Jain et al. [54] and Williams [60] assert that higher order theories such as Stokes' are more appropriate for storm conditions. Shyam Sunder et al. [48] maintain that for deep water the two wave theories, linear and Stokes, are similar.

The 100 year storm wave is commonly used as a basis for riser design [54,37], although it is pointed out [35,36] that a riser system has only to function for the life of the mineral field. Sanchez-Arcilla [61] deals with the long-term analysis of the wave climate using short term techniques. He is mainly concerned with the durations of the storms, the durations of the calms, and the intensities of the storm peaks.

Stansberg [62] investigates the slow-drift responses of a marine riser system, as the typical riser has long fundamental mode periods which are excited by the long period-components of the sea-state.

1.4.4 Wave-current interaction

Nolte et al. [26] compare the effect of random multi-directional waves and currents with a colinear system, and found that a two-dimensional study is conservative, over predicting the drag forces produced on the riser by about 20%. Wolfram et al. [37] report that non-colinearities of wind and waves occur, especially during decreasing sea-states. Jain et al. [54] show that the non-colinearity of waves and current reduce the maximum surge displacement of the riser, and this is a least upper bound for orthogonal waves and current, but complex, hazardous whirling motions result.

Li et al. [63] investigate the changes in wavelength and celerity when waves interact with currents, and present simple nomograms as design tools.

The current distribution chosen is important, as there are annual, seasonal and geographical changes in the current profiles [8-11]. Triangular or constant steady velocity distributions are usually chosen for in the interests of simplicity [28,29].

1.5 VORTEX INDUCED OSCILLATIONS

Flexible marine structures, such as risers, are susceptible to vortex-induced oscillations. Griffin [53] reports on an oil rig situated in the English Channel where vortex-induced resonant vibrations caused large amplitude oscillations of the riser, and resonant behaviour in the drilling machinery on deck. Two fatigue failures resulted, and substantial financial losses were incurred.

In the past, these effects have often been ignored or overlooked, as reliable data was lacking, and the design methods to cope with vortex effects did not exist. Vortex considerations have become more important as mining operations have moved into deeper and more hostile environments [53].

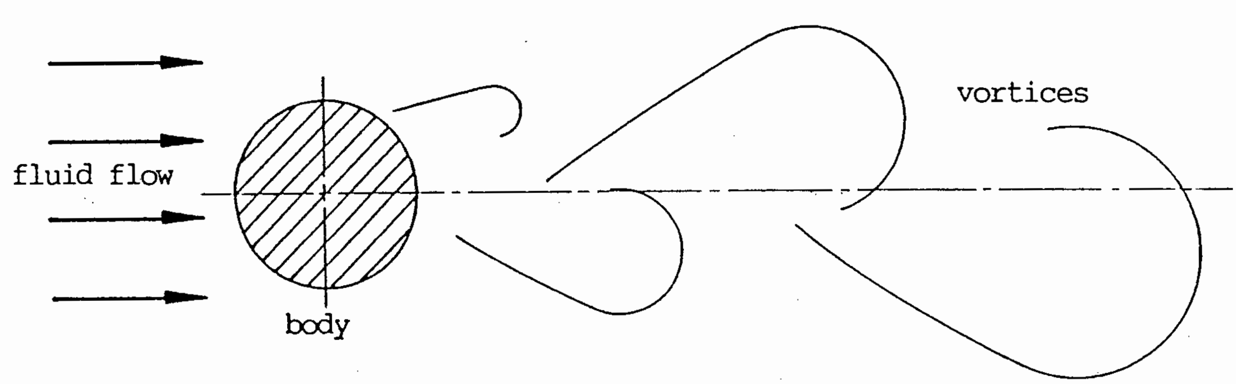

fig. 1.2 - Vortex-shedding

When fluid flows past a submerged body, vortices may be shed, as may be seen in figure 1.2. When the vortex-shedding frequency approaches the natural frequency of a flexible body, the marine riser in this case, the body takes control of the shedding process. This phenomenon is termed "lock-on", "wake capture", or "synchronisation" [50].

During lock-on, large resonant oscillations occur, and amplified lift and drag forces are generated. Transverse and in-line oscillations occur. Every et al. [52] and Griffin et al. [53] show that the in-line response amplitudes are of an order of magnitude less than the transverse vibrations.

Much work has been done in the study of vortex-related effects, papers including those by Rajabi et al. [51], Every et al. [52], Griffin et al. [53], Patrikalakis et al. [64], Overik et al. [65,66], and Sarpkaya [50]. Most of these papers are primarily experimental in nature, as the theoretical background to vortex-shedding is not well developed.

Paniker et al. [33] observe that flow-induced vibrations will be present with almost any flow case, as there are infinite natural modes in any real structure, but maintain that such vibrations do not present a serious hazard except in strong currents where high frequencies and large curvature variations may result.

Rajabi et al. [51] indicate that there is a 'clear lack of a physically sound model' of the vortex-shedding process, and hence that empirical data and correlations must be resorted to. Rajabi et al. show that vortex-shedding may be induced by currents or waves, although previous work has been limited more to the effects of current-induced vortices.

The vortex-induced transverse oscillations result in an increase in the in-line drag forces of between two and three factors [51-53]. Nomographs are available for design purposes, for estimating the increased hydrodynamic forces associated with this phenomenon [53]. The codes (DNV; BS 3351; ANSI B31.3, B31.4, B31.8) are also supposed to account for vortex-shedding effects, but their applicability to deeper water and more hostile environments is questionable [1,2].

Rajabi et al. show that the ratio of the dominant shedding frequencies to the wave frequency is related to the Reynolds number, R_e, and the Keulegan-Carpenter number, KC. Griffin et al. show a functional dependence on the Froude number as well.

For wave-induced vortex-shedding, the effect of the amplified drag is to reduce the response amplitudes of the lower portions of the riser, and to increase them in the upper. This may be beneficial, as the maximum bending moment usually occurs near the bottom of the riser. However, vortex-shedding is usually detrimental when a steady current is present as well [51].

When the situation is complicated by the presence of multiple risers or other bodies in proximity to the riser, the flow field is complicated and the vortex effects become more complex [33] and severe [65,66]. Overik et al. [65,66] deal with vortex effects in multi-tube risers. They investigated the problem experimentally, but experienced difficulties.

Overik et al. [65,66] and Demirbilek et al. [67] correlate the vortex effects in multi-tube riser systems with single-tube risers. They suggest the use of a "pitch" or "effective" tube diameter for the multi-tube configuration, in which case single-tube theory may be used.

Griffin et al. [53] show that the vortex-induced response is very sensitive to the hydrodynamic damping in the system, which is, in turn, not very well understood. Experimental data is available, but the results are fairly uncertain. A heavily damped system has smaller vibration amplitudes, and a wider lock-on response band. Hysteresis effects associated with the exciting flow velocity and the system response have been observed. [50,53,65,66]

In his paper, Sarpkaya [50] discusses the mathematical models that are most commonly used to describe vortex phenomena, the model developed by Harten and Currie being the most common. Other models used are those developed by Landle, Szechey, and Iwan and Blevins.

Sarpkaya indicates that there are serious flaws in these models, as the underlying processes are not very well understood, and that there is a serious lack of correlation between the theory and the experimental results. The theoretical problems may be due to the complex nature of the boundary layers, associated with laminar and turbulent effects.

Fluid-structure interaction experiments are notoriously difficult to conduct, and vortex related experiments are particularly complex. The validity of the modelling and scaling techniques used experimentally is also questionable. Most of the experiments are done with short, fixed cylinders, which respond in a fashion different to very long, flexible risers.

Most experiments are conducted on vertical cylinders, and there is the problem of how to model inclined pipes. King and Ramberg [50] demonstrated that the oscillations of circular cylinders are largely independant of angle of attack.

Usually the component of the fluid velocity normal to the pipe, or the projected area of the pipe, is used in the calculations. Sarpkaya maintains that tube-proximity effects greatly reduce the exciting force and width of the lock-on range, which is at odds with Overik [65,66].

Chakrabarti et al. [47] and Sarpkaya have indicated that the vortex-induced effects in three dimensions are much more complicated than in two dimensions, and more difficult to implement in a model.

1.5.1 Vortex-shedding control

The riser response characteristics may be changed in the design phase to try and reduce the vortex-induced effects, but the phenomenon is not very well understood, and adequate site data might not be available. It is possible to redesign on site. Bernitsas et al. [3] investigate riser redesign, using a nonlinear inverse perturbation method to calculate the changes in riser design necessary to change its response characteristics.

To effect this change, buoyancy and weight modules may be attached to the riser, the drilling-mud density may be changed, the riser tube geometry may be changed, or the riser top-tension may be adjusted. One may also use flow spoiling devices to modify the flow field around the riser in order to suppress the vortex-shedding.

Several types of devices are commercially available. Griffin et al. refer to Zdravkovich's paper (1981) as being the authoritative work in this field. Zdravkovich catalogues the various types of vortex-suppressing devices, their effectiveness and associated drag coefficients, and gives recommendations for effective design against vortex-induced vibrations.

Some devices, such as the aerofoil shaped one, reduce drag, while other types increase drag, although this increase is less severe than the increased drag due to the transverse vortex-induced vibrations. Every et al. [52] indicate that the functioning of the vortex suppressors is not very well understood, and that some devices have actually increased the vibrations in the system.

1.6 MULTI-TUBE RISERS

Floating production platforms usually require multi-tube risers to perform the functions of mooring, pumping crude and treated oil and injection fluids, and of providing power and communications services. Multi-riser or multi-tube riser configurations may be used. In the multi-tube case there is usually a large primary pipe with smaller secondary tubes attached to it, either internally or externally, as shown in figure 1.3.

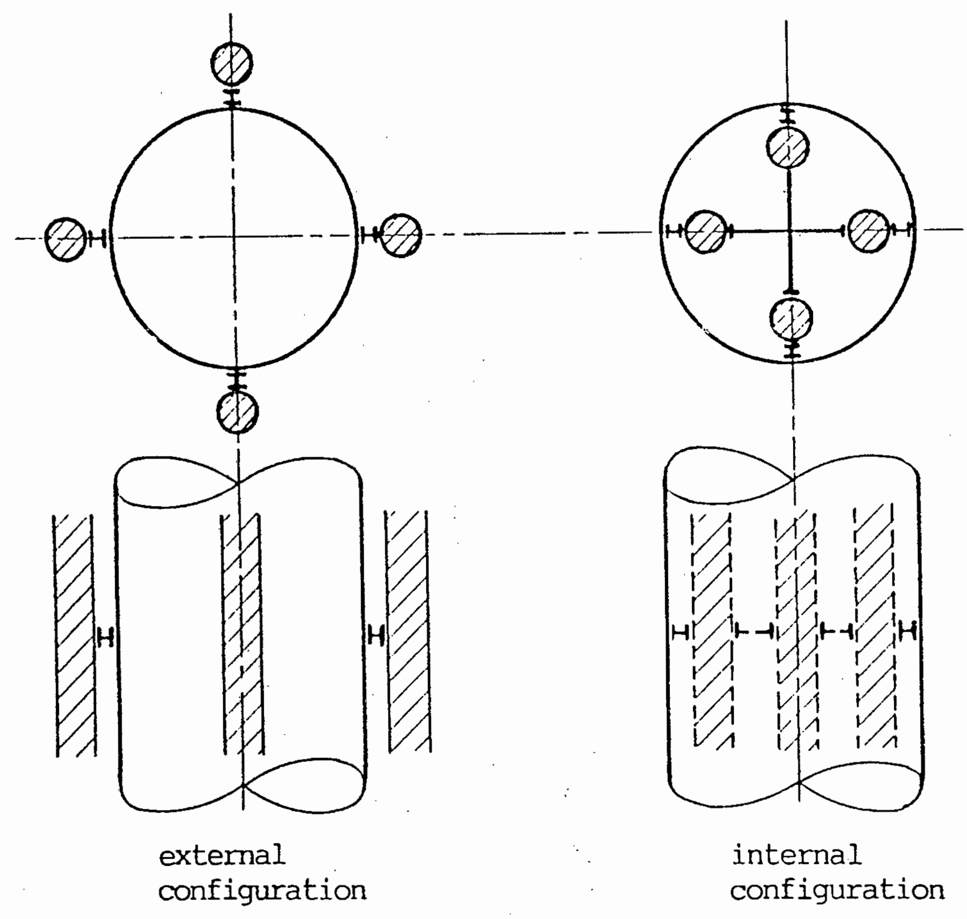

fig. 1.3 - Multi-tube riser configurations

The presence of multi-tube risers complicates the riser analysis in two ways. Firstly, the fluid-structure interaction is affected (if the secondary tubes are external), and secondly, the structural properties of the system are altered.

Several papers attempt to solve the fluid-structure interaction problem, including Demirbilek et al. [67] and Overik et al. [65,66]. The reader is referred to section 1.2 and 1.3 where single-tube risers are discussed, and to section 1.5 for the vortex-induced effects of multi-tube risers.

Overik et al. and Demirbilik et al. experimentally relate the drag, inertia and lift coefficients of various riser configurations to Reynolds number, R_e, Keulegan-Carpenter number, KC, and Strouhal number, S.

Demirbilek et al. account for vortex-shedding, stochastic effects, and steady and unsteady flow. The results are sensitive to pipe roughness, flow blockage, turbulence, and free surface effects.

Huang et al. [31] and Bennett et al. [68] deal with techniques for the modelling of the structural characteristics of multi-tube risers. Huang et al. maintain that the response of the riser system is usually dominated by the stiffness of the primary pipe, and suggest that the response of the system may be calculated considering the primary pipe only.

This response is then imposed on each secondary pipe separately, for the detailed design of those pipes. Huang warns that high local stresses may occur owing to clamps, contact, etc. and that these effects must be dealt with separately.

Bennett et al. [68] provide three modelling approaches, which they call, in ascending order of complexity, accuracy, applicability and cost, the "uncoupled" or independent, "composite" and "coupled" or interactive methods. The uncoupled technique involves the separate analysis of each distinct tube in the production riser bundle, ignoring any interaction between them.

The composite method is an extension of this, where a single riser equivalent is used. The final method involves coupling the individual risers at specific points of interaction along their lengths, allowing for full simulation of the riser system. This method is more complicated and expensive, but the results are more accurate. Bennett et al. give a tabular comparison of the three methods.

Bennett et al. conclude by remarking: 'As long as riser designs continue to evolve and change, no computer code, no matter how advanced, will become a "black box" into which one need only input dimensions, weights, etc., push the button, and await "the answers". A specific program of riser analysis should be tailored to fit the riser design and its environment.'

1.7 DYNAMIC CONSIDERATIONS

Originally, most of the work done in the field was concerned with the static analysis of marine riser systems. As mining operations moved into deeper and more hostile environments, it was necessary to incorporate dynamic aspects into the analysis.

The analysis procedure usually takes the form of a static evaluation, which is then used as a starting position for the dynamic analysis [9,15,54]. Care must be taken to handle the combined static and dynamic effects correctly, because the static and dynamic effects are coupled through the nonlinear drag force [34].

Spanos et al. [23-25] maintain that dynamic effects may be neglected in the case of shallow water depths, moderate sea-states and drilling-vessel motions, and relatively small riser diameters. Wybro et al. [35] assert that low frequency effects may sometimes be dealt with statically.

Wolfram et al. [37] indicate that offshore mining structures should be designed to ensure that the mean of the response spectrum of the structure varies from that of the wave energy spectrum. A schematic representation of the response characteristics of various offshore structures may be seen in figure 1.4.

The more rigid structures, such as steel frame towers, are suitable for shallower waters. A riser system is the only practical system for deep waters in terms of construction, installation and maintenance. For these deep water structures, dynamic analysis is important. Dynamic effects in the risers occur due to wave, current, wind and geotechnical excitation. In the analysis of marine risers the last two effects listed above are usually neglected.

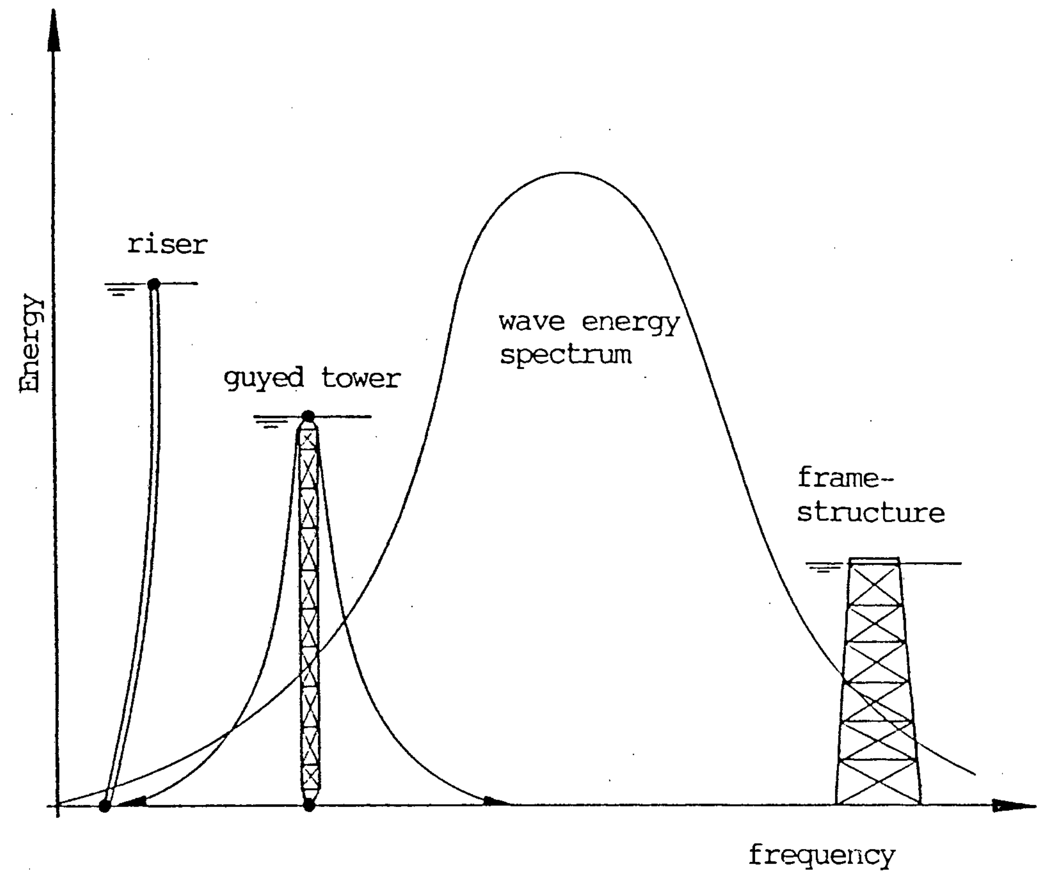

fig. 1.4 - Response characteristics of offshore structures

Sparks et al. [12-14] maintain that the wave-induced vibration is not of great concern in the study of long risers, since the amplitudes of these oscillations decrease rapidly as they descend the riser, owing to the strong hydrodynamic damping. Also, the irregular nature of the wave-action makes build-up of regular vibration unlikely. This is not true of the current-action, where vortex-shedding and lock-on may cause large oscillations [12-14].

In contrast, most authors [18,22-25,28,32,35,37,48] consider wave-induced effects important. Rajabi et al. [51] show that wave-induced vortices also play an important role in the dynamics of the riser system.

1.8 FINITE ELEMENTS IN THE ANALYSIS OF MARINE RISERS

The reader is referred to section 3 for the computational aspects of marine riser analysis.

Finite element analysis is now the most frequently used tool in the modelling of marine risers. The beam finite element is most commonly employed. Usually Bernoulli-Euler beam theory is sufficient to model the riser. Owing to the slim nature of the riser, shear deformation is negligible [6,34, 51,69].

Hibbitt et al. [15,46], Nordgren [34], and Huang et al. [30] have developed special, hybrid, beam elements in order to model this type of large deformation, nonlinear system.

Owing to the "string-like" behaviour of the riser, Bergan et al. [7] suggest the use of truss elements as they are inexpensive to use, but question the accuracy of the results. Davies [70] found that truss elements were difficult to use in this type of application, as the zero bending stiffness between the elements generated numerical instabilities.

McNamara et al. [15] agree that the riser behaves like a cable away from the end points, but must be modelled as a beam near the ends. Spanos et al. [23-25] indicate that neglecting the bending stiffness in the model, affects more the maximum bending stress at the bottom ball-joint, than the maximum angle, and that this effect decreases with increasing riser length.

Some authors have developed elements to cater for specific assumptions, such as McNamara et al. [18], who developed a simple beam element using convected boundaries with rigid body rotation assumed to be constant over each element. Garrett [71] has developed a three-dimensional torque-free, inextensible element, but admits that these assumptions are not always valid.

Other element theories used include the tensioned beam-column theory for near-vertical, straight risers [34], and Timoshenko and Cosserat beam theory, which include shear effects [15]. Warping effects are usually neglected, so shell elements are only required for the analysis of riser details [6,15].

A special element is required to model an articulation, as is found in the catenary configuration. Jain et al. [54] suggest that in a model containing an articulation, the rest of the riser may be assumed to be rigid. Fewer numerical difficulties are experienced if this is done, since the large difference in stiffness would cause the system of equations to be poorly conditioned, and the coupling effects would be complex.

Bergan et al. [7], and McNamara et al. [15] suggest the use of a short, very flexible element to model the articulation, although Bergan's solution did experience numerical difficulties.

1.8.1 Stiffness, damping and mass matrices

As the structural configuration changes, the stiffness of the structure changes. A geometrically nonlinear model must include the option for updating the stiffness matrix. The stiffness matrix may be updated every increment of the analysis, or at intervals specified by the user [7]. Patel et al. [22] update the stiffness matrix for the static solution if the deflections are large, but do not update during the dynamic analysis.

The mass in the system may be treated in a manner consistent with the finite element formulation, or lumped at the nodes. The consistent approach is often considered to be more accurate, but this is not always true, and is problem-dependent [22,72]. Consistent mass formulations result in rotational and translational coupling effects [22]. A lumped mass system is easier to formulate, and results in the elimination of rotational inertia, unless included separately [22].

Vugts et al. [73] define four causes of damping in the system: Material (plastic deformation, hysteretic effects, heat generation, etc.); structural (friction in pinned joints, etc.); environmental (fluid drag, wave and current interaction with the structure, etc.); and foundation damping (soil-structure interaction).

Most authors tend to neglect the foundation effects, apply the fluid drag as a force, and combine the material and the structural damping. Numerical damping may be used to simulate the structural and the material damping, as many time integration operators, such as the Houbolt, Newmark, and Hilber-Hughes-Taylor, include the facility for artificial damping [7,8,11,32,72,74]. This is not recommended [75], as the damping effects in these operators are complicated. The damping in these operators should rather be used to damp out spurious, numerically generated higher order frequency modes. This is discussed in section 4.

Often the so called Rayleigh damping is used [7,9,15,18,22, 49,73], which can simplify the computational aspects of the problem, in that the system of equations may be uncoupled, and modal analysis used, if the system is linear. The Rayleigh damping matrix is of the form: $\underline{C} = a.\underline{K} + b.\underline{M}$, where a and b are constants.

Structural damping is usually assumed to be small when compared to the hydrodynamic drag effects. Structural damping of between 5% and 10% is usually assumed [7,22]. The higher order values of damping are suitable for the synthetic/metallic composites sometimes used in riser manufacture [7].

Sparks et al. [12-14] maintain that the damping effects are only significant near resonance, and that the distribution of damping in the model is not critical, but rather that the rate at which energy is dissipated from the system is important.

1.9 UNCERTAINTY CONSIDERATIONS IN MARINE RISER ANALYSIS

Many engineering problems involve processes and phenomena that are inherently random in nature. The degree of sensitivity of a structure to either deterministic design changes or to randomness of the design parameters, is of great importance to the engineer when making decisions under conditions of uncertainty.

1.9.1 Modelling uncertainties

There are two basic types of uncertainty that occur in the design process [16,17,76-78]:

1) There are uncertainties associated with the randomness of the parameters in the process. These uncertainties may stem from the inherent randomness of that parameter, or they may be generated by the imperfect manner in which that parameter is measured. If the latter, then uncertainties may be reduced by increasing the number of samples or by improving sampling techniques.

2) There are uncertainties associated with the modelling process itself. Any model is an imperfect representation of the real world, and the degree of this misrepresentation is a measure of the uncertainty of the model. These uncertainties may be reduced by improving the modelling assumptions, and the modelling algorithms.

A full description of the uncertainty in a process involves the use of probabilty density functions (PDFs), which are often not known. The PDF describes the distribution of a random parameter. The PDF may be assumed, or the mean value and the variance (a measure of dispersion) of the process may be used to represent the nature of the uncertainty.

Ibrahim [78] differentiates between two types of parameter uncertainties:

1) The analysis of structures with deterministic properties and random excitation involves stochastic differential equations with random coefficients.

2) The analysis of structures with random properties involves differential equations with coefficients represented by random variables. These random variables may be discrete, or continuous, in which case random field theory must be used.

The modelling process is represented schematically in figure 1.5.

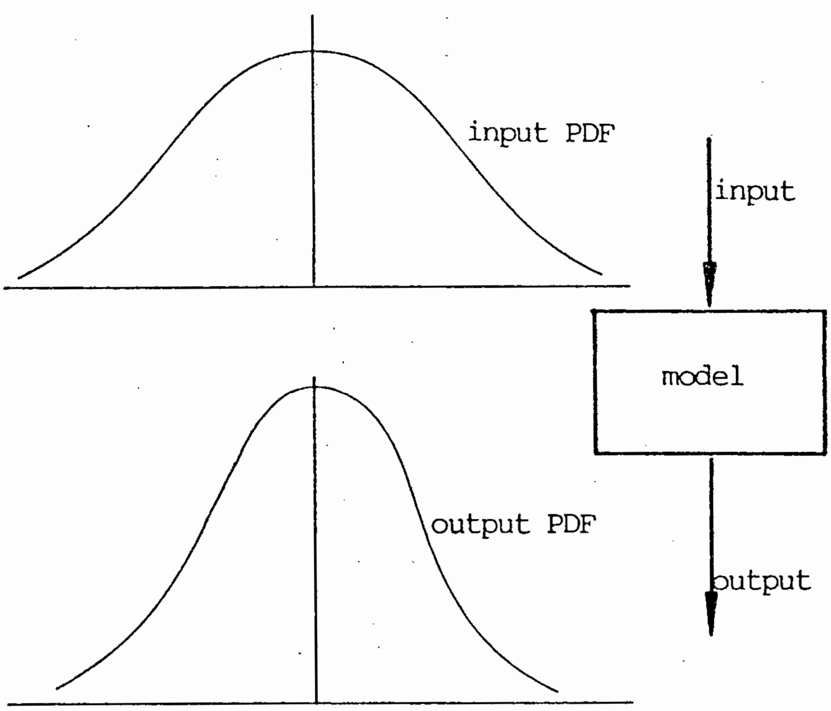

fig. 1.5 - Schematic diagram of random process

In the above figure, the model is developed to predict the response of a system to an input. There might be uncertainties associated with the input, or with the model. One would like to be able to predict the uncertainty in the response caused by the uncertainty in the input.

Standard techniques, such as impulse and frequency response functions, and perturbation methods, may be used [78], or numerical methods, such as the stochastic finite element method (SFEM), may be used.

SFEM methods include statistical and non-statistical methods. Statistical methods comprise techniques such as Monte Carlo simulation, stratified and latin-hypercube sampling. These methods usually require that full probabilistic information concerning all uncertainties be known, which is often not the case.

The uncertain parameters are usually assumed to have a Gaussian distribution, and to be uncorrelated [79]. If not, a Rosenblatt transformation might convert the process to an uncorrelated Gaussian one [78].

Non-statistical methods include the probabalistic finite element method (PFEM) developed by Liu et al. [16,17], which will be introduced in section 8., and applied to the marine riser system.

1.9.2 Uncertainties in marine riser analysis

The analysis of marine riser systems is complicated by the fact that there are serious uncertainties that have to be accounted for. The two most important effects are those of the random sea excitation, and the random nature of the system parameters. The parameters that are the most uncertain are the hydrodynamic coefficients associated with the fluid loading, C_d and C_m.

Also of importance is the uncertainty inherent in the model. This uncertainty is difficult to quantify. The model must be tested in some way against an analytical solution, or against a superior model. The geometrically linearised model developed in section 6 was tested against ABAQUS, a sophisticated nonlinear program, and the results of this comparison may be found in section 6.

The uncertainties in the model, which include the uncertainty inherent in the application of Morison's equation, can be reduced by applying more sophisticated theories and modelling techniques.

Much more work has been done in an attempt to model the effects of the random sea-state than to model the uncertainties of the system parameters, and includes work by Sigbjörsson [58], Nolte et al. [26], Shyam Sunder et al. [48], Dareing et al. [28], Kao [42], Spanos et al. [23-25], Spidsöe et al. [59], Stansberg [62], Grigoriu et al. [79], Burrows [80], Leonard et al. [81] and Kirk [20].

The emphasis in this project, will be on the parameter uncertainties associated with marine riser analysis, and in particular with the uncertainties in the hydrodynamic loading coefficients C_d and C_m.

Hogben et al. [55] summarise much of the experimental work done, in an effort to measure and correlate these coefficients which appear in Morison's equation. These experiments are difficult to carry out as there are so many parameters that may vary. The problems are worsened by the fact that the applicability of Morison's equation to highly flexible structures is questionable.

Hogben et al. report that errors of as much as 50% are common. Clearly, the effect of these large uncertainties on the response of the systems is significant. The uncertainties are particularly severe in the regime where drag and inertia effects are both important, which is unfortunately where risers usually operate [48].

The PFEM is applied to the problem of marine riser analysis, and the uncertainties associated with the hydrodynamic coefficients in sections 7 and 8. The method is implemented with the geometrically linearised finite element riser model developed in section 6.

2. MODELLING RISERS WITH ABAQUS

"Generic" models have been developed for the three configurations described in section 1.1. These are the standard, the catenary and the hanging configurations.

For convenience of analysis, this study was broken up into two sections, static and dynamic. This was done for three reasons. Firstly, the dynamic portion of an analysis usually begins with the configuration in static equilibrium, and so this is a reasonable point at which to break up the analysis.

Secondly, a full dynamic analysis is complicated and expensive, and it is not practical to investigate the effects of all the parameters. A more efficient approach is to investigate as many of the parameters as possible in the static analysis, and to apply this information to the dynamic analysis.

Thirdly, the static and the dynamic analyses have different modelling difficulties associated with them, and these may be more easily resolved by conducting the two analyses separately.

The analysis may also be broken up into modelling and design considerations. Design considerations include the effects of parameters such as the length of the riser, and the hydrodynamic coefficients, which are decided by the constraints on the design.

The sensitivity of the model to such parameters may be investigated, to be used by the designer as an indication of how reliable the data for the design must be. The design aspects of these factors are too specific to a particular design to be dealt with in this study, which will be limited to the numerical and computational aspects.

Modelling considerations include such factors as the type of elements used in the model, and the start-up procedures employed. The efficiencies of the models are sensitive to the start-up procedure, in terms of the convergence characteristics and the computational cost of the solution, and indeed, whether or not a solution can be achieved at all. The reasons for this are discussed in section 5. ABAQUS uses "steps" in order to define the history of the model, and these steps are employed to implement the various start-up procedures.

The way in which this analysis was conducted is as follows: An "average" model for each configuration was chosen, after investigating the available literature. For each of these average models, the modelling considerations were investigated in a static analysis. The most efficient model, in terms of cost and accuracy, was termed the "generic" model, and formed the basis of all further analysis.

The generic models for the three configurations are illustrated below:

2.1 Standard Riser configuration [4,22-23,28,29,34,38,51]

This configuration is the most commonly used riser system. The generic model, showing the step-wise analysis procedure, may be seen in figure 2.1.

Start-up procedure:

i) Initial position: see dashed line in figure 2.1
ii) Step 1: application of the top-tension.
iii) Step 2: application of the drag forces and self-

weight, displacement of top node to a point near to where expected equilibrium position will be.

iv) Step 3: release of top node, to achieve equilibrium.

v) Step 4: dynamic analysis.

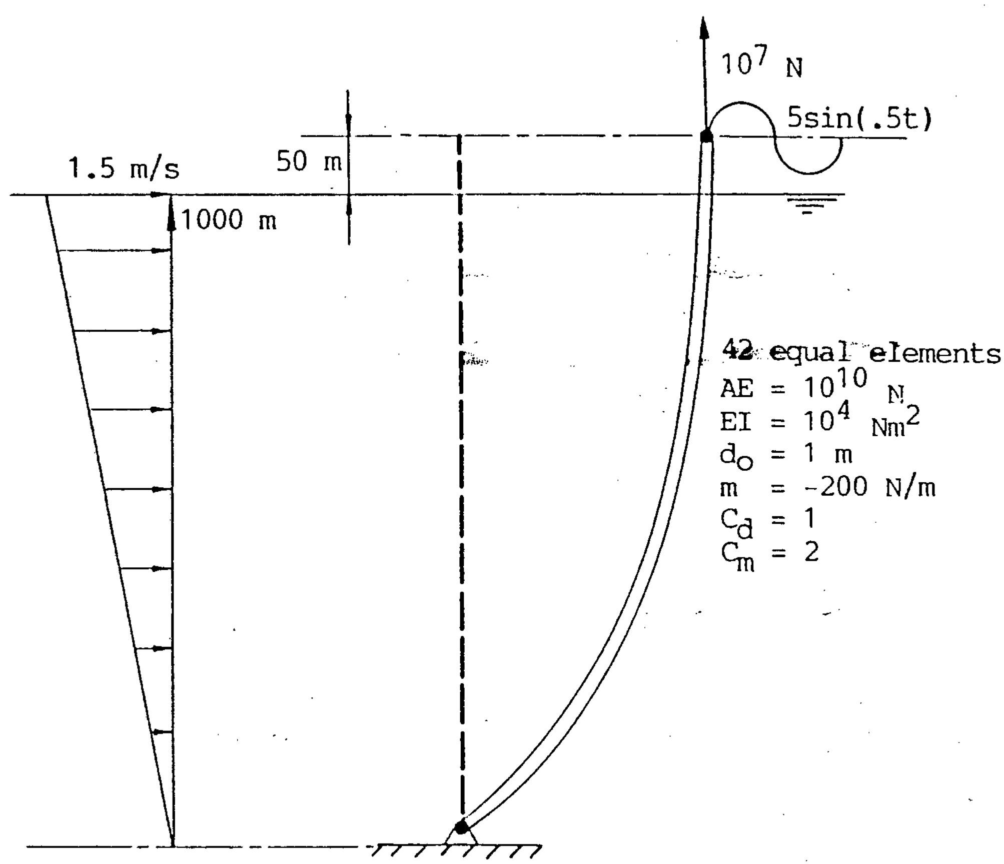

fig. 2.1 - Generic standard riser configuration

2.2 Catenary configuration [7,15,33]

The generic model, showing the step-wise analysis procedure may be seen in figure 2.2.

Start-up procedure:

i) Initial position: see dashed line in figure 2.2

ii) Step 1: application of buoyancy force, displacement of central node in the catenary section of the model to a point near to where equilibrium position is expected to be.

iii) Step 2: application of self-weight, and drag forces.

iv) Step 3: displacement of end node to the sea surface, to a position near to where the equilibrium position is expected to be.

v) Step 4: release of top node to achieve equilibrium on surface.

vi) Step 5: dynamic analysis.

The articulation was modelled by two short, very flexible beam elements on either side of a short, stiff beam element. A point buoyancy load was applied to the central element.

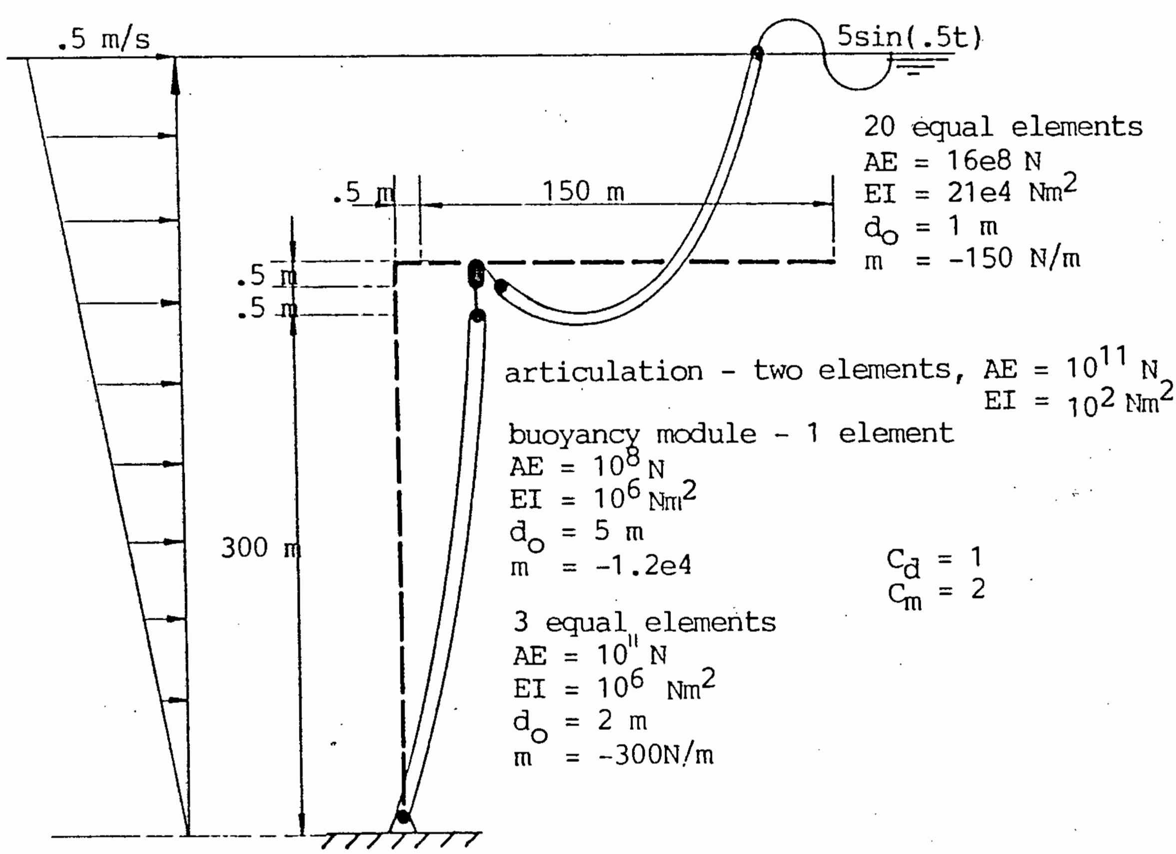

fig. 2.2 - Generic catenary riser configuration

2.3 Hanging configuration [8-11]

The generic model, showing the step-wise analysis procedure, may be seen in figure 2.3.

Start-up procedure:

i) Initial position: see dashed line in figure 2.3

ii) Step 1: application of self-weight, and the displacement of the bottom node to a point near to where the equilibrium position is expected to be.

iii) Step 2: release of bottom node to achieve equilibrium.

iv) Step 3: dynamic analysis.

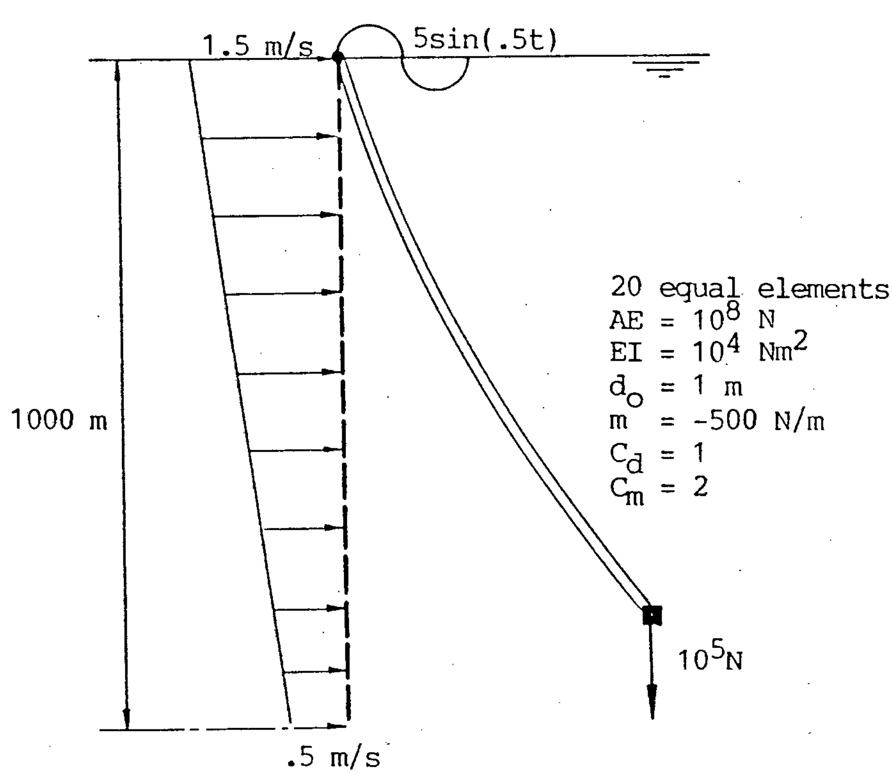

fig. 2.3 - Generic hanging riser configuration

2.4 Modelling with ABAQUS

i) Dynamic models have been implemented with ABAQUS for the three configurations, and enough experience has been acquired to confidently model this type of problem.

ii) The models discussed in this section are two-dimensional, which is a simplification of the actual riser configuration. Physically, the situation is complicated by non-co-planar currents and waves, which result in complex whirling motions [54].

Numerically, a three-dimensional model may be difficult to implement, as spurious higher order modes may be generated by numerical "spill-over" between the planes [32]. Nolte et al. [26] maintain that a two-dimensional model is conservative by about 20%. A three-dimensional model in which the waves and current were co-planar was developed with ABAQUS, and the computational effort was only marginally greater than the two-dimensional model.

iii) It would be useful to obtain data and design requirements for an actual riser system, as there are simply too many parameters to try and draw conclusions from the general case, especially for the dynamic analysis. Kirk [20] says: 'Attempts to optimise riser design over a wide range of environmental parameters cannot achieve meaningful results.'

iv) Some user subroutines of ABAQUS are versatile, such as the material specification routines, but others are limited. For example, it is not possible to implement a linearised version of Morison's equation through the subroutines, as some of the pertinent parameters, such as nodal velocities, are not passed to the subroutine.

Without changing ABAQUS' source code, the linearisation cannot be effected. It is possible, though, to attempt the relatively small displacement configurations using the linear stepping options, and to investigate the validity and cost saving of doing this.

v) A modal solution requires an eigenvalue search, and since the stiffness matrix generated with the *AQUA option is non-symmetric, this cannot be done. That is, the *FREQUENCY option cannot be evoked. A modal analysis neglecting the drag and added-mass effects would not be very useful.

vi) The version of ABAQUS (4-5-169) used in this study does not have the facility for spectral analysis and random vibration analysis, although future versions will. This facility would only be useful for this type of study if a linearised version of Morison's equation were also implemented. Thus the potential for computational work with ABAQUS in this field is limited at present.

3. NUMERICAL ASPECTS OF MARINE RISER ANALYSIS

3.1 Introduction

The procedure adopted by an engineer in the analysis of marine riser systems depends very much on the objectives of that particular study. The researcher might be interested in a specific aspect of the system, such as vortex-induced oscillations [51-53,64-66], or in the response of multiple riser systems [31,37,65-67].

The engineer might be concerned with the detailed design of the system, or in its maintenance [36]; or in the modes of failure of the system, such as buckling [5,6], or fatigue failure [35]. Each problem requires its own methodology and modelling algorithms. In this study, the numerical and computational aspects will be investigated, with the application of the finite element program, ABAQUS.

Numerical aspects include those aspects associated with the algorithm and the mechanics of the problem, and the manner in which they affect the solution. Computational aspects apply more to the implementation of that algorithm on a computing machine. The two concepts are interrelated, and cannot be considered in isolation. For example, the stiff nature of a marine riser causes poor conditioning of the stiffness matrix, which may cause convergence problems owing to the finite representation of the computer.

Chakrabarti et al. [47] give a good general overview of the analysis techniques available for marine riser modelling. As is shown in fig. 3.1, the general analysis may be broken up into static and dynamic portions, a static analysis usually being obligatory in order to determine the initial conditions for the dynamic run. Dynamic considerations are complicated, and are considered in section 4.

3.2 Governing equations of the riser system, and their solution

As figure 3.1 shows, it is first necessary to develop a system of partial differential equations which describe the riser behaviour. This is done by considering a force or energy balance on an elemental segment of the riser. These equations relate the forces applied to the system to the properties of that system, including its mechanics and geometry (compatibility), and are called the governing equations of the system. The geometrically linearised set of governing equations is derived in appendix B.

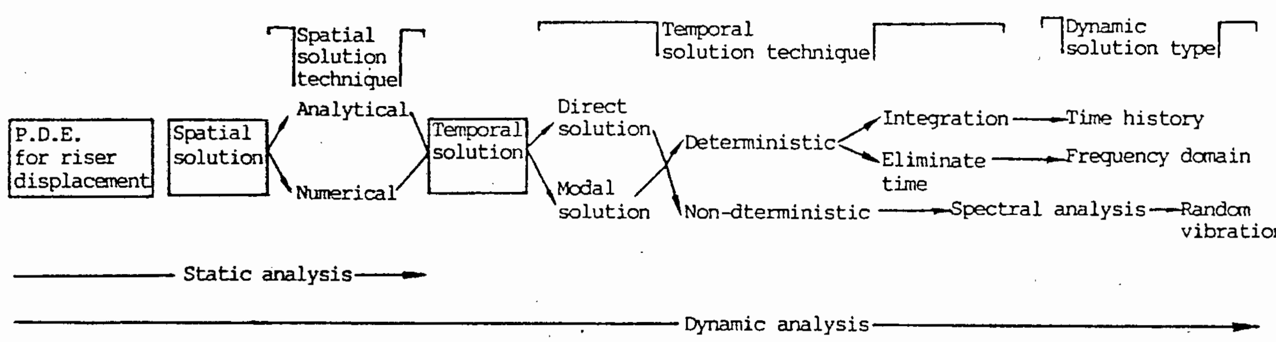

fig. 3.1 - Flow chart of solution procedures
[Chakrabarti et al., 47]

An energy balance results in a system of equations involving energy functionals which may form the basis of a finite element formulation. Papers dealing with the derivation of the governing systems of equations for large deformation, three-dimensional risers include those by Bernitsas et al. [3-6], Chung et al. [8-11], Huang et al. [30,31], Kim et al. [44], Konuk [82], Natvig [32] and Garret [71].

These equations may be simplified for the small displacement, planar case, as is done by Bernitsas et al. [3-6], or the small displacement model may be derived idependently, as is done by Spanos et al. [23-25], Patel et al. [22] and McIver et al. [38]. Other authors just quote these results. The final set of governing equations derived by the various authors are usually of the same form.

The static and dynamic analysis begins with the spatial [47] solution of the governing equations, which results in the displaced shape of the structure under the action of statically applied forces. There are numerous techniques for the solution of these equations, but they may be divided broadly into analytical and numerical classes.

3.3 Analytical solutions

The marine riser problem is generally complicated in that it is highly nonlinear, nonlinearities arising from the large displacements of the riser, and the hydrodynamic loading. The geometry of the riser may be non-uniform, with cross-section changes, articulations, weight and buoyancy modules, and attached cables. These considerations, combined with the nonlinearities of the system, make analytical solutions, to any but the most simple of configurations, impossible. However, an analytical solution, even for a simple riser configuration, may give the engineer important insight into the mechanics of the problem.

Bernitsas [6] uses Airy stress functions to solve a linearised set of equations in order to investigate buckling effects in marine risers. Other types of analytical solutions assume a deformed shape of the riser, often an elastic catenary shape, or the sum of a truncated series. Modal analysis is sometimes used, but the governing equations must first be linearised [47]. Kirk, Dareing and Huang [47] use modal superposition techniques. These methods are limited in their application, and are not exact.

3.4 Numerical solutions

Many types of numerical solution schemes also exist. Numerical solutions allow for complete generality of geometry. Any nonlinearities may be handled in principle, but convergence problems and high computation costs may result. The two most frequently used methods are the finite difference method [51,85], and the finite element method [5,79,15,18, 22-23,30,34,49,71]. The finite element method has the advantage that it is more flexible, and may be more readily applied to various geometries.

Finite difference codes are generally much simpler to generate on a one-off basis, but are not as versatile as the finite element schemes. Chakrabarti et al. [47] maintain that finite difference schemes are better suited for two-dimensional problems, while the finite element method may be used for three-dimensional problems with large deformations. Finite difference schemes have been used by Bennett et al. [68] and Young et al. [83], although their formulations are not described in detail in their papers.

Finite element schemes for problems related to structural mechanics usually result in banded, symmetric matrices, the solution procedures for which are well documented [47]. Finite difference schemes may result in unbanded, non-symmetric matrices, and are hence not as efficient for large systems. The *AQUA option in ABAQUS generates a non-symmetrical system of equations. Since the finite element method is the most popular, some aspects are discussed in more detail in section 1.8.

Other numerical schemes have been developed and applied to the riser problem, but are usually more specific, and not as versatile as the afore-mentioned methods. The developers of these methods usually report advantages of their schemes, which include improved accuracy, reduced computational costs, improved computational speed, and simpler formulation. These methods include the use of Laplace transfer-matrices by Nielsen et al. [40], the projection of the solution along the eigenmodes of the system by Kim et al. [44], block integration by Jain et al. [54], Galerkin method by Kirk [20], modal analysis by Dareing et al. [28], and transfer functions by Chung et al. [11].

The numerical solution of the governing system of equations is by no means simple. The equations are highly nonlinear, and modifications to the conventional numerical schemes are usually required. Iterative techniques are used for the solution of the nonlinear equations; or the equations may be linearised, or partly linearised, to simplify the problem. The degree to which the linearisation of the system of equations affects the solution is of major concern. ABAQUS can deal with the general nonlinear problem, and so may be used as a basis for comparison of linearised models.

3.5 Numerical difficulties

Most workers in the field report numerical problems. Natvig [32] reports severe stability problems in the three-dimensional analysis as opposed to a two-dimensional analysis, even when the structure motion, waves and currents are all co-linear. He attributes this effect to higher order vibration modes being excited owing to numerical round-off in the plane perpendicular to that in which the excitation takes place.

A co-planar, three-dimensional model implemented with ABAQUS in this study presented no problems, as described in section 5.3.3, although these effects were not investigated in detail. The three-dimensional analysis cost approximately 20% more than the two-dimensional one. Jain et al. [54], in their analysis of the three-dimensional motion of risers generated by non-co-linear waves and a steady current, report complex whirling motions of the riser.

The poor conditioning of the system of equations, combined with these round-off errors, may cause convergence problems. McNamara et al. [18] report numerical stability problems arising from high frequency axial vibration modes. Natvig [32] implemented a numerical filter in order to damp out these higher order modes.

Bergan et al. [7] encountered numerical difficulties during start-up procedures, owing to high frequency, numerically generated, spurious modes, and recommend efficient start-up procedures to overcome this. Bergan et al. attribute these high frequency modes to discontinuous velocities between the time steps, which generate artificial impulses. Bergan et al. used linear interpolation, and proposed that these effects might disappear with higher order interpolation. This effect was not noticeable in the ABAQUS and RISER models developed in this study.

Hibbitt et al. [29] also report start-up difficulties, which they attribute to the highly flexible nature of the unstressed riser in its initial configuration. After some loading is applied, the axial stresses stabilise the system, and convergence is more rapid. McNamara et al. [18] suggest the slow application, or "ramping-on" of the applied loads, in order to overcome this problem. This technique has been used with some success in the dynamic analyses in this study, using ABAQUS, where the loads or kinematic boundary conditions are applied in increments over the dynamic step.

The solution of Bergan et al. experienced uncontrolled oscillations within two wave cycles in one of their numerical examples [7]. They were fairly inconclusive as to the cause of the problem, not being sure whether the solution was picking up response characteristics of the real system, or whether they were just spurious, numerically generated modes, worsened by the poor conditioning of the system.

Much of the work done in this field is concerned with overcoming the stability problems inherent in this type of nonlinear, large deformation problem. The Newton method, or a modified version, is the most popular method for solving these problems, and is used by ABAQUS. The Newton method will be discussed in more detail in section 5.2.

Some computer programs have the facility for the inclusion of a small degree of damping, in order to damp out the higher order spurious modes that are often the cause of numerical instability. Some of the dynamic analysis algorithms, such as the Newmark, Houbolt, Wilson and the Hilber-Hughes-Taylor used in ABAQUS, provide artificial numerical damping [15,74,75]. Konuk [82] points out that 'strong intuitive understanding' is necessary for the application of such a scheme, as the damping effects are complex.

McNamara et al. [15], Nordgren [34] and Huang et al. [30] have developed hybrid finite elements in order to cope with the convergence problems associated with this type of analysis. In the formulation of the hybrid element, both displacements and forces are iterpolated independently, instead of just the displacements being interpolated, as is done with the standard finite element. The advantages and disadvantages of hybrid elements, specifically in ABAQUS, will be considered in section 5.6.3.

The convergence rate of the solution is affected by the non-linearity of the problem, and the poor conditioning that results from axially stiff systems such as risers, which often have axial stiffnesses of orders of magnitude larger than the bending stiffness [15]. In the extreme case, this results in a singularity for the instance of an articulation of zero bending stiffness. The conditioning of the system will be dealt with in section 5.3.

Konuk [82] indicates that when "stiffness is combined with strong nonlinearity of the problem, the convergence of any classical iterative technique is mostly a matter of chance". Most current models thus employ modified algorithms in an attempt to overcome these problems.

4. NUMERICAL CONSIDERATIONS IN THE DYNAMIC ANALYSIS OF MARINE RISERS

4.1 Introduction

Dynamic analyses are usually required for a marine riser design. The reader is referred to figure 3.1 for a flow diagram of analysis procedures. The reader is also referred to section 3 for details on the spatial solution of the governing equations, and some background to the numerical aspects of the problem. See also section 1.7, as regards the dynamic modelling considerations.

The solution of the dynamic riser problem falls into two main categories: deterministic (time and frequency domains) and non-deterministic or stochastic methods [47] (see figure 3.1). The time versus frequency domain, and the deterministic versus non-deterministic questions, are discussed in sections 4.3 and 1.9. The most important aspect of a time domain solution is the choice of time integration scheme, and this choice will be dealt with in some detail.

4.2 Solution techniques, and numerical aspects of the dynamic analysis

Several algorithms are available for direct time integration, that have been used in the literature for this type of problem. McNamara et al. [15] use the Hilber-Hughes-Taylor method, which is implemented in ABAQUS. This operator will be discussed in more detail in section 5.4. The most commonly used algorithms are the Newmark (average acceleration or trapezoidal) method [7,22], and the Wilson [32] and Houbolt methods [18,34] which are extensions of the Newmark method and have the capabilities of including artificial numerical damping.

Other methods used are the Crank-Nickolson [49], the Adams-Moulton predictor-corrector [71] and the Runge-Kutta by Wybro et al. [35], which Hall et al. [49] deem specifically unsuitable for this type of problem. Hall et al. [49], Konuk [82], Park [84], and McNamara [74] deal with the rationale behind choosing an algorithm for this class of problem.

Hall et al. [49] indicate that the "stiff" nature of marine risers is characterised by responses containing many frequency components, some rapid, some slow. The system is "stiff" in that its eigenvalues are widely separated [82]. Faddeev et al. [85] show that the ratio of the largest to the smallest eigenvalue is a direct measure of the condition number of the system, which is discussed in section 5.3.

The governing equations are neither parabolic nor hyperbolic, but rather, in general, complicated and nonlinear in nature, and thus do not fall into any standard classification of partial differential equations [49]. Hall et al. [49] recommend the use of a modified Crank-Nicholson scheme, with artificial damping, which gives a stable solution.

McNamara [74] critically appraises the main solution techniques available for the solution of nonlinear stuctural dynamic problems involving large deformations and possible plastic deformation. McNamara compares the Houbolt, Newmark, Wilson and central-difference operators.

An important factor in the choice of methods is the fact that the scheme must be coupled with an already existing structural model. Most of these schemes were developed for the analysis of linear systems, and the extension to nonlinear systems is not trivial [74]. Weeks [84] concludes that the characteristics of a linear system are maintained in the corresponding nonlinear system, which is in contention with McNamara.

The Runge-Kutta scheme is conditionally stable, and requires very small time steps. The Wilson scheme is judged the most accurate of the algorithms evaluated by McNamara, with the Houbolt method requiring small time steps of $dt/T \leq 0.005$, where dt is the time step, and T the period of the mode of interest. For linear problems, McNamara suggests the Newmark or Wilson operators, which give stability and accuracy with relatively large time steps.

For nonlinear problems accuracy, and not stability, is usually the most important factor in choosing an algorithm. If a high degree of accuracy is required, a single-step operator, such as the central-difference scheme, is best, although the cost is higher than multi-step methods. Regardless of the operator chosen, for nonlinear problems the time step must be quite small, smaller than 0.01 of the period of the highest modal frequency of interest [74].

The stiffness of the system need only be updated periodically, and McNamara suggests that every ten time steps is adequate. Hibbitt [86] maintains that for the general case where severe nonlinearities may occur, the stiffness matrix should be updated every analysis step, and this is done in ABAQUS.

In many algorithms, the small time step required for sufficient accuracy precludes the necessity of an iterative scheme, the Wilson operator being an exception [74]. Because the Newmark scheme has a limited stability range, and the Wilson and central-difference schemes are expensive and difficult to implement, McNamara suggests the use of the Houbolt operator for most applications. Hughes [75] maintains that the Houbolt operator is outdated, as other more accurate algorithms have been developed, such as Park's modified Gear's operator [84].

McNamara concludes by saying: " The nature of nonlinear analysis does not lend itself easily to rigid conclusions, and further numerical experimentation with other operators and more complex structures is required" [74]. This statement is supported by the contradictions apparent in the literature.

A general problem in the dynamic analysis of riser systems is the transient part of the solution, especially in the case of rapid, or random motion, such as may be found in storms, or due to impact loads that might occur during the mooring of the vessel [39]. Spurious, high frequency modes occur in the transient part of the analysis, and usually result in numerical instabilities [7,15,18,32].

Damping is usually introduced into the system in order to filter out these unwanted modes. Jain et al. [54] report that the transient response is almost immediately suppressed, owing to the large damping inherent in these problems, caused by the hydrodynamic drag effects.

Sparks et al. [12] maintain that the damping effects are only significant near resonance, and that the position of damping in the system is unimportant, but rather that the rate of energy dissipation from the system is important. When a flexible system near resonance moves in compliance with the wave motion, the system can effectively filter out wave forces near the natural frequency of the system, which may result in a reduction in the response of the system [42].

Some authors, including Chung et al. [8,11] and Kao [42], have undertaken sensitivity analyses to determine which parameters influence the dynamic analysis of marine riser systems the most. Kao reports that when the natural frequency of the structure is greater than that of the dominant sea-state's, a conservative response spectrum results.

Kao also indicates that when the pipe diameter is increased, the errors in the computed response decrease. This is because the drag nonlinearity becomes less severe. This concept may be extended. Any nonlinearity that can be reduced in some way, without compromising the system with artificial linearisation, leads to reduced errors.

Bergan et al. [7] report that the response of this type of system is very sensitive to the loading and displacement history of the system. McNamara et al. [15], on the other hand, maintain that, owing to the linearly elastic material assumptions, the starting position and loading path have no effect on the final results of the analysis. Numerically, there appears to be some dependence on the start-up procedure and solution path, in terms of convergence characteristics and ease of solution. Some efficient start-up procedures are described in section 2, and the reasons for these efficiencies in section 5.

4.3 Time/frequency domain considerations

The reader is referred to figure 3.1 in order to place these issues in context. The deterministic solution includes both the time and frequency domain analysis. The frequency domain analysis requires the governing equations to be linear, and so, linearisation techniques must be implemented, and these techniques are not always satisfactory. A time domain analysis is more general in that all nonlinearities may, in theory, be handled, but this sort of analysis is more expensive and time consuming than the frequency domain option [47].

Several researchers have used time domain analysis, including Natvig [32], McNamara et al. [15,18], Wybro et al. [35], Bergan et al. [7], Nordgren [34], and others. Amongst those that have employed the frequency domain are Patel et al. [22] and Shyam Sunder et al. [48].

Young et al. [21], McIver et al. [38], Vugts et al. [73] and Chakrabarti et al. [47] give useful comparisons between frequency and time domain analyses.

The frequency domain analysis assumes that all the time varying terms are of the form $X = X_o e^{iwt}$. When this substitution is made into the governing equations of motion, time (t) cancels, and the independent variable becomes frequency (w). Frequency domain calculations typically take 2 to 5 iterations to converge to a solution [57].

The time domain solution must be checked to ensure that steady-state has been achieved, while the frequency domain solution contains no transients. Young et al. [21] recommend that the frequency domain be used to carry out repetitive parameter studies, as the cost of time domain analyses is prohibitive, but admit that the necessary linearisation is a drawback, although there is promise in the current, sophisticated, linearisation schemes. McIver et al. [38] recommend that a combination of frequency and time domain methods be used in an analysis.

Chakrabarti et al. [47] suggest that the frequency domain solution is better suited for investigations into fatigue failure, as the cost of the required long time domain runs is prohibitive. On the other hand, Patel et al. [22] suggest that a time domain solution is essential for fatigue and fracture analysis, as only a time domain analysis gives the detailed information necessary for a meaningful study in irregular sea-states.

The frequency domain solution is more sensitive to minor changes in wave spectra [47], but McIver et al. [38] assert that the frequency domain solution has the same degree of reliability as the time domain solution. A combination of both techniques is recommended. The time domain analysis can give credibility to the linearised frequency domain solution. Young et al. [21] suggest that the frequency domain analysis is ideally suited to the study of random sea effects, as the time domain analysis of this problem requires the solution of at least 1000 waves, which is very expensive.

McIver et al. [38], and Young et al. [21] report cost-savings, using the frequency domain analysis, of 20 to 50 times that of the time domain. Young et al. recommend doing most of the analysis in the frequency domain, and checking the key results in the time domain. ABAQUS (version 4-5-169) does not have the facility to conduct an analysis in the frequency domain. In order to do so the equations must be linearised. Care must be taken in doing so, due to the large geometric nonlinearities that occur in some of the riser configurations. The hydrodynamic drag must also be linearised.

5. NUMERICAL ASPECTS OF MODELLING MARINE RISER SYSTEMS WITH ABAQUS

5.1 Introduction

The main constraint in this type of problem, that is, the large displacement analysis of axially stiff members (combined with bending flexibility), is the ability of the model to converge to a solution. This problem arises in both the static and the dynamic analyses, owing to the poor conditioning of the system of equations. The unstable behaviour of the solution manifests itself in the high residuals that appear in the analysis steps.

In order to model a particular riser configuration, one has the option of several start-up procedures, as described in section 2. In this section each of these options will be termed a different model. When a different riser configuration is being discussed, it will be explicitly stated as such.

With the automatic time stepping facility of ABAQUS in operation, which is necessary for many of these problems, it is difficult to objectively measure the relative efficiencies of the various elements and models. After the first iterative attempt, the different models follow different solution paths, or at least the time steps are different.

From experience gained with ABAQUS, the analyses that experienced the greatest convergence difficulties also had the largest initial residuals. Therefore, the initial residuals, of the first iterative attempt, of the first increment of each step, appear to be the best measure of the convergence characteristics.

The total number of increments in a step is not always a good measure of the solution efficiency, as a step may take fewer increments, with more iterations per increment, and still take up more computational time. The total computational time and the accuracy of the results are measures of the over-all efficiency of the model.

5.2 Handling of nonlinearities: Newton's method

The nonlinear nature of the marine riser system requires nonlinear algorithms for solving the system's equations. Newton's method is the most popular, and is used in ABAQUS.

Cook [72] likens a nonlinear analysis to "following a winding path in a dense fog". Hibbitt [86] remarks that Newton's method is difficult to use, and is one of the most severe limitations faced in the application of codes such as ABAQUS.

Newton's method is well documented, and so will not be discussed in detail here, but it basically operates by predicting a new configuration by projecting along the tangent of the solution path, and by correcting the solution to reach equilibrium. The algorithm in ABAQUS iterates at each increment until the solution lies within a user-defined tolerance. The equilibrium equations, in incremental form, may be represented as follows:

$$\underline{K}\ \underline{\delta d} = \underline{\delta f}$$

where - $\underline{K}$ is the current or tangent stiffness matrix, a function of $\underline{d}$.
- $\underline{\delta d}$ is the incremental displacement vector.
- $\underline{\delta f}$ is the incremental load vector.

The above set of equations is nonlinear, and the solution must be iterated until the difference, or residual, between the predicted forces, and the equilibrium forces, is within a specified tolerance, PTOL and MTOL in ABAQUS. Strictly speaking, the iterations should continue until the displacement residuals are within a defined tolerance as well. For cost reasons, ABAQUS only iterates the force terms, although the displacement residuals are calculated and printed [101].

As the system becomes more ill-conditioned, the stiffness matrix experiences large diagonal decay in the equation solving routine, and large incremental displacements are predicted. The residuals become large, the algorithm finds it difficult to converge to within the force tolerances, and the solution becomes unstable. This process will be discussed later in this section.

5.2.1 Effectiveness of Newton's method

The effectiveness of Newton's method depends on several factors: the conditioning of the system of equations, which will be dealt with in section 5.3, and the type of system being analysed; that is, whether the solution hardens or softens. Softening and hardening systems, and the manner in which Newton's method operates on them are illustrated in figure 5.1

The riser problem falls into the hardening type of classification, that is, as the displacement increases, the system becomes stiffer because the axial forces increase. For this type of problem the stiffness should be up-dated at every increment [72], as is done in ABAQUS. The automatic increment stepping facility in ABAQUS is very useful in allowing a large range of problems to be solved.

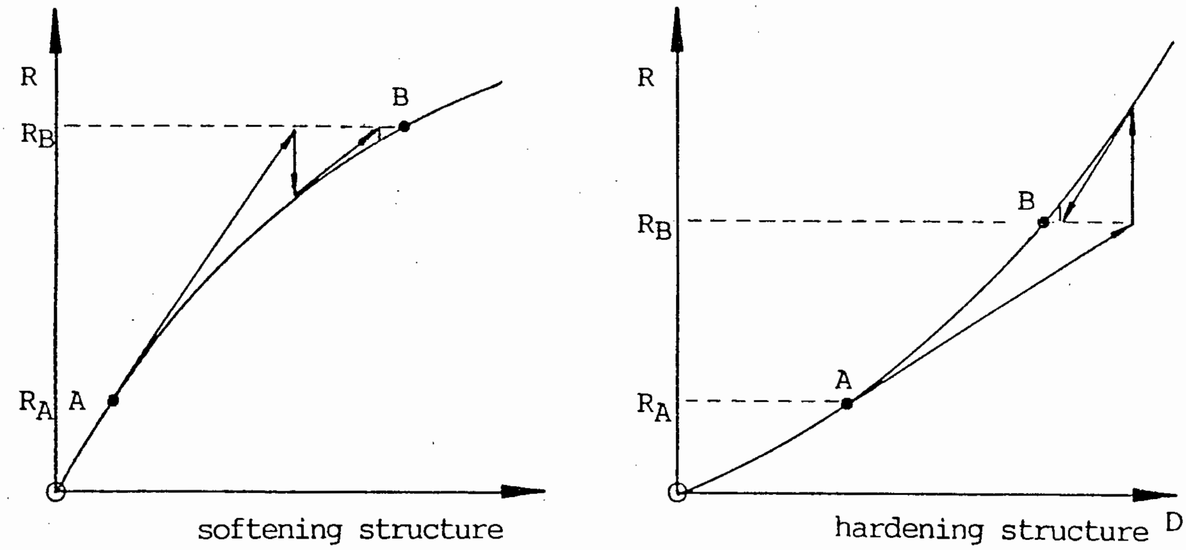

fig. 5.1 - Newton's method on hardening/softening systems [Cook, 72]

The effectiveness of Newton's method depends on the accuracy of the solution, an accurate solution allowing for rapid convergence, and large incremental steps. Errors in the solution arise from both numerical and modelling considerations. Modelling errors are errors generated by poor idealization of the real problem, such as an insufficient number of elements, or poor material assumptions.

Numerical errors arise from truncation and round-off error, truncation error being the more severe [72]. Truncation and round-off error may cancel out to some extent. They may be reduced by working in double precision. Irons [87] says that 'when round-off occurs, we are still solving a set of equations, which just happen to be the wrong ones', and that 'round-off is like a venereal disease. We all talk about it, but nobody admits to having it.'

The solution accuracy, under the influence of the competing effects of discretization and truncation error, is shown in figure 5.2.

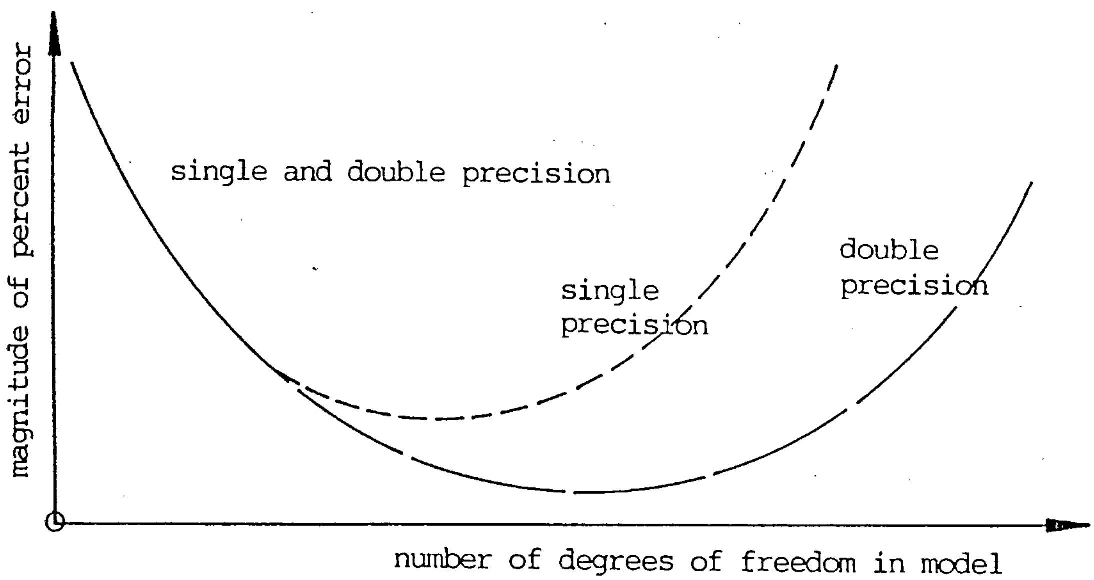

fig. 5.2 - Discretization and truncation effects on accuracy [Cook, 72]

5.3 Numerical ill-conditioning of system equations

A main source of error arises from the poor conditioning of the system of equations. Equations $\underline{K}\ \underline{d} = \underline{f}$ are termed "ill-conditioned" if small changes in $\underline{K}$ or $\underline{f}$ may lead to large changes of coefficients in the solution vector $\underline{d}$ [72]. This would suggest that in some way the inverse of $\underline{K}$ is "large".

Ill-conditioning may be caused by the physical situation, such as the axially stiff nature of the marine riser (combined with its flexible bending nature). The effects of poor conditioning may be worsened by numerical factors, such as the severity of the truncation error, which depends on the precision at which the computer is operating.

A measure of the conditioning of a coefficient matrix $\underline{K}$ is the condition number $C(\underline{K})$. $C(\underline{K})$ is defined as [88]:

$$C(\underline{K}) = \|\underline{K}\| \; \|\underline{K}^{-1}\|$$

where $\|\bullet\|$ indicates the ∞-norm
$\underline{K}$ is the stiffness matrix
$\underline{K}^{-1}$ is the inverse of $\underline{K}$

where: $$\|\underline{K}\| = \max_{1 \le i \le n} \sum_{j=1,n} |K_{ij}|$$

It should be noted that there is some confusion in the literature as to the meaning of the condition number. The condition of $\underline{K}$ should actually be represented by a matrix representing the sensitivity of the vector $\underline{d}$ to small changes in the vector $\underline{f}$ [88], but it is generally simpler to use a single value, as defined above. This value is an upper-bound of the actual matrix condition.

Other types of matrix norms, or the ratio of the largest to the smallest eigenvalue of $\underline{K}$, may be used as a measure of the condition [72,85,88,89]. Attempts [85,88] have been made to scale the matrix $\underline{K}$, to form $\underline{K}'$, by pre- and post-multiplying $\underline{K}$ by constants. The condition of $\underline{K}'$ is the same as for $\underline{K}$. The scaling factors may be chosen so as to minimise the condition number, which is an upper-bound of the actual condition.

If the coefficients of $\underline{K}$ are presented with d digits in the computer, computed results are accurate to s digits, where

$$s \approx d - \log C(\underline{K})$$

which is the worst case [72,89].

5.3.1 Effect of element numbering sequence on conditioning

The effect of the conditioning of a system is illustrated in the following example, from Haggenmacher et al. [90], where the effect of the elemental numbering sequence on the condition is illustrated:

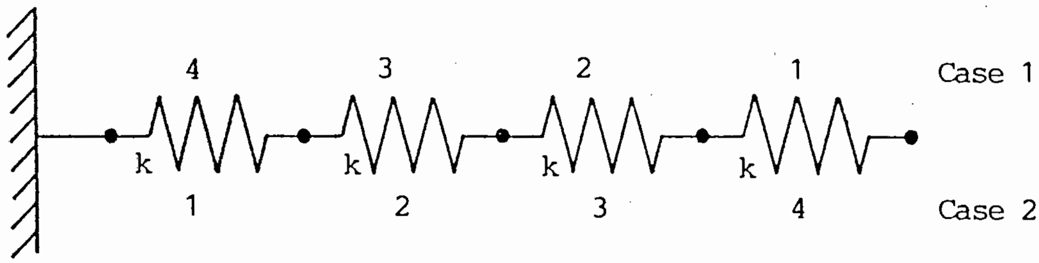

case 1: $$[\underline{K}] = \begin{bmatrix} k & -k & 0 & 0 \\ -k & 2k & -k & 0 \\ 0 & -k & 2k & -k \\ 0 & 0 & -k & 2k \end{bmatrix}$$

$$\text{Pivot } [\underline{p}] = \begin{bmatrix} k \\ k \\ k \\ k \end{bmatrix} \qquad [p_{ii}/K_{ii}] = \begin{bmatrix} 1 \\ 1/2 \\ 1/2 \\ 1/2 \end{bmatrix}$$

worst pivot ratio =1/2, independent of n

case 2: $$[\underline{K}] = \begin{bmatrix} 2k & -k & 0 & 0 \\ -k & 2k & -k & 0 \\ 0 & -k & 2k & -k \\ 0 & 0 & -k & k \end{bmatrix}$$

$$\text{Pivot } [p] = \begin{bmatrix} 2k \\ 3k/2 \\ 4k/3 \\ k/4 \end{bmatrix} \qquad [p_{ii}/K_{ii}] = \begin{bmatrix} 1 \\ 3/4 \\ 2/3 \\ 1/4 \end{bmatrix}$$

worst pivot ratio = 1/4, decreasing to 1/n, where n is the dimension of the problem

The pivot ratio, p_{ii}/K_{ii}, is a direct measure of the computational error in the solution of the system of equations [90]. A pivot ratio of zero would indicate singularity. Each negative power of ten for the pivot ratio represents an accuracy loss of that many leading digits in the solution. A pivot ratio of one means that the degree of freedom is totally independent, while a pivot ratio of zero means total dependency.

The above example indicates that the choice of pivot, or the elemental numbering sequence, is important. One should always number from the region of flexibility toward the region of stiffness in the model [Melosh, 72].

In the riser problem, the elements are numbered from the free end to the fixity. Numbering the elements from the fixity to the free end, in the analysis of the standard riser configuration with ABAQUS, resulted in the analysis aborting in the second step, owing to numerical difficulties, with initial residuals of between 7 and 18 orders of magnitude greater. J. Zugg [91] solved convergence problems that her solution was experiencing, in her analysis of marine pipe laying with ABAQUS, by simply altering the ordering of the elements in her model.

It is the decay of the diagonals, as reflected by the pivot number, and not the magnitude of the diagonal coefficients, that is of significance. Small pivots and large multipliers do not necessarily provoke large error [72].

5.3.2 Effect of large stiffness ratio on conditioning

The combination of high axial stiffness and low bending stiffness found in most riser problems leads to diagonal decay and ill-conditioning of the stiffness matrix. The stiffness ratio is the ratio of the axial stiffness, AE, to the bending stiffness EI.

Consider the following problem:

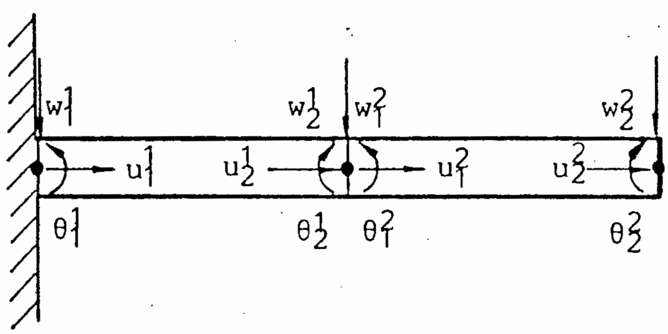

Element stiffness matrix for Euler beam:

$$
[\underline{k}] = \begin{array}{c} \begin{array}{cccccc} u_1 & \Phi_1 & w_1 & u_2 & \Phi_2 & w_2 \end{array} \\ \begin{bmatrix} 12EI/h^3 & 6EI/h^2 & 0 & -12EI/h^3 & 6EI/h^2 & 0 \\ & 4EI/h & 0 & -6EI/h^2 & 2EI/h & 0 \\ & & AE/h & 0 & 0 & -AE/h \\ & & & 12EI/h^3 & -6EI/h^2 & 0 \\ & \text{symmetrical} & & & 4EI/h & 0 \\ & & & & & AE/h \end{bmatrix} \end{array} \begin{array}{c} u_1 \\ \Phi_1 \\ w_1 \\ u_2 \\ \Phi_2 \\ w_2 \end{array}
$$

for case 1 $\quad h = 1, \; EI = .5, \; AE = 10, \quad C(\underline{K}) = 420$

for case 2 $\quad h = 1, \; EI = .5, \; AE = 1000, \quad C(\underline{K}) = 42\ 000$

where $C(\underline{K})$ is calculated as defined in section 5.3

It may be seen from the above example that an increase in the axial stiffness increases the ill-conditioning of the system. This trend is illustrated in figure 5.3, which shows how the initial residuals increase for larger values of axial stiffness of the riser, in a typical catenary riser analysis on ABAQUS, for a typical analysis step. The other riser configurations show similar trends.

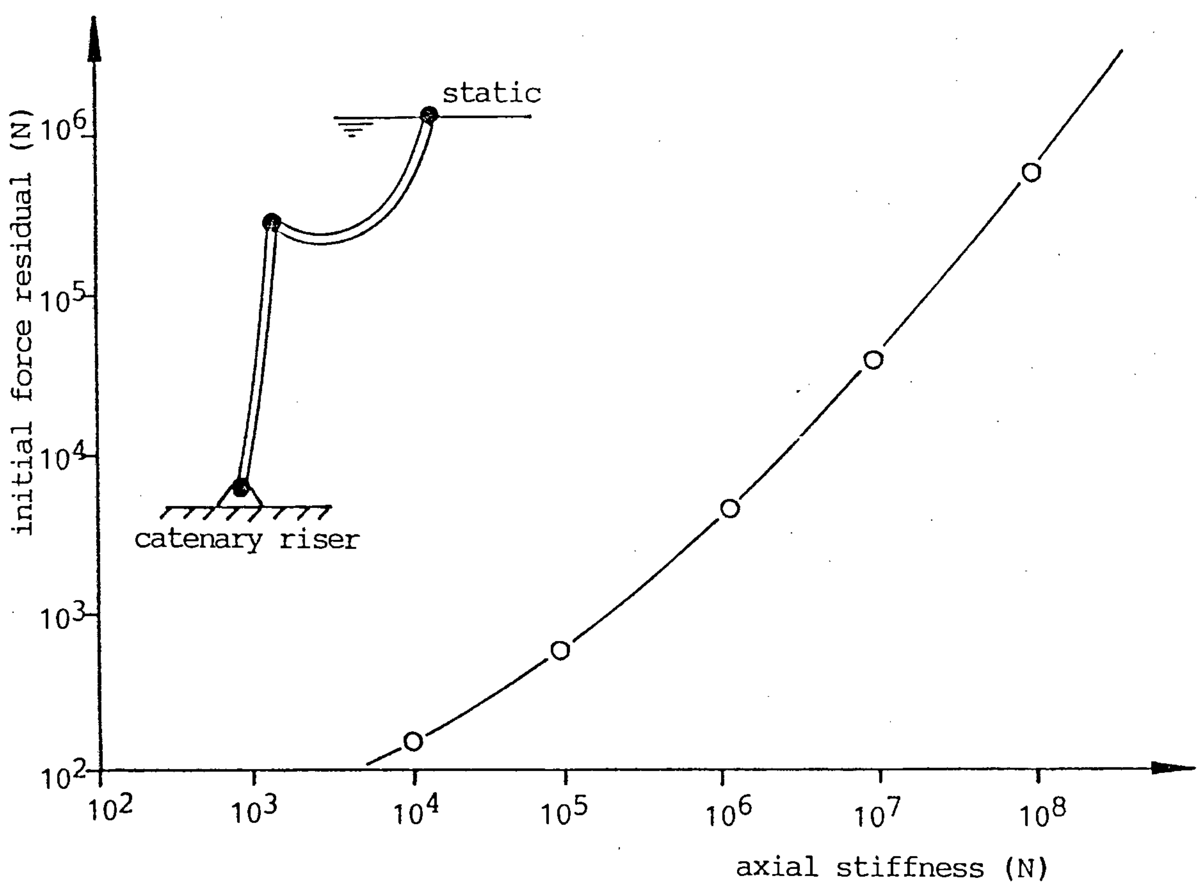

fig. 5.3 - Effect of axial stiffness on convergence rate.

Changing the bending stiffness appreciably, by several orders of magnitude, does not change the deformed shape (to four significant figures). The bending moment carried by the riser does, however, depend on the bending stiffness, and is in fact directly proportional to it. This has been verified with ABAQUS, and with the linearised riser model, RISER, developed in section 6.

A major cause of ill-conditioning in the system of equations is a region of high stiffness supported by a region of low stiffness [72]. This shifts the essential information to the end bits of the coefficients during the solution of the system of equations, where they may be lost by truncation and round-off. This is evidenced by the small pivot ratios of such a system, as described in section 5.3.1, where some of the pivots become very small. An example of this is the articulation in the catenary configuration, which was modelled successfully using a short, very flexible element.

5.3.3 Other sources of ill-conditioning

Other sources of poor conditioning include too few supports, an increased number of elements, and sudden changes in element size within the model [72]. The order of the governing differential equations and the dimension of the problem also play a role in deciding the condition number. Smaller elements are more flexible than large elements owing to the constraints of the interpolating function, and therefore a sudden change of element size in the model may produce larger condition numbers. $C(\underline{K})$ is proportional to [72]:

$$(h_{max}/h_{min})^{2m-1} . N^{2m/n}$$

where - h_{max} and h_{min} are the maximum and minimum element lengths in the model.

- 2m is the order of the governing system of differential equations.
- N is the number of elements in the model.
- n is the dimension of the problem, 2 for plane problems

In the catenary configuration, the effect on the convergence rate of modelling with ABAQUS in three dimensions was unclear, with some portions of the 3-D analysis requiring more iterations, and others, less.

The effect of changing the number of elements on the convergence of the solution was considerable, as is shown in figure 5.4. This figure is typical of all of the riser analyses conducted with ABAQUS. These effects are reflected in the total computational cost for these runs as well. The curve flattens off at higher values of N owing to the effect of the improved accuracy of the smaller elements. This effect is illustrated in figure 5.2, and will be discussed in section 5.6.2.

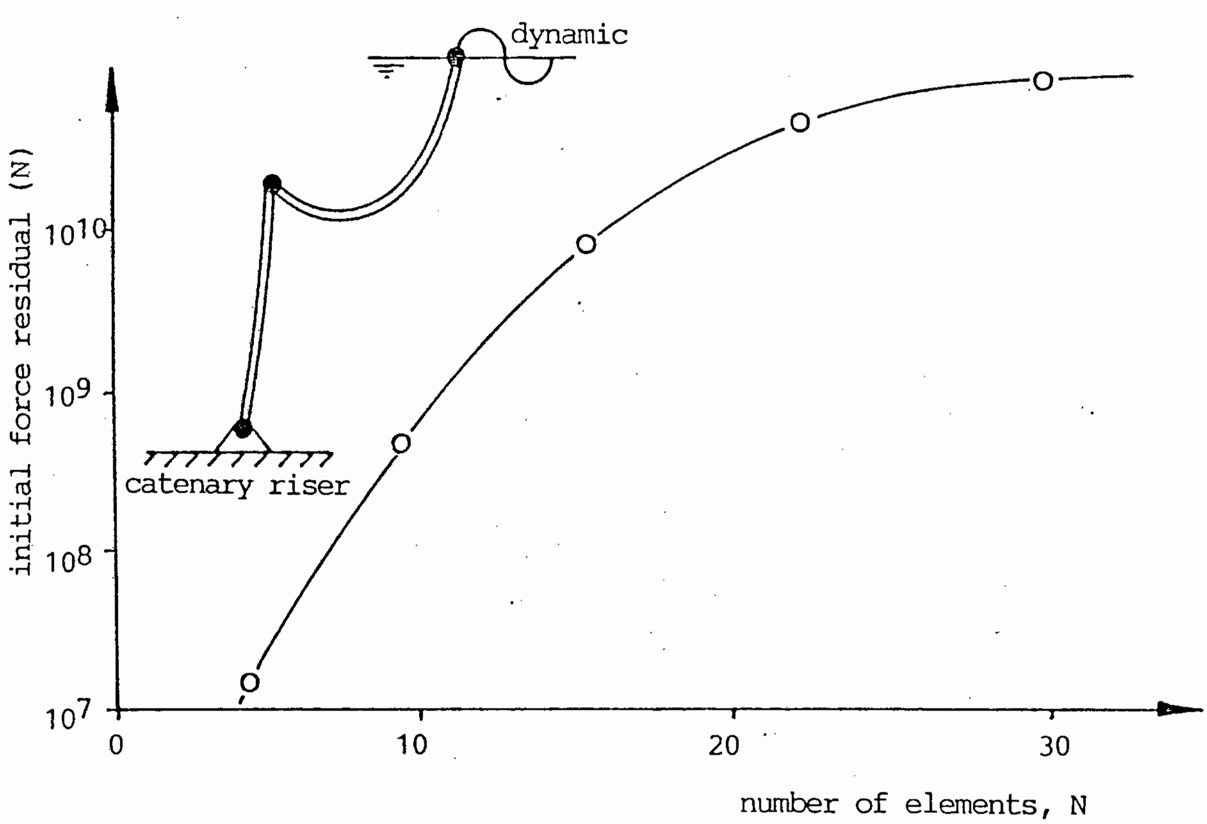

fig. 5.4 - Effect of the number of elements on convergence

The choice of the basis functions also influences the condition of the system, although orthogonal polynomials yield fairly well conditioned matrices [92]. Strang [93] shows that the condition number increases slightly with the order of the polynomial basis function, but that the improved accuracy of the higher order elements outweighs this effect.

To quote J. W. Tukey, "If a thing is not worth doing, it is not worth doing well" [88]; if a system of equations is very poorly conditioned, it is better to reformulate the problem in some way rather than make "heroic" efforts to extract a good solution [72]. This may be done by resequencing the elements, using fewer elements, varying the loading history, using hybrid elements, etc.

5.4 Dynamic riser modelling

For the direct time integration of the system equations in the dynamic analysis, ABAQUS employs the α-, or Hilber-Hughes-Taylor operator, which is a modified Newmark method [75,86]. The H-H-T operator is an unconditionally stable, implicit scheme, which has numerical damping capabilities. This operator is designed for "inertial" problems, such as risers where wave propagation effects are negligible.

The size of the incremental step in a dynamic run is decided by modelling considerations as well as numerical concerns. McNamara [74] recommends that a time step of up to a two-hundredth of the period of the highest modal frequency of interest is necessary for accurate results in nonlinear problems. He also maintains that accuracy, and not stability, is the critical factor in most nonlinear problems, even for conditionally stable algorithms.

The effect of altering the time step in the dynamic analysis was not investigated. The automatic time stepping option in ABAQUS allows the time step to vary within the analysis, and thus the solution errors may be restricted to the user-defined tolerances.

5.4.1 Error monitoring in the dynamic analysis

ABAQUS uses the half-step residual of each dynamic step to monitor the accuracy of the solution, and to adjust the time step in the automatic time stepping mode. The H-H-T operator ensures equilibrium, to within the user defined tolerances MTOL and PTOL at the end of each time step, but not within the time step. The degree to which the system is not in equilibrium (in the d'Alembert sense) within the time step is a measure of the error of the algorithm. ABAQUS uses the equilibrium residual at the half step as this measure. In the automatic mode the program can vary the time step until the half-step residual is within a user-defined tolerance, HAFTOL.

The growth and decay of the half-step residual in a typical riser dynamic analysis is shown in figure 5.5.

In figure 5.5, the large initial residuals are shown. The time step is automatically reduced to overcome this, and later increases as the residuals decrease. The residual oscillates owing to the forced displacement oscillation at the top node. The figure represents two full cycles of this excitation. The mean residual decreases as the system is damped, to the steady-state value.

There appears to be a limit to which the initial half-step residual in the dynamic analysis can be reduced, and once this limit has been reached, decreasing the time step has no further effect. A large HAFTOL must be used initially, which may be decreased after a *RESTART.

In the transient portion of the analysis, spurious higher order modes are generated [7,15,18,32]. This problem is more severe in the case of the standard riser configuration, which is very stiff owing to the large top-tension. These higher order modes cause large velocities and accelerations in the initial portions of the analysis. Large accelerations cause large forces, and hence the initial force residuals may be high.

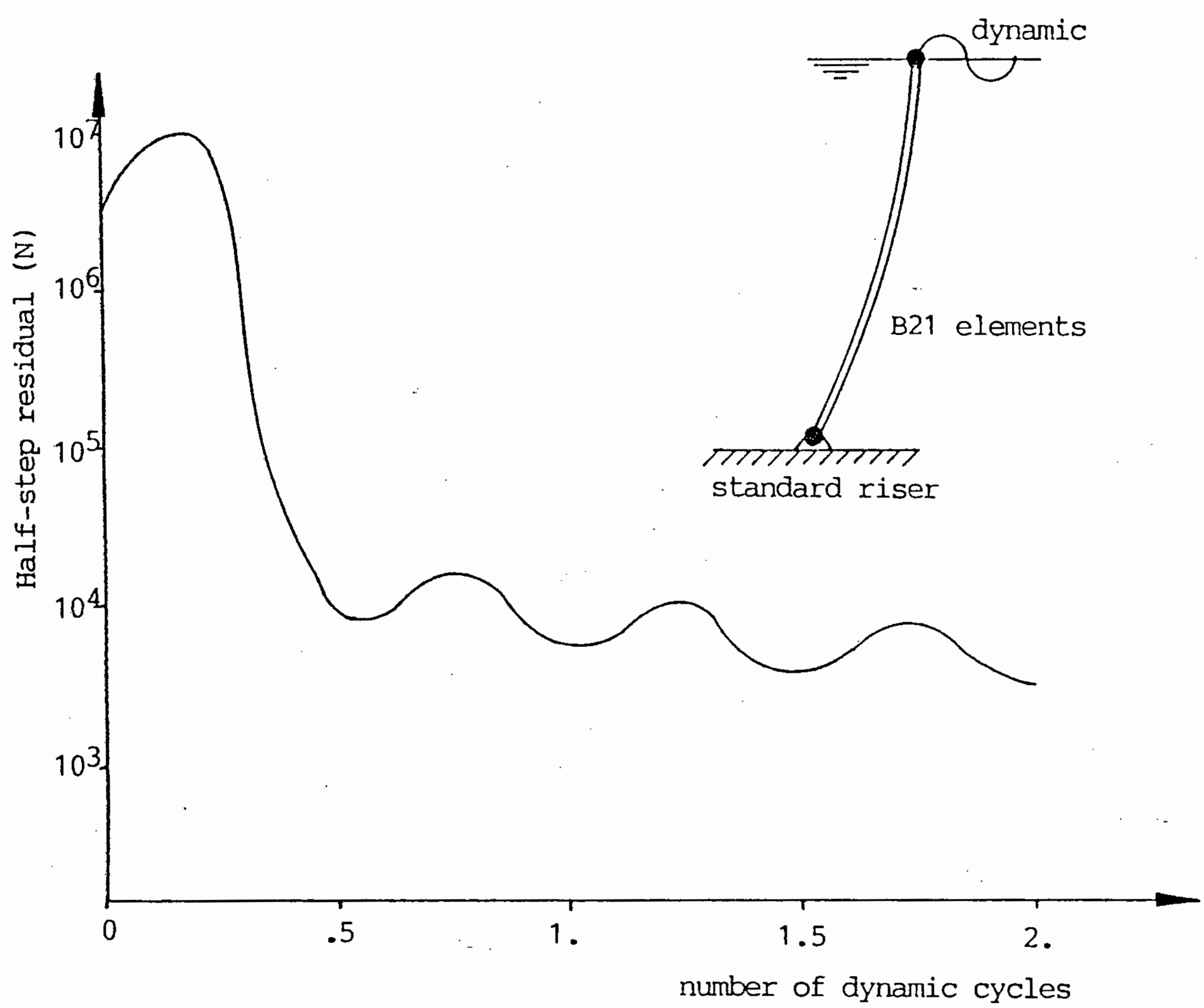

fig. 5.5 - Half-step residual for a typical dynamic analysis

The Hilber-Hughes-Taylor direct integration operator used in ABAQUS has an artificial damping coefficient, α, which is user-defined. The use of α at its default value was found sufficient to filter out the spurious, higher-order modes. In order to overcome these initially high residuals, which are typical of this type of problem, one must initally set the tolerances high. If necessary, the tolerances may be refined with a *RESTART after the residuals have decreased.

5.5 Static riser modelling

In the static analysis, the riser is initially highly flexible, and unstable, in the sense that a small load produces a large displacement. After some loading is applied, the axial stresses stabilise the system, and convergence is more rapid [29]. This effect is illustrated in figure 5.6, where the initial residuals are large at the start of a step, and decrease as the system stabilizes.

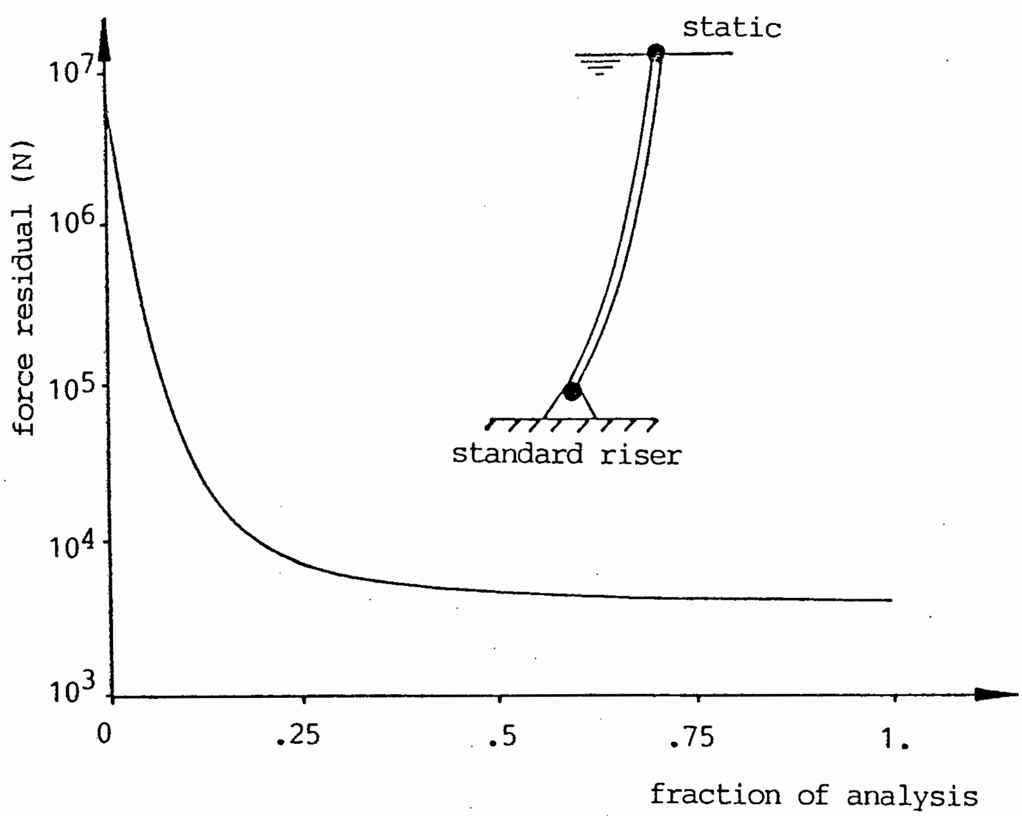

fig. 5.6 - Force residual for a typical static analysis

An axial tension, which has the effect of stiffening the system, thus stabilizes the static solution. The relationship between the axial tension and the initial residuals of a typical standard riser configuration is shown in figure 5.7. This axial tension may have an adverse effect on the dynamic solution, where problematic high frequency modes may be generated.

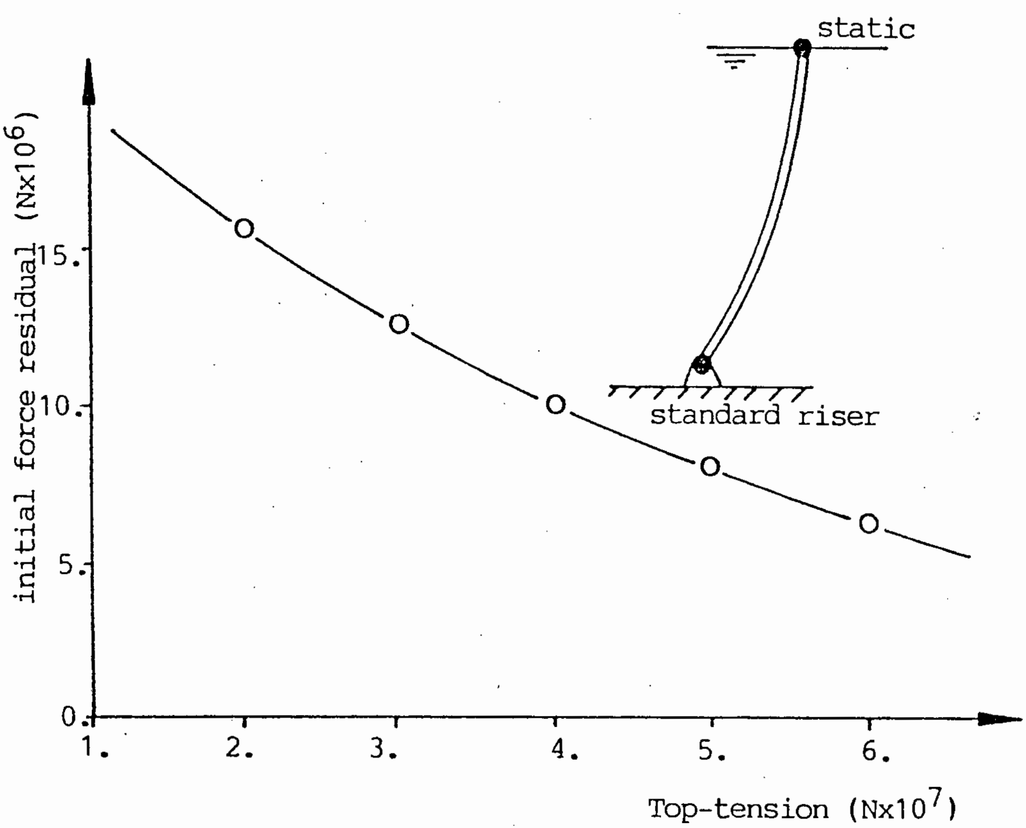

fig. 5.7 - Effect of axial tension on convergence

The application of this stabilizing tension to marine riser analysis, with ABAQUS, may be seen in the following examples. It was found that applying the top-tension in the standard riser configuration in the first step, and displacing the top-node in the second, decreased the computional time by more than 50%, as compared to applying the tension and moving the node in one step. The maximum residuals also decreased dramatically, from 10^{24} to 10^{5} for the force residuals, and from 10^{7} to 10^{1} for the displacement residuals.

In the catenary configuration, it was found that displacing the central node of the catenary portion of the model in the first step speeded up the convergence, because if the self-weight was applied directly, the force residuals were very large, of the order of 10^{20}, and convergence problems were encountered. The reader is referred to section 2 for more information on these modelling techniques.

5.6 Effect of element type on convergence and accuracy

Other effects that influence the convergence rate and accuracy of the solution are the number and type of elements. ABAQUS has various types of elements in its library, including linearly and quadratically interpolated shear beams, B21 and B22, and a cubically interpolated Euler beam, B23. These elements are designed for two-dimensional analysis. Equivalent three-dimensional elements, B31, B32 and B33, are available. Hybrid versions, B21H, B22H, B23H, B31H, B32H and B33H are also available.

5.6.1 Choice of the order of element

McNeal [94] indicates that there has been a long controversy regarding the choice of the order of the element. He quotes Zienkiewicz as saying that a significant cost saving may be achieved by using the fewer higher order elements necessary to achieve a given accuracy. However, the reduced number of higher order elements might be insufficient to represent all of the local geometries. This was found to be true in the case of the marine riser.

The results of the static analysis showed little dependence on the type of element used, in terms of accuracy, with the displacement results agreeing to within .02%, and the force results the same to four places. In the dynamic analysis the B21 elements did not perform as well, the displacement results varying by as much as 2%. The improved accuracy of the higher order elements did manifest itself in the rate of convergence, and this is shown in figure 5.8.

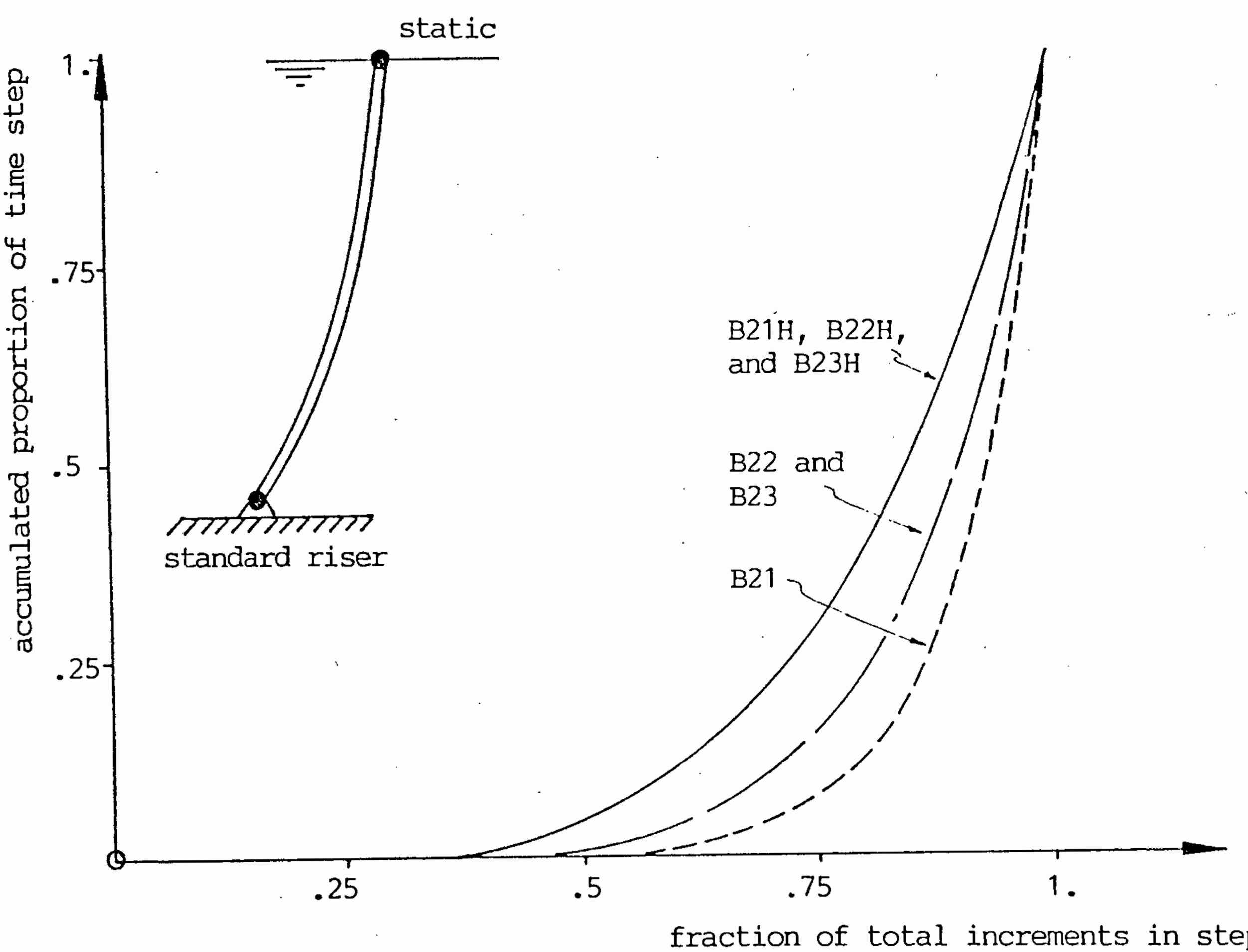

fig. 5.8 - convergence characteristics of various elements

In figure 5.8 one can see that the hybrid elements have the fastest convergence rate, followed by the cubic and quadratic elements, and lastly, the linear element. The computational costs of typical static analyses of the standard riser is illustrated in figure 5.9, so as to compare the different elements that are available with ABAQUS.

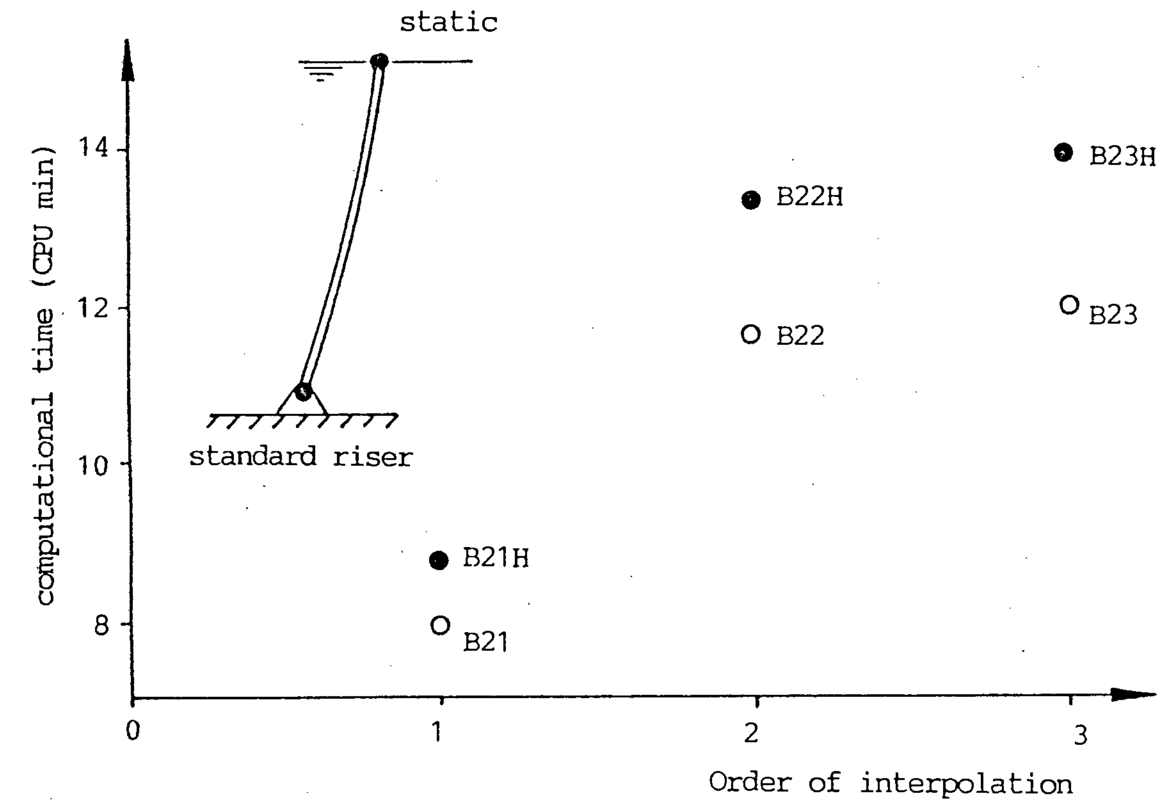

fig. 5.9 - Effect of the order of the element on computational cost

Typically, the hybrid beams were 20% more expensive than the equivalent standard elements.

5.6.2 Choice of the number of elements

In the riser problem, it was found that where the force results changed rapidly, the displacement results did not, and where the displacement results changed rapidly, the force results did not. Thus it was decided, in order to resolve both the displacement and stress results, to use a mesh of equally sized elements.

It was found that the resolution of the displacement and stress results was the most important criteria for deciding element size, not accuracy. For an equal number of elements the higher order elements were considerably more expensive than the linear elements (by up to 200%).

McNeal [94] shows that the cost of generating the stiffness matrix is proportional to $N_g^2 . N_i$ where N_g is the number of connected nodal points, and N_i the number of internal integration points. The cost of processing a higher order element is also larger.

Increasing the number of elements in the model not only increases the resolution of the output, but also increases the accuracy of the solution, at the cost of slower convergence, and greater computational expense. Numerical experiments on the marine riser using ABAQUS show an approximately linear relation between computer cost and number of elements. As the number of elements in the model increases to infinity, the discretization error converges to zero, but the truncation errors diverge. This effect is shown in figure 5.2.

The requirements for this type of convergence, or h-convergence, are as follows: the displacement field within the element must be continuous; the element must be able to assume a state of constant strain; the element must be capable of rigid-body motion; and elements must be compatible. These conditions are satisfied for the beam elements in ABAQUS. The convergence of the solution as the order of the element increases is called p-convergence, and is faster than h-convergence [72]. For accuracy alone, it is thus better to use fewer, higher order elements.

Carey et al. [95] show that the error of the finite element method is proportional to h^{μ}, where h is the element size, and $\mu = \min(k + 1 - m, r - m)$, where k is the degree of the largest complete polynomial in the assumed displacement field, 2m is the order of the governing differential equation, and r is the order of the solution to the governing differential equation, u. If u is regular, so that r - m is large, one may increase the convergence rate by increasing the order of the complete polynomials, k. If the solution is so irregular that $r - m < k + 1 - m$, the rate of convergence is completely unaffected by k.

5.6.3 Hybrid beam elements in ABAQUS

ABAQUS has in its library a full range of hybrid beam elements. These elements have been developed in an attempt to alleviate the numerical problems that occur in this type of problem, that of ill-conditioned, thin beams. These elements use mixed methods of formulation, involving both assumed displacement and force fields. Mixed formulations usually use Lagrange multipliers to impose constraints.

A special type of mixed formulation is the hybrid formulation, which is based on an assumed stress field in the domain, and an assumed displacement field on the boundary. These two assumptions are independent, and hence the nodal degrees of freedom are displacement, and these elements may be joined to any standard element [72,95].

Henshell [96] has found that hybrid elements generally give better results than standard elements for a course mesh, but as the mesh becomes more refined, the advantages diminish.

The meaning of the words "mixed" and "hybrid" are not standardised, but the above interpretations seem to be the most generally accepted.

5.6.3.1 Performance of hybrid beams

ABAQUS's hybrid beams have their advantages and disadvantages. In a quasi-linear analysis such as the standard riser configuration, where the displacements are not too large, the hybrid beams do not perform as well as the standard elements. The convergence rates for the two types are similar, but the computational effort of the hybrid beams is up to 75% greater. These problems may be described as "force dominant", in that it is the force convergence that is the slowest, and the extra displacement iterations of the hybrid beam are wasted.

In "displacement dominated" problems, such as the catenary and hanging configurations, which have significant geometric nonlinearities, the hybrid elements fare better, converging faster, and costing about the same as the standard elements, and in the case of the linear beam, costing 25% less. In these problems the displacement convergence is slower than the force convergence.

This is evidenced by the fact that the force residuals are very low by the time that the displacement residuals are within tolerance for the hybrid beams. The standard elements do not iterate the displacements, and so the force residuals may still be quite large at the end of an increment (just within tolerance). The initial force residuals for the hybrid beams are typically several orders of magnitude less than those for the standard elements in this type of problem.

The accuracy of the solution does not improve with the use of the hybrid elements, only the convergence characteristics do. The accuracy is more affected by the order and number of elements in the model.

A disadvantage of the hybrid element is that, in this version of ABAQUS, (4-5-169), the displacement tolerances are internal to the program, and may not be adjusted by the user. This means a certain loss of versatility in tackling some of these problems, where the residuals are high for some parts of the problem, and low for others.

The *AQUA options in ABAQUS caused convergence problems in the displacement dominated problems such as the catenary and the hanging configurations, particularly in the dynamic analysis. These problems were more severe in the case of the hybrid beams, and are caused by an error in ABAQUS that should be corrected in version 4-5-170 [97].

The standard elements were not as affected by the *AQUA convergence problems, because it was the displacement residuals that were large. The standard elements do not check the displacement residuals for convergence, while the hybrid beams do, and consequently only the hybrid beams experienced difficulties.

The results for the standard elements were questionable, owing to the large displacement residuals. To overcome these problems, small time steps had to be used, along with high initial tolerances, modified in a *RESTART. Care had to be taken to ensure that the initial conditions for the dynamic analysis were taken from the static equilibrium position, as this reduced the initial residuals, and convergence was faster.

5.6.3.2 Interpretation of element stress and displacement results

Thin beams are prone to shear locking if full numerical integration is used. This is because the bending energy depends on the cube of the element thickness, while the shear energy depends linearly on the thickness. As the beam becomes thinner, the shear term dominates, and the beam "locks". This problem may be alleviated by under integrating the element.

The standard element formulation is too stiff, owing to the constraints of the assumed displacement field and, in the case of the hybrid beams, the assumed force field. Reduced integration has the effect of relaxing the stiffness matrix, which may be beneficial, but spurious zero, or low energy modes may occur.

Spurious modes may occur if the element is "rank deficient". Spurious modes do not occur with the standard beam elements. For example, the B22 element has 9 degrees of freedom (3 per node), and hence its order is 9. There are 3 strain terms per Gauss point, and three rigid body modes, giving the element a rank of 9. Thus rank $\leq$ order, and no spurious modes occur.

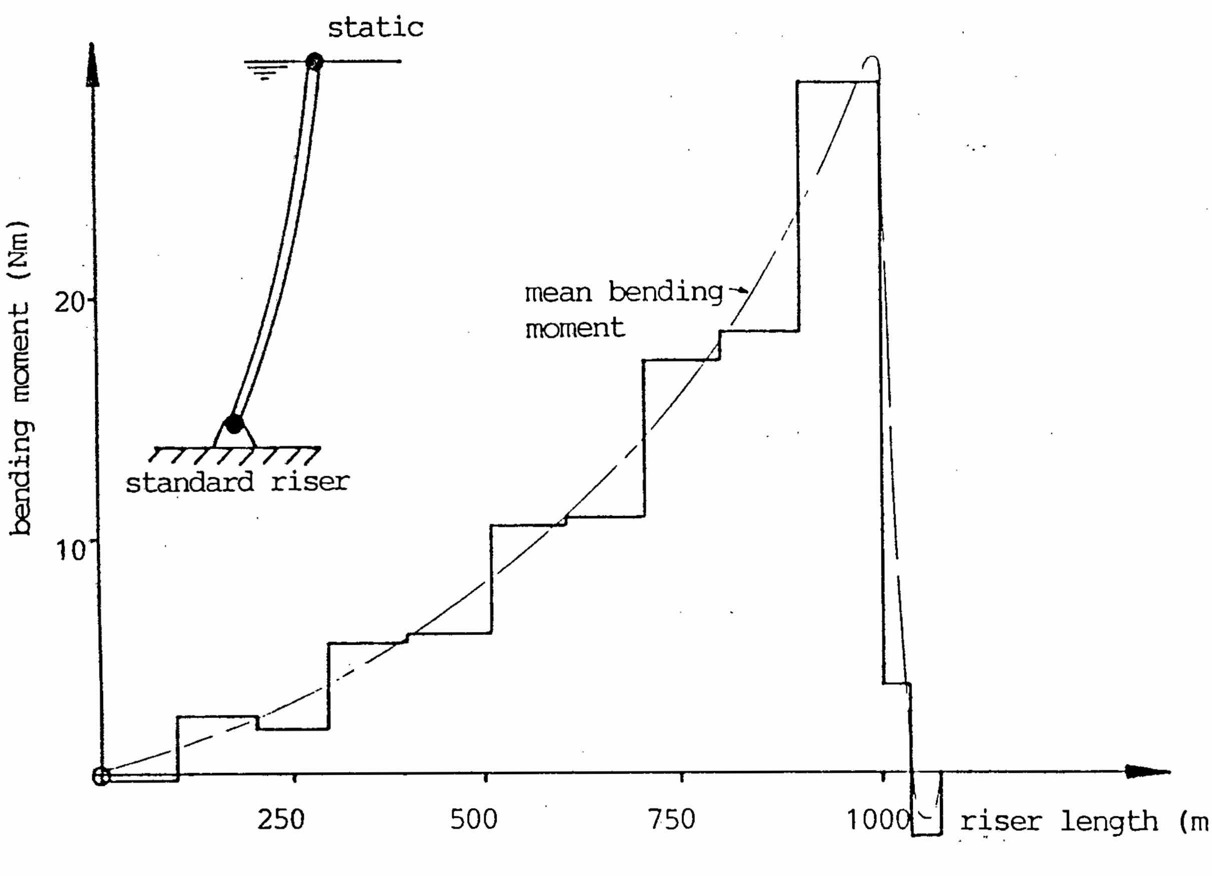

fig. 5.10 - bending moments in riser, using hybrid elements

Oscillatory stress results were observed when using the hybrid elements, as is shown in figure 5.10. In this figure, the bending moment is plotted against length for the standard riser configuration. The mean of the hybrid stress results agrees with the results of the standard elements, which do not have these oscillatory modes. The negative bending moments are due to the top 50 m of the riser being above the water line.

At first it was thought that the oscillatory behaviour shown in figure 5.10 might be a "spurious mode" in the stress results, equivalent to the displacement spurious modes that may occur with the standard elements, since the element forces are interpolated in much the same way as the displacement field.

An analysis similar to that carried out in a previous paragraph on an hybrid beam element is difficult, as it is unclear whether or not the notions of rank and order are general to all formulations. Spurious displacement modes are not apparent in the hybrid beam displacement results, and no mention of spurious stress results in mixed elements could be found in the literature.

P. Burger [103] of Hibbitt, Karlsson and Sorensen Inc. has indicated that this behaviour may be caused by an error in the stress processing subroutine of ABAQUS. This error is not serious, in that the mean force result agrees with that of other standard elements. These errors are to be corrected in version 4-6 of ABAQUS [97]

A mesh that gives good displacements may be too coarse to yield accurate stresses [72], and care should be taken with the interpretation of the stress results.

5.7 Marine riser modelling recommendations with ABAQUS

The following modelling guidelines were found useful:

i) Use the smallest number and simplest type of elements compatible with the stress gradients and structure geometry [72]. Equal length linear elements were found to be the best in terms of cost, stress and displacement representation.

For the force dominated problems, such as the standard riser configuration, the B21 elements performed best in terms of cost, accuracy and convergence characteristics. For the displacement dominated problems, such as the catenary and hanging configurations, the hybrid beam element was best. Reducing the number of elements in the model can drastically reduce the computational cost, and improve the condition number and hence the convergence rate.

ii) Mesh grading should be done in such a way that abrupt changes in element size are minimised [72]. This reduces the condition number of the system of equations.

iii) If a direct-integration scheme is used, masses less than approximately 1 000^{th} of the average mass should be eliminated by combining them with other masses [72]. Numerical difficulties may arise, owing to round-off, if this is not done.

iv) A mesh that gives good displacement results may be too coarse to yield accurate stresses [72], and care should be taken in the interpretation of the stress results.

v) A useful concept in developing a reliable finite element model is that of modular design. In ABAQUS, this is enhanced by the "steps" used to define the model history. This concept is more important as the model becomes more complex.

For example, in the catenary configuration, the catenary portion of the model was developed before the rest of the model. In all the models the static analysis was completed before dynamic runs were attempted.

vii) The elements should be numbered toward the fixity, since this increases the pivot ratio and improves the convergence rate.

viii) If possible, the analysis should be conducted in two dimensions. Assuming the current and waves co-planar is a conservative assumption, by approximately 20% [33]. A two-dimensional analysis is cheaper to run than a three-dimensional analysis. The literature [31] reports possible numerical difficulties in conducting three-dimensional analyses.

ix) In the static analysis, it was found that pre-tensioning the riser stabilised the system, and convergence was faster. This axial tension might have a detrimental effect on the dynamic analysis.

x) This class of problem typically produces high residuals at the beginning of a step. The tolerances must be set high to overcome these initial residuals, but may be refined with a *RESTART after this. The automatic, incremental stepping option is useful in coping with this type of problem where the residuals fluctuate, although the initial residuals are not always that sensitive to changes in time step.

xi) When developing the model, it is better to begin with large tolerances, and after the first run, once the magnitude of the forces and residuals is known, to refine the tolerances.

xii) If convergence problems are encountered at the beginning of a step, the loads or kinematic boundary conditions may be ramped on. This technique has been used successfully in the dynamic analysis using ABAQUS, but was not necessary in the static analyses. In the dynamic analysis the damping coefficient, α, in the Hilber-Hughes-Taylor operator, may be ajusted in order to reduce the convergence problems.

xiii) It is expensive to drive the *AQUA options in ABAQUS, as several nested iterations are required for the solution. The reasons for this will be dealt with in section 6, where the geometrically linearised model, RISER, is developed. Convergence difficulties associated with the Morison drag in ABAQUS may be due to an error in ABAQUS [97], but this should be corrected in version 4-5-170. The use of Stokes' wave theory may cause errors, which should be corrected in version 4-5-188 [97].

6. SMALL DISPLACEMENT FINITE ELEMENT RISER MODEL

6.1 Statement of problem

The governing equations of the simplified system, bearing in mind figure 6.1, and the assumptions discussed in sections 1 and Appendix B, are as follows:

$$f_x = m_x \frac{\delta^2 x}{\delta t^2} + \frac{\delta^2}{\delta y^2}\left(EI \frac{\delta^2 x}{\delta y^2}\right) - \frac{\delta}{\delta y}\left((T_e)\frac{\delta x}{\delta y}\right) - (W_e)\frac{\delta x}{\delta y} \quad \text{.........(6.1)}$$

term 1   term 2   term 3   term 4

where:

$$f_x = C_m \mu_o \frac{\pi d_o^2}{4}\left(a_w - \frac{\delta^2 x}{\delta t^2}\right) + C_d \mu_o \frac{d_o}{2} \$\left(v_c + v_w - \frac{\delta x}{\delta t}\right)\left(v_c + v_w - \frac{\delta x}{\delta t}\right)^2 \quad \text{.(6.2)}$$

term 5   term 6

$$T_e = T + (p_i A_i - p_o A_o) \quad \text{...............................(6.3)}$$

$$W_e = (\mu_r (A_o - A_i) + \mu_i A_i - \mu_o A_o).g \quad \text{.....................(6.4)}$$

with boundary conditions:

$x = 0$ at $y = 0$

$\frac{\delta x}{\delta y} = 0$ at $y = H$

with initial conditions specified (these will be discussed in detail later).

These equations are similar in form to those employed by Young et al. [83], Kirk [20], Bernitsas [6], Dareing et al.

[28], Huang et al. [30], Kim et al. [44], McIver et al. [38], Patel et al. [22] and Chakrabarti et al. [47].

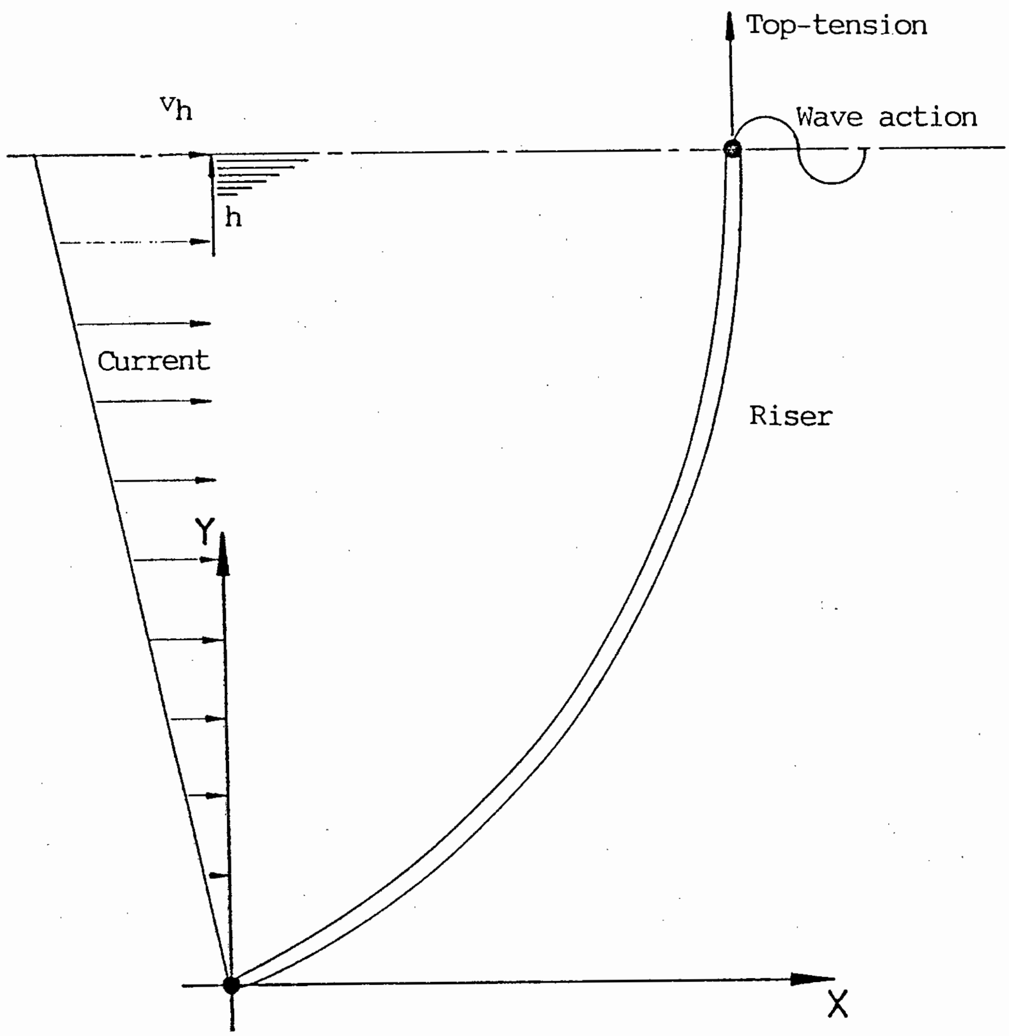

fig. 6.1 - Riser system to be modelled

The most important simplifications inherent in the above equations are that they are restricted to two dimensions, and that they are geometrically linear. As a result, movement in the x and y directions is uncoupled, and the above equations have only x as their dependent variable, which represents the transverse motion of the riser. The uncoupled, axial behaviour of the riser may easily be incorporated into the model at a later stage. The geometric linearity would suggest limitations in the application of the above equations, and these limitations will be discussed in section 6.4.

The nonlinear nature of the drag force, term 6, equation 6.2, has been preserved, although linearisation techniques are well documented [22-25,38]. This was done because the effect of the uncertainty of the drag coefficient, C_d, in this term, was still to be investigated, and so it was deemed unwise to modify this term. Also, some of the linearisation techniques described in the literature involve iterative techniques anyway, so it was decided to leave the drag term nonlinear.

6.2 Simplfying assumptions

The following assumptions were made in order to simplify the model formulation:

i) The effects of the drill-string were neglected. The drill-string has the effect of increasing the total weight of the system, as well as providing contact loads with the riser. The error owing to this assumption is negligible [6].

ii) The drilling-mud's velocity is small, and so the centrifugal and Coriolis forces may be neglected, as may the frictional effects of the drilling mud [6].

iii) All local effects such as contact, impact and stress concentrations are neglected. These effects do not have a significant effect on the overall mechanical properties of the system, and should be the subject of a detailed design, in which case, shell theory might be necessary.

iv) The riser material is assumed to be homogenous, isotropic, and linearly elastic.

v) Variations in the fluid with depth, such as viscosity, density, and temperature, are neglected.

vi) All three-dimensional effects are neglected. Nolte [33] maintains that assuming that waves and current are co-planar is conservative.

vii) Loading effects, such as wind loading, residual loads and vortex excitation, are neglected. An increased drag coefficient may be assumed, to account for the increased drag owing to vortex excitation, although the resonant effects will be neglected.

viii) Drag and mass coefficients, C_d and C_m, will be assumed constant.

ix) The effects of partially submerged elements will be neglected.

x) The dependence of the hydrodynamic loads on the inclination will be neglected. This effect is usually accounted for by using the area of the riser projected onto the vertical plane, but this requires a further iteration. For small displacements this effect can be neglected, in accordance with the assumptions made in Appendix B.

xi) Term 4, equation 6.1, will not be updated for every dynamic step, as this would involve an extra iterative loop for every step, which would be expensive. The slope variations about the mean should be small for the dynamic analysis, and therefore not updating term 4 should not cause large errors.

All of the above assumptions are made in order to simplify the development of a prototype model, and may be included in a more sophisticated model at a later stage.

6.3 Description of finite element program RISER

A version of a small, finite element program, ONEDEE, based on methods and notation developed by Hinton et al. [98], was available. This program was applicable to linearly elastic, plane truss problems, and was implemented in Fortran on a Bondwell 39 micro computer by Brown [99]. Extensive modifications were necessary to facilitate the modelling of marine risers. The modified version is called RISER.

6.4 Program modification

Equations 6.1 and 6.2 may be rewritten as:

$$\underline{M}\,\underline{a} + \underline{C}\,\underline{v} + \underline{K}\,\underline{x} = \underline{f} \quad \ldots\ldots (6.5)$$

where: $\underline{a} = \frac{\delta^2 \underline{x}}{\delta t^2}$ $\qquad \underline{v} = \frac{\delta \underline{x}}{\delta t}$

$\underline{K}$ is the stiffness matrix, and incorporates terms 2 and 3. $\underline{C}$ is the structural damping matrix, which is assumed to be stiffness-proportional. $\underline{M}$ is the mass matrix, and incorporates term 1, and the second part of term 5. $\underline{f}$ is the force vector, and incorporates terms 4, 6 and the first part of term 5.

6.4.1 Stiffness matrix

The standard Bernoulli-Euler beam element was used to model the riser. Because the riser is slender, shear deformation is considered to be negligible, and Bernoulli-Euler theory is adequate. Bernouli-Euler theory is adequate for low frequency excitation [3]. The degrees of freedom employed by this element are shown in figure 6.2.

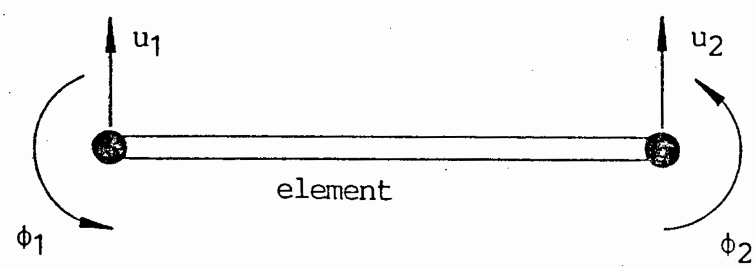

fig. 6.2 - Bernoulli-Euler beam element

Standard cubic Hermitian shape functions are used to approximate the displacement field over each element. The resulting elemental stiffness matrices for terms 2 and 3, equation 6.1, are shown below:

Term 2:

$$\frac{EI}{h^3}\begin{array}{c} \begin{array}{cccc} u_1 & \Phi_1 & u_2 & \Phi_2 \end{array} \\ \begin{bmatrix} 12 & 6h & -12 & 6h \\ & 4h^2 & -6h & 2h^2 \\ & & 12 & -6h \\ \text{symmetrical} & & & 4h^2 \end{bmatrix} \end{array} \begin{array}{c} u_1 \\ \Phi_1 \\ u_2 \\ \Phi_2 \end{array}$$

Term 3

$$T_e\begin{array}{c} \begin{array}{cccc} u_1 & \Phi_1 & u_2 & \Phi_2 \end{array} \\ \begin{bmatrix} 6/5h & 1/10 & -6/5h & 1/10 \\ & 2h/15 & -1/10 & -h/30 \\ & & 6/5h & -1/10 \\ \text{symmetrical} & & & 2h/15 \end{bmatrix} \end{array} \begin{array}{c} u_1 \\ \Phi_1 \\ u_2 \\ \Phi_2 \end{array}$$

Term 2 represents the bending stiffness of the riser, while term 3 represents the stiffness owing to the effective tension in the riser. As this tension increases, the riser behaves more and more like a string, as the bending effects become insignificant.

The stiffness of each element is evaluated, and the global stiffness matrix is assembled in the usual manner.

6.4.2 Damping matrix

There are two types of damping in the system: structural and hydrodynamic. The hydrodynamic effects are included in term 6, equation 6.2, and are applied in the force vector, $\underline{f}$, of equation 6.5.

The structural damping is assumed to be stiffness-proportional. No mass proportionality is assumed for two reasons: firstly, there should be no correlation between the structural damping in the system, and the added mass owing to the fluid entrapment, as expressed by the second part of term 5, equation 6.2; secondly, assuming that there is no dependence of the damping matrix on the mass coefficient, C_m, which will be considered a random variable in section 7, simplifies the formulations in that section.

6.4.3 Mass matrix

The consistent mass matrix for the Bernoulli-Euler beam element, as defined by Cook [73], is:

$$[\underline{m}] = \frac{m}{420}\begin{array}{cc} \begin{array}{cccc} u_1 & \Phi_1 & u_2 & \Phi_2 \end{array} & \\ \begin{bmatrix} 156 & 22h & 54 & -13h \\ & 4h^2 & 13h & -3h^2 \\ & & 156 & -22h \\ \text{symmetrical} & & & 4h^2 \end{bmatrix} & \begin{array}{c} u_1 \\ \Phi_1 \\ u_2 \\ \Phi_2 \end{array} \end{array}$$

where m is the mass of the element.

Term 1, and the second part of term 5, in equations 6.1 and 6.2, are included in the mass matrix. Term 1 represents the mass of the riser and its contents, while term 5 represents the added-mass owing to fluid entrapment.

The global mass matrix is assembled in the usual fashion.

6.4.4 Force vector

The force vector includes the effects of term 4 (which represents the lateral component of the riser weight and buoyancy), term 6 (which represents the hydrodynamic drag), and the first part of term 5 (which represents an added mass effect).

The lateral component of the weight and buoyancy depends on the final slope of the riser, the nodal values of which are degrees of freedom of the model. To calculate this component of the force vector, a simple iterative scheme was employed, approximately five iterations being usually necessary for convergence to within acceptable tolerances.

To implement terms 5 and 6, a wave theory must be used in order to evaluate the wave velocity, v_w, and wave acceleration, a_w. A current profile must also be assumed in order to evaluate v_c. For this model, a linear current profile was assumed, and linear Airy wave theory was employed [22, 38,83].

A consistent elemental load vector was used to apply all distributed loads:

$$\{\underline{f}\} = ph \begin{Bmatrix} \overset{u_1}{1/2} & \overset{\Phi_1}{h/12} & \overset{u_2}{1/2} & \overset{\Phi_2}{-h/12} \end{Bmatrix}^T$$

Loads were assumed constant over each element, equal to p in the above expression.

6.4.5 Static and dynamic analysis

The static displacement of the riser under the action of a current may be determined by neglecting all terms in the governing equations containing $\delta x/\delta t$, $\delta^2 x/\delta t^2$ and a_w. The resulting displacement field may be used as the initial condition for the dynamic analysis; the initial velocity and acceleration fields are usually assumed to be zero, or to be compatible with the wave action.

The dynamic analysis is conducted using the Newmark scheme derived by Cook [72]. This implicit operator is unconditionally stable for linear systems, but this stability is not guaranteed for nonlinear systems. A time step of less than one tenth of the lowest mode of interest is recommended in order to resolve that mode, although numerical stability requirements might dictate the use of a smaller time step.

Artificial damping may be introduced if required. Using the suggested values of the Newmark coefficients of $\alpha=.5$ and $\beta=.25$, results in no artificial damping (which is recommended if not absolutely necessary [75]), no amplitude errors, and slight phase errors. These effects have been verified by applying the Newmark scheme used in RISER to a simple two degree-of-freedom system. In these tests, the phase error detected was less than .1% of the response period.

In the dynamic analysis, the force vector changes with time owing to the wave action. A kinematic boundary may be implemented at the top node, to simulate the motion of a floating vessel. This is done in the standard fashion, by modifying the load vector and stiffness matrix appropriately, during the solution procedure.

6.4.6 Drag nonlinearity

An iterative scheme is required to evaluate the drag force, expressed in term 6. Consider the forces acting on a node of the riser, as shown in figure 6.3.

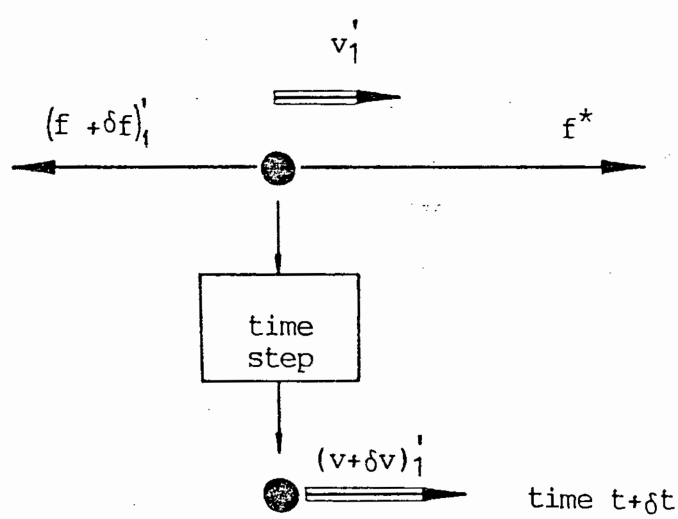

fig. 6.3 - Forces acting on riser node

In figure 6.3 the node is in equilibrium in the d'Alembert sense at the current time t. The force pair, $f+\delta f$ and f^*, required to produce dynamic equilibrium at time $t+\delta t$ depends on the velocity, $v+\delta v$, at time $t+\delta t$. The velocity $v+\delta v$ is unknown, and so an iterative scheme must be implemented. f^* is the sum of the forces acting on the node, besides that of drag. $f+\delta f$ is the drag force owing to the relative velocity of the node.

A guess, v'_1, of the velocity, $v+\delta v$, must be made; the force, $(f+\delta f)'_1$ evaluated, and the resulting nodal velocity $(v+\delta v)'_1$ determined. This velocity must be used to make a new guess, v'_2, and so on. When v'_n is sufficiently close to $(v+\delta v)'_n$ convergence has been achieved, and the solution $v+\delta v$ has been found. By considering the effect of making a guess, v', the required iterative process may be clarified, as shown in figure 6.4.

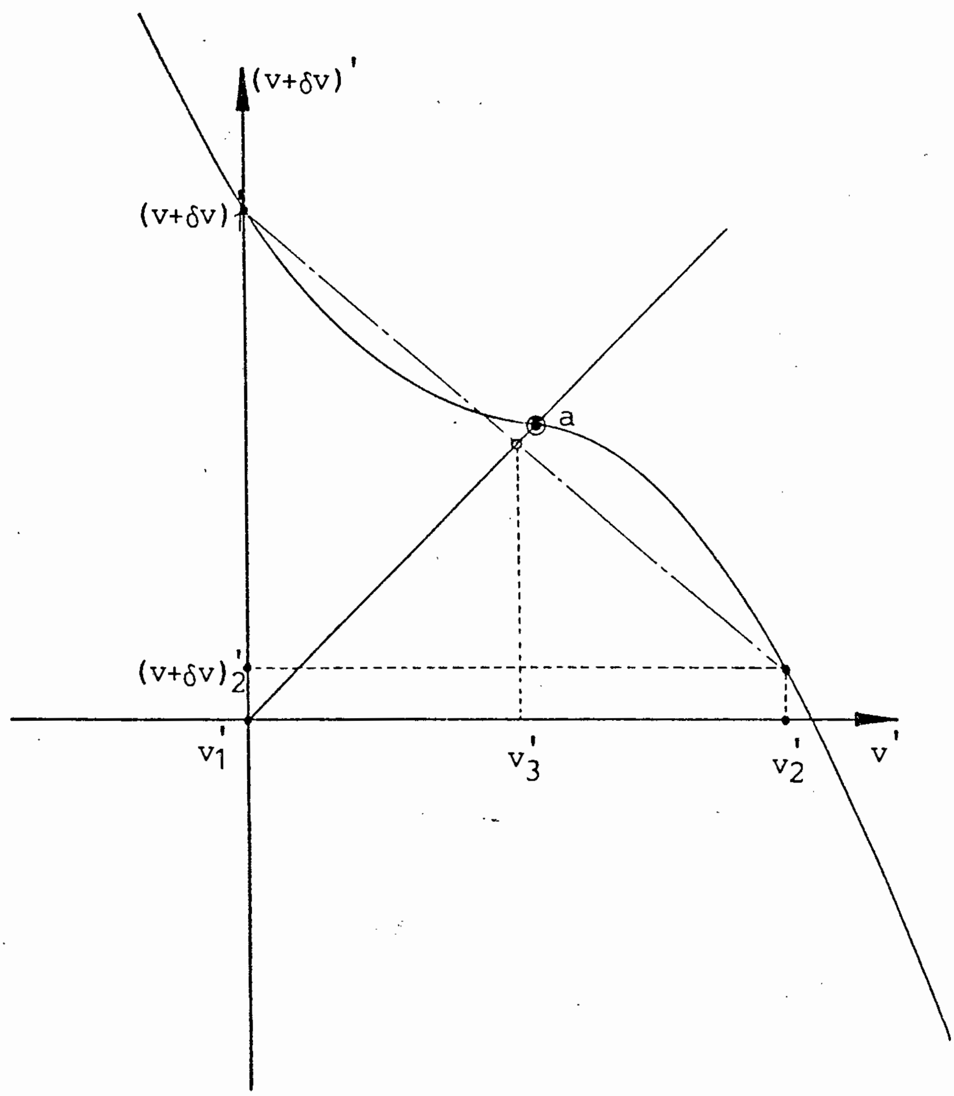

fig. 6.4 - Schematic diagram of velocity iterative procedure

The solution, $v+\delta v$, lies at $v' = (v+\delta v)'$, or the point 'a' in the figure. It may be seen that a large positive guess of v' results in a large negative predicted $(v+\delta v)'$, and vice versa. Thus a simple iterative scheme will not converge to the solution, but will oscillate, and diverge.

A quasi-Newton scheme was used to achieve convergence. The intersection of the line joining the two previous guesses and the 45°-degree line was used as the current guess.

It was found that this algorithm's stability was dependent on the size of the time step employed by the Newmark scheme. For reasonable time steps, sufficiently small so as to resolve the details of the fundamental mode of the riser, the algorithm was stable. The stability is independent of the initial two guesses, and convergence is approximately quadratic.

For convenience, the first guess, v'_1 was taken as the previous time step's velocity, v, and the second guess, v'_2, as a fraction, ϵ, of the first guess's velocity prediction, $(v+\delta v)'_1$. The value of ϵ is user-controlled, and may be adjusted in order to "tune" the algorithm. A value of ϵ=.05 gave consistently good results, the solution usually converging within five iterations.

6.5 Program validation

In order for a model such as this to be used with confidence, the performance of the program must be gauged. A measure of the mechanical behaviour of the riser model is the performance of the static model. The resulting lateral top-node displacements for various top-tensions predicted by RISER were compared to those predicted by ABAQUS, which is a fully nonlinear program. The results of this comparison are illustrated in figure 6.5.

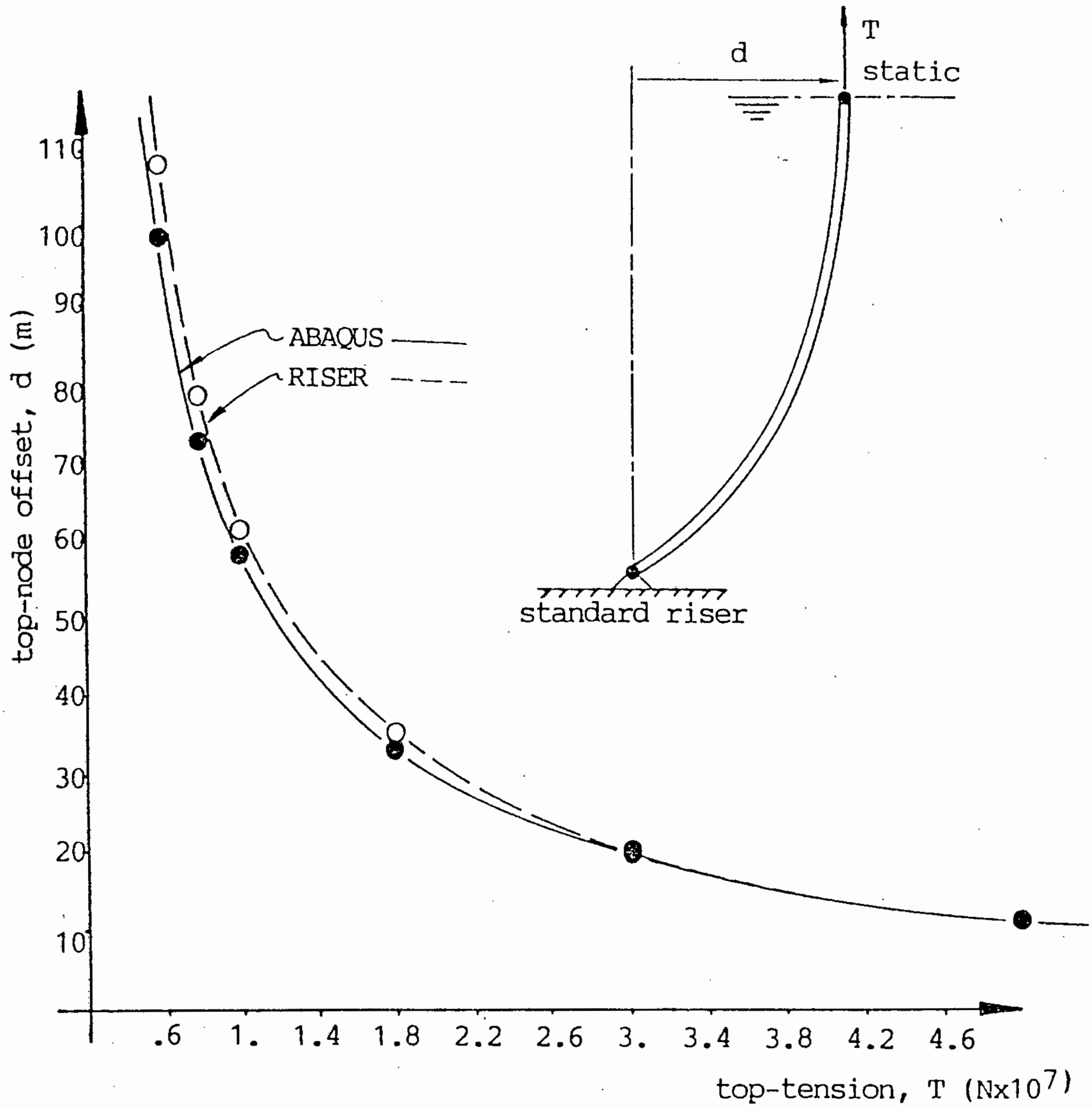

fig. 6.5 - Offset of top node for different top-tensions

A geometrically nonlinear model allows for the lateral hardening effect at large lateral displacements. The stiffness owing to the geometry of the system is termed the geometric stiffness. Thus, at larger displacements, the two solutions depicted in the figure diverge, the model used by ABAQUS hardening, or at least softening more slowly. The dominant softening effects acting on the system at lower top-tension values are those that are due to the decreased tension, and the increased lateral component of weight and buoyancy. At top node displacements of less than 10% of the vertical height of the riser, the error predicted by RISER is restricted to less than about 10%, when compared to ABAQUS.

It is therefore recommended that RISER only be used for small displacements, of less than 10% of the riser height. This restriction is not a limitation for the modelling of riser configurations, such as the standard or the hanging configuration, where the maximum deflection is usually less than 10% of the largest model dimension, but prohibits the modelling of configurations such as the catenary configuration.

The shape of the riser predicted by RISER agreed with the one predicted by ABAQUS. The resulting error at any point along the riser was approximately the same as the error at the top-node.

The implications of the effective tension, T_e (equation 6.3), on the riser behaviour are interesting, and this has been the subject of much research and comment (see section 1.3). The effective tension at any point in the riser is not simply equal to the applied top-tension, but is modified by the axial component of the hydrostatic pressure force. This is caused by the fact that the ends of any portion of the riser are not open to the surrounding fluid. This pressure effect acts as a tension. Sparks [12-14] describes in detail the mechanism of the effective tension.

The riser derives most of its stiffness from the effective tension. In fact, reducing the bending stiffness, EI, to zero in this model, had a negligible effect on the deformed shape, although the bending moment carried by the riser is proportional to the bending stiffness. The riser behaves in a "string-like" fashion. This is in agreement with the results obtained with ABAQUS.

The effective tension may be varied by varying the drilling-mud density in the model. The hydrostatic pressure depends on the density of the fluid, and so the effective tension, as defined in equation 6.3, is also density-dependent. The effect of doing this is shown in figure 6.6.

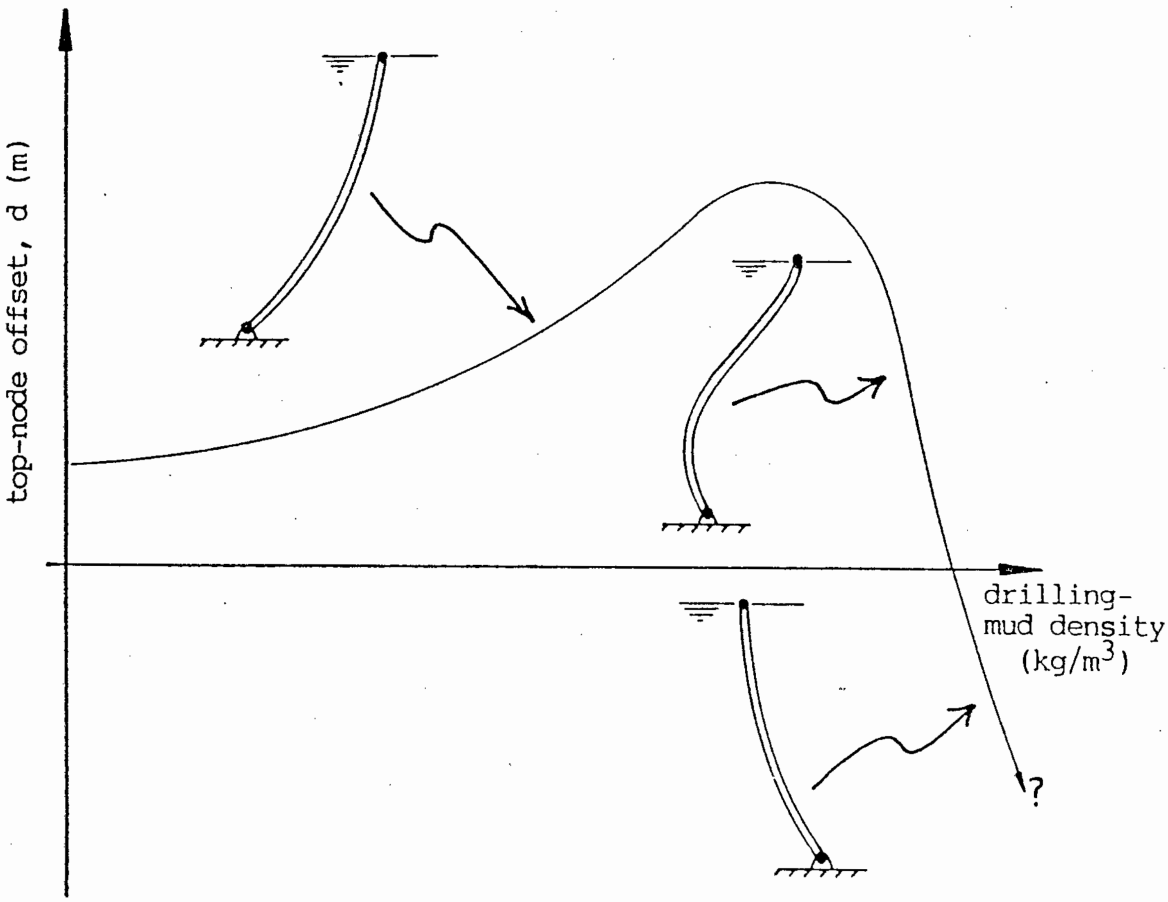

fig. 6.6 - Schematic diagram showing the effect of changing the density of the drilling-mud

The effective tension decreases with depth owing to the increasing hydrostatic pressure. The lateral stiffness of the riser depends on this effective tension, and may become negative if the effective tension decreases sufficiently. A negative stiffness is an indication of buckling, and this effect may be seen in the above figure. The riser buckles first near the bottom, where the pressure is greatest (in the static case). The results predicted after this happens are questionable, and should be disregarded.

This buckling problem is particularly severe for deep water risers, and has been investigated by Bernitsas et al.[3-6]. Practically, the effective tension may be increased by changing the drilling-mud density, or by using buoyancy modules at intervals along the riser.

It is important to know something about the convergence of the model's solution, with the increase of the number of elements in the model. This has been investigated with RISER for a static analysis, and typical results are shown in figure 6.7.

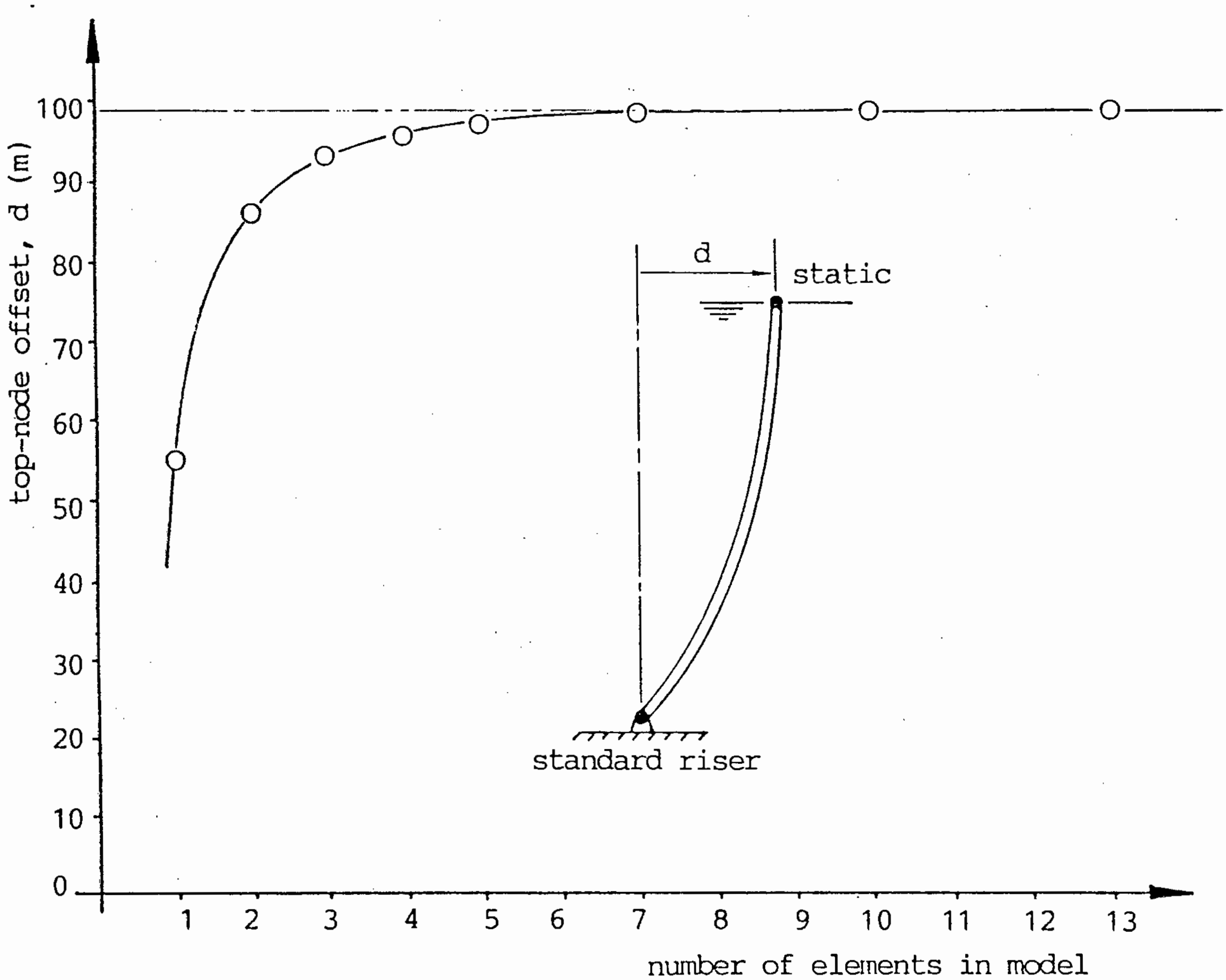

fig. 6.7 - Effect of the number of elements in the model on convergence

As the number of elements in the model increases, the solution rapidly converges. The stiff nature of the finite element formulation may also be observed. It is recommended that approximately ten elements be used in the model. Using more elements becomes prohibitively expensive in terms of computing time, and storage space.

With the probabalistic finite element model (PFEM), derived in section 7, implemented, using more than 15 elements exceeded the 640K capacity of the micro computer. This limit could be increased slightly by optimising the program.

The PFEM program takes approximately 10 to 20 seconds per time step to run on the Bondwell 39 micro computer, depending on the convergence characteristics, and the size of the arrays being processed. If any extensive use were to be made of this program, the implementation of the program on a more powerful machine would be warranted. This discussion will be extended in section 8.

The dynamic portion of the algorithm is more difficult to verify against ABAQUS, since the dynamic model is much more complicated than the static model. Small differences in the formulation of the problem may result in phase differences, which give large, apparent errors at any given time within the analysis. The transient portion of the analysis will vary, depending on how the wave loading is applied, and so the programs must be compared at steady state.

The Newmark scheme used in this program has been validated independently, and the results of the dynamic analyses are credible in the sense that the response amplitude, period and phase are compatible with the wave excitation, and similar to those given by ABAQUS, although it would be difficult to quantify this.

7. THE PROBABALISTIC FINITE ELEMENT METHOD APPLIED TO MARINE RISERS

The probabalistic finite element method was developed in 1986 by Liu et al. [16,17]. The applicability of the Probabalistic Finite Element Method (PFEM) to marine riser analysis is investigated in this section.

The PFEM employs a second-order approximation of the input mean, and a first order approximation of the input variance, to predict the response characteristics of a system with random parameters.

7.1 The Probabalistic finite element method

Liu et al. tested the PFEM against a Monte Carlo (MC) and an Hermite-Gauss quadrature (HGQ) simulation. A stiff, two degree-of-freedom system and a ten bar truss, with uncertain elemental stiffnesses, were investigated. Material and geometric nonlinearities were included in the truss formulation. The following points are pertinent:

1) The method is easily integrated with an existing finite element model, as many of the same subroutines may be employed.

2) The method developed by Liu et al. [16], for discrete random variables, may be extended to random fields [17]. The random field is discretised in the same fashion as the displacement field. The correlated variables are transformed by an eigenvalue orthogonalisation to a set of uncorrelated variables. These techniques are illustrated by the application of the method to a one-dimensional elastic-plastic wave propagation problem, and compared to a Monte Carlo simulation.

3) The predicted mean and variance are second and first order accurate respectively. Only information concerning the first two moments of the random variables is required.

4) The PFEM is more efficient than the MC or the HGQ methods for small to medium sized problems. The number of time integrations required for a linear dynamic problem, with q random variables, is q+2 for the PFEM, 3^q for the HGQ method, and N for the MC simulation, where N is the number of sample values required.

5) The PFEM's accuracy compared favourably with the MC and the HGQ methods, for values of the coefficient of variation of the random variables of 10% or less. The accuracy of the PFEM decreases for larger values of time, and is better suited to short time history analysis, such as impulsive loading. This decrease of accuracy with time is owing to the nature of the resonant excitation of the response sensitivity vectors (derived in section 7.3). A detailed description of this reasoning may be found in Appendix C.

6) The PFEM is easier to apply to linear problems, as the sensitivity vectors (derived in section 7.3) that one must calculate are easily obtainable. One must often resort to finite difference approximations of these vectors in a nonlinear analysis, and the formulation becomes problem dependent.

7.2 Statistical background

In order to understand the PFEM, some statistical concepts must first be clarified. Consider a general function $\Omega(b)$, as shown in figure 7.1.

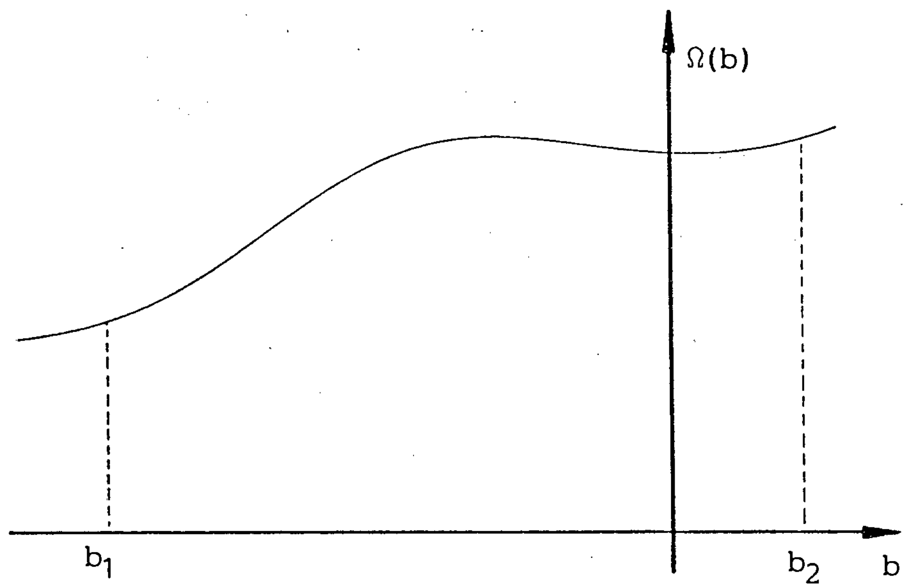

fig. 7.1 - A general function, Ω(b)

The average, mean, or first moment, of the function Ω over the interval B is defined by the expectation operator E[Ω]:

$$E[\Omega] = \int_B \frac{\Omega(b)}{B}\, db \quad \ldots\ldots (7.1)$$

The variance, or second moment, of the function Ω is defined by:

$$\mathrm{Var}(\Omega) = \sigma^2 = E[(\Omega - E[\Omega])^2] \quad \ldots\ldots (7.2)$$

where σ is the standard deviation, a measure of dispersion. That is, the variance is the mean of the square of the deviation of Ω from its mean level, E[Ω] [76,100]. The statistical "moments" described above are mathemetically analogous to the "moments" of inertia used in mechanics.

7.3 Formulation of the PFEM

Consider the system of equations that describes the behaviour of the marine riser (as formulated in section 6):

$$\underline{M}\ \underline{a} + \underline{C}\ \underline{v} + \underline{K}\ \underline{d} = \underline{f} \quad \text{.........................(7.3a)}$$

where:

$$\underline{f} = C_m \mu_o A_o \underline{a}_w + \tfrac{1}{2} C_d \mu_o d_o \$(*)(*)^2 + (\mu_i A_i - \mu_o A_o)\delta \underline{x}/\delta y \quad \text{..(7.3b)}$$

where:

$$(*) = (\underline{v}_c + \underline{v}_w - \underline{v}) \quad \text{.........................(7.3b)}$$

and

$\$(*)$ is the sign of $(*)$

We will be considering the hydrodynamic coefficients C_d and C_m to be random. These are the most serious uncertainties in a marine riser analysis, as discussed in section 1.9. Using the notation of Liu et al., the vector of random parameters is $\underline{b} = \{C_d \quad C_m\}^T$, with the dimension of $\underline{b}$ being q. The acceleration, velocity and displacement vectors are functions of the random variables, as is the mass matrix, which is a function of the mass coefficient. All other parameters in equation 7.3 will be considered to be deterministic in nature.

It can be shown that a second order approximation of the mean of a function $\Omega(\underline{b})$ can be given by a Taylor series expansion about the mean value of Ω [16,102]:

$$E[\Omega(\underline{b})] \approx \bar{\Omega} + \tfrac{1}{2} \sum_{i,j=1}^{q} (\delta^2 \bar{\Omega}/\delta b_i \delta b_j)\ \mathrm{Cov}(b_i, b_j) \quad \text{.........(7.4)}$$

$$E[\Omega(\underline{b})] \approx \bar{\Omega} + \tfrac{1}{2}\sum_{i=1}^{q} (\delta^2\bar{\Omega}/\delta b_i^2)\ \mathrm{Var}(b_i) \quad \text{.....(7.6)}$$

$$\mathrm{Var}(\Omega(\underline{b})) \approx \sum_{i=1}^{q} (\delta\bar{\Omega}/\delta b_i)^2\ \mathrm{Var}(b_i) \quad \text{.....(7.7)}$$

The expectation operator may be applied to equation 7.3:

$$E[\ \underline{M}\ \underline{a} + \underline{C}\ \underline{v} + \underline{K}\ \underline{d}\ ] = E[\ \underline{f}\ ] \quad \text{.....(7.8)}$$

which may be expanded owing to the linearity of the expectation operator. Employing equation 7.6 and the chain rule, and noting that $\delta^2\bar{\underline{M}}/\delta b_j^2 = \delta^2\bar{C}_m/\delta b_j^2 = \delta^2\bar{C}_d/\delta b_j^2 = 0$:

$$E[\underline{M}\ \underline{a}] \approx \bar{\underline{M}}\cdot\underline{a} + \tfrac{1}{2}\sum_{j=1}^{q} \{2(\delta\bar{\underline{M}}/\delta b_j)(\delta\bar{\underline{a}}/\delta b_j) + \bar{\underline{M}}\delta^2\bar{\underline{a}}/\delta b_j^2\}\ \mathrm{Var}(b_j) \quad \text{.....(7.9a)}$$

$$E[\underline{C}\ \underline{v}] \approx \bar{\underline{C}}\ \underline{v} + \tfrac{1}{2}\sum_{j=1}^{q} \{\bar{\underline{C}}\delta^2\bar{\underline{v}}/\delta b_j^2\}\ \mathrm{Var}(b_j) \quad \text{.....(7.9b)}$$

$$E[\underline{K}\ \underline{d}] \approx \bar{\underline{K}}\ \underline{d} + \tfrac{1}{2}\sum_{j=1}^{q} \{\bar{\underline{K}}\delta^2\bar{\underline{d}}/\delta b_j^2\}\ \mathrm{Var}(b_j) \quad \text{.....(7.9c)}$$

$$E[\underline{f}] \approx \bar{\underline{f}} + \tfrac{1}{2}\sum_{j=1}^{q} \mu_o d_o \$(*)\{2(*)(-\delta\bar{\underline{v}}/\delta b_j)(\delta\bar{C}_d/\delta b_j) + \bar{C}_d(\delta\bar{\underline{v}}/\delta b_j)^2 + \bar{C}_d(*)(-\delta^2\bar{\underline{v}}/\delta b_j^2)\}\ \mathrm{Var}(b_j) \quad \text{.(7.9d)}$$

Equations 7.9 may be rewritten:

$$\bar{\underline{M}}\ \bar{\underline{a}} + \bar{\underline{C}}\ \bar{\underline{v}} + \bar{\underline{K}}\ \bar{\underline{d}} = \bar{\underline{f}} \quad \text{.....(7.10)}$$

$$\underline{\bar{M}}\ \delta\underline{\bar{a}} + \underline{\bar{C}}\ \delta\underline{\bar{v}} + \underline{\bar{K}}\ \delta\underline{\bar{d}} = \delta\underline{\bar{f}} \quad \ldots\ldots\ldots\ldots\ldots\ldots\ldots\ldots (7.11)$$

where

$$\delta\underline{\bar{a}} = \tfrac{1}{2}\sum_{j=1}^{q}\{\delta^2\underline{\bar{a}}/\delta b_j^2\}\ \mathrm{Var}(b_j) \quad \ldots\ldots\ldots\ldots\ldots\ldots\ldots (7.12a)$$

$$\delta\underline{\bar{v}} = \tfrac{1}{2}\sum_{j=1}^{q}\{\delta^2\underline{\bar{v}}/\delta b_j^2\}\ \mathrm{Var}(b_j) \quad \ldots\ldots\ldots\ldots\ldots\ldots\ldots (7.12b)$$

$$\delta\underline{\bar{d}} = \tfrac{1}{2}\sum_{j=1}^{q}\{\delta^2\underline{\bar{d}}/\delta b_j^2\}\ \mathrm{Var}(b_j) \quad \ldots\ldots\ldots\ldots\ldots\ldots\ldots (7.12c)$$

$$\begin{aligned}\delta\underline{\bar{f}} = \tfrac{1}{2}\sum_{j=1}^{q}\mu_o d_o \$(\bar{*})\{&2(\bar{*})(-\delta\underline{\bar{v}}/\delta b_j)(\delta\bar{C}_d/\delta b_j) + \\ &+ \bar{C}_d(\delta\underline{\bar{v}}/\delta b_j)^2 + \bar{C}_d(\bar{*})(-\delta^2\underline{\bar{v}}/\delta b_j^2) - \\ &- 2(\delta\underline{\bar{M}}/\delta b_j)(\delta\underline{\bar{a}}/\delta b_j)\}\ \mathrm{Var}(b_j) \quad \ldots\ldots\ldots (7.12d)\end{aligned}$$

Equation 7.10 is used to evaluate the first order components of the mean acceleration, velocity and displacement vectors at any time, t. The second order components may be evaluated using equation 7.11. The second order approximations of the means are therefore:

$$E[\underline{a}] \approx \underline{\bar{a}} + \delta\underline{\bar{a}} \quad \ldots\ldots\ldots\ldots\ldots\ldots\ldots\ldots\ldots\ldots (7.13a)$$

$$E[\underline{v}] \approx \underline{\bar{v}} + \delta\underline{\bar{v}} \quad \ldots\ldots\ldots\ldots\ldots\ldots\ldots\ldots\ldots\ldots (7.13b)$$

$$E[\underline{d}] \approx \underline{\bar{d}} + \delta\underline{\bar{d}} \quad \ldots\ldots\ldots\ldots\ldots\ldots\ldots\ldots\ldots\ldots (7.13c)$$

The first order approximations of the response variances are:

$$\mathrm{Var}(\underline{a}) \approx \sum_{j=1}^{q} (\delta\bar{\underline{a}}/\delta b_j)^2 \,\mathrm{Var}(b_j) \quad \text{......................(7.14a)}$$

$$\mathrm{Var}(\underline{v}) \approx \sum_{j=1}^{q} (\delta\bar{\underline{v}}/\delta b_j)^2 \,\mathrm{Var}(b_j) \quad \text{......................(7.14b)}$$

$$\mathrm{Var}(\underline{d}) \approx \sum_{j=1}^{q} (\delta\bar{\underline{d}}/\delta b_j)^2 \,\mathrm{Var}(b_j) \quad \text{......................(7.14c)}$$

In order to evaluate equations 7.12 and 7.14, the sensitivity matrix, $\delta\bar{\underline{M}}/\delta b_j$, the first order sensitivity vectors, $\delta\bar{\underline{a}}/\delta b_j$, $\delta\bar{\underline{v}}/\delta b_j$ and $\delta\bar{\underline{d}}/\delta b_j$, and the second order sensitivity vectors $\delta^2\bar{\underline{a}}/\delta b_j^2$, $\delta^2\bar{\underline{v}}/\delta b_j^2$ and $\delta^2\bar{\underline{d}}/\delta b_j^2$ must all be evaluated.

The dependence of the mass matrix on $\underline{b}$ is found in term 5 of equation 6.2. $\delta\bar{\underline{M}}/\delta b_j$ is evaluated at the elemental level, and assembled in exactly the same way as the mass, stiffness and damping matrices.

It should be noted that for $\underline{b} = \{C_d \quad C_m\}^T$,

$$\delta\bar{C}_d/\delta b_1 = 1, \qquad \delta\bar{C}_d/\delta b_2 = 0$$

$$\delta\bar{C}_m/\delta b_1 = 0, \qquad \delta\bar{C}_m/\delta b_2 = 1$$

The first and second order sensitivity vectors may be evaluated by differentiating equation 7.3, with respect to b_j:

$$\begin{aligned}
&\bar{\underline{M}}(\delta\bar{\underline{a}}/\delta b_j) + \bar{\underline{C}}(\delta\bar{\underline{v}}/\delta b_j) + \bar{\underline{K}}(\delta\bar{\underline{d}}/\delta b_j) = \\
&\quad = (\delta\bar{C}_m/\delta b_j)\mu_o A_o a_w + \mu_o d_o \$(\bar{*})\{(\delta\bar{C}_d/\delta b_j)(\bar{*})^2/2 + \\
&\quad + \bar{C}_d(\bar{*})(-\delta\bar{\underline{v}}/\delta b_j)\} - \bar{\underline{a}}(\delta\bar{\underline{M}}/\delta b_j) \quad \text{......................(7.15)}
\end{aligned}$$

$$\underline{\bar{M}}(\delta^2\underline{\bar{a}}/\delta b_j^2) + \underline{\bar{C}}(\delta^2\underline{\bar{v}}/\delta b_j^2) + \underline{\bar{K}}(\delta^2\underline{d}/\delta b_j^2) =$$
$$= \mu_o d_o \$(\bar{*})\{2(\bar{*})(\delta\bar{C}_d/\delta b_j)(-\delta\underline{\bar{v}}/\delta b_j) + \bar{C}_d(\delta\underline{\bar{v}}/\delta b_j)^2 +$$
$$+ \bar{C}_d(\bar{*})(-\delta^2\underline{\bar{v}}/\delta b_j^2)\} - 2(\delta\underline{\bar{M}}/\delta b_j)(\delta\underline{\bar{a}}/\delta b_j) \quad \ldots\ldots\ldots\ldots\ldots (7.16)$$

Equations 7.10, 7.11, 7.15 and 7.16 are all of the same form, $\underline{M}\ (\underline{\bullet}) + \underline{C}\ (\underline{\bullet}) + \underline{K}\ (\underline{\bullet}) = (\underline{\bullet})$, and the same time integration scheme may be used to evaluate each one. These equations are also nonlinear in $\underline{\bar{v}}$, $\delta\underline{\bar{v}}/\delta b_j$ and $\delta^2\underline{\bar{v}}/\delta b_j^2$. The algorithm developed in section 6.4.5 is used to solve these equations.

7.4 Solution procedure

1) $\underline{\bar{K}}$, $\underline{\bar{C}}$, $\underline{\bar{M}}$ and $\delta\underline{\bar{M}}/\delta b_j$ are evaluated at the elemental level, and assembled into the global form.

2) The static elemental load vectors are evaluated and assembled into the global load vector.

3) The boundary conditions are applied, and the system of equations solved, giving the static response of the structure.

4) The static response is used as the initial displacement condition for the dynamic analysis. Initial velocity and acceleration vectors are applied. The initial conditions are assumed to be deterministic. That is, the first and second order initial sensitivity vectors are assumed to be zero.

   This assumption is made because the initial velocity and acceleration sensitivity vectors are not known. The initial displacement sensitivity vectors could be evaluated simply, by applying the PFEM to the static problem.

5) The time integration is started, using the Newmark operator. The following six procedures are conducted for each time step:

6) The global load vector, $\bar{\underline{f}}$ in equation 7.10, is assembled. $\bar{\underline{a}}$, $\bar{\underline{v}}$ and $\bar{\underline{d}}$ are evaluated from equation 7.10, iterating for $\bar{\underline{v}}$. The following two procedures are conducted for each j:

7) The global load vector in equation 7.15 is assembled, $\underline{a}$ from step 6 being required. Equation 7.15 is solved for the first order sensitivity vectors $\delta\bar{\underline{a}}/\delta b_j$, $\delta\bar{\underline{v}}/\delta b_j$ and $\delta\bar{\underline{d}}/\delta b_j$, iterating for $\delta\bar{\underline{v}}/\delta b_j$.

8) The global load vector in equation 7.16 is assembled, $\delta\bar{\underline{a}}/\delta b_j$ from step 7 being required. Equation 7.16 is solved for the second order sensitivity vectors $\delta^2\bar{\underline{a}}/\delta b_j^2$, $\delta^2\bar{\underline{v}}/\delta b_j^2$ and $\delta^2\bar{\underline{d}}/\delta b_j^2$, iterating for $\delta^2\bar{\underline{v}}/\delta b_j^2$.

9) $\delta\bar{\underline{a}}$, $\delta\bar{\underline{v}}$ and $\delta\bar{\underline{d}}$ may either be evaluated from equations 7.12, or 7.11, which require the formulation of a extra load vector, and an extra time integration.

10) $E[\underline{a}]$, $E[\underline{v}]$ and $E[\underline{d}]$ are evaluated from equations 7.13.

11) $Var(\underline{a})$, $Var(\underline{v})$ and $Var(\underline{d})$ are evaluated from equations 7.14.

8. APPLICATION OF THE PFEM TO UNCERTAINTIES IN THE HYDRODYNAMIC COEFFICIENTS

Hogben [55] summarises much of the experimental work done in the field of the hydrodynamic loading of structures. The variation in the values of the drag coefficient, C_d, and the mass coefficient, C_m, is large. C_d values of between 0 and 2.75, and C_m values of between 0 and 5, are recorded. Errors of over 50% are common. Data on the scatter of the experimental results is scarce.

Provisionally it was decided to use the values given by Reid [55] of:

$$C_d = 0.53 \qquad \mathrm{Var}(C_d) = 0.04$$

$$C_m = 1.47 \qquad \mathrm{Var}(C_m) = 0.13$$

These values were recorded in the Gulf of Mexico. Current effects were included in the analysis. The above coefficients result in coefficients of variation of 38% for C_d, and 25% for C_m.

The correct hydrodynamic coefficients to use in an actual design analysis would probably be vary from the above values; however, the applicability of the PFEM, developed in section 8, to marine risers may still be investigated.

8.1 Limitations of the PFEM

Liu et al. [16] mention four limitations of the PFEM:

1) The coefficients of variation (cov's) of the random parameters in the system are limited to about 10%. That is, $\sigma/\mu \leq 0.1$, where σ is the standard deviation, and μ is the mean value of the parameter.

2) The accuracy of the solution decays with time, and so the method is only applicable to short, transient analyses (see Appendix C for details).

3) The PFEM is cheaper than other simulation methods, such as the Monte Carlo (MC) and the Hermite Gauss Quadrature (HGQ) method for small to medium sized problems, but this advantage diminishes as the size of the problem increases.

4) The formulation of the sensitivity vectors may be comlicated for a nonlinear analysis, and is problem dependent.

In the formulation of the PFEM, applied to the marine riser, there are nonlinearities in $\bar{\underline{v}}$, $\delta\bar{\underline{v}}/\delta b_j$, and $\delta^2\bar{\underline{v}}/\delta b_j^2$, as described in section 7. These nonlinearities are handled successfully by employing the agorithm developed in section 6.4.5. Typically, 3 to 6 iterations are required for each j, for both the first and second order sensitivity equations (equations 7.15 and 7.16 in section 7), and 3 to 6 iterations for the first order components of the mean response, represented by equation 7.10.

It is now clear that for large, nonlinear problems the PFEM may become more expensive than simulation techniques such as the Monte Carlo. If, on average, n iterations are required, and there are q random parameters, each time step will require n(2q + 1) iterations, while a MC simulation will require N·n iterations, where N is the number of simulations.

Typically, for the PFEM, each time step takes between 10 and 20 seconds CPU time on a Bondwell 39 micro computer, each step requiring between 20 and 30 iterations.

Since the PFEM's accuracy decays with time, it is difficult to obtain the response characteristics of the system at steady-state, as is required for the analysis of marine risers. One can obtain steady-state results by letting the system run deterministically until steady-state has been achieved, and then applying the PFEM, assuming the response at the instant of application of the PFEM to be deterministic. That is, the initial sensitivity vectors are set to zero. Initial values for these senstivity vectors can be assumed, but it is difficult to assign them meaningful values.

It is not possible, as Liu et al. [16] have done, to simply put a bound (of 10%) on the coefficient of variation of the random parameters. It is the size of the second order components of the response means, as described by equations 7.11 and 7.12, that limit the effectiveness of the PFEM. These second order components should be less than about 10% of the first order components of the means for the method to be effective. The first order components are used to evaluate the second order components, as is described in equations 7.9, 7.12, 7.15 and 7.16. The second order components are then added to the first order components in equations 7.13 in order to evaluate the second order approximations of the response means.

The second order means are proportional to the variances of the random parameters, as described by equations 7.12. Thus there is a dependence of the magnitude of the second order components on the means on the coefficients of variation. It must be stressed that the magnitudes of these second order components are also problem dependent, and so, for each problem the cov bound will be different, as will be illustrated in the next section.

8.2 Coefficient of variation bounds for the PFEM

The effects of the uncertainties of C_d and C_m can be investigated independently by setting $Var(C_m)$ and $Var(C_d)$ to zero respectively. It was found that for a typical standard riser configuration, as described in section 2, the uncertainties in C_m dominated.

Typically, with $Var(C_m)$ set to zero, the second order components of the means remained several orders of magnitude less than the first order components. However, when $Var(C_d)$ was set to zero, the second order components of the means were of the same order of magnitude, or even larger, than the first order components. Under these conditions the response of the system pedicted by the PFEM was erratic.

For this riser configuration it was found that the cov bounds were about 95% for C_d, and about 1% for C_m. The system is very sensitive to the uncertainties in the mass coefficient, owing to the magnitude of the last terms in equations 7.15 and 7.16. The sensitivity matrix $\delta\underline{\bar{M}}/\delta b_j$ dominates the right-hand side of these equations. The magnitude of the added-mass in the system is of the same order as the rest of the mass in the system.

The PFEM is thus not applicable to riser problems where the inertial effects are large. The PFEM may be applied if the inertial dependence of the response is reduced in some way. The inertial effects are proportional to the square of the external diameter of the riser, while the drag is related linearly to the external diameter. The importance of the inertia thus decreases as the diameter of the pipe decreases.

It was found that for the values of the hydrodynamic coefficients used by Reid [55] (quoted near the beginning of this section), the PFEM was applicable to the riser system for external diameters of less than about 5 mm, which is of no use in the analysis of marine risers, or even cables. However, for C_m cov values of approximately 10%, the permissible diameter increases to about 30 mm. Therefore, if more accurate data is available, the PFEM might be applicable to the analysis of the uncertainties associated with mooring cables.

The PFEM, in its present form, therefore cannot be used to model the uncertainties inherent in the mass coefficient, C_m, but can be used to model the sensitivity of the response to uncertainties in the drag coefficient, C_d. The modelling of the system uncertainties, while ignoring the most important, that of C_m, would not be of much use. Other simulation techniques, such as the Monte Carlo method, are required; or perhaps the PFEM may be modified, although this has not been attempted in this study.

8.3 Description of the PFEM's general characteristics

A typical set of results for a standard riser configuration is shown in figure 8.1. Var(C_m) is set to zero, so as to neglect the effects of the mass coefficient uncertainties. Figure 8.1 shows the lateral, top node displacement, second order mean, second order component of that mean, and variance, as functions of time.

The second order component of the mean oscillates in much the same fashion as the mean, although out of phase, and several orders of magnitude smaller. The variance is aways positive, and the magnitude tends to increase with time. The velocity and acceleration response characteristics show the same trends.

The simple two degree-of-freedom example that Liu et al. [16] used to demonstrate the PFEM shows slightly different characteristics. The second order compoment of the mean for this example oscillates at about twice the frequency of the mean, and so does the variance. This trend is not obvious in the marine riser results illustrated in figure 8.1. It is therefore clear that some of the characteristics of the PFEM solution are problem dependent. Smaller time steps might be necessary in order to resolve these higher frequency second order component means.

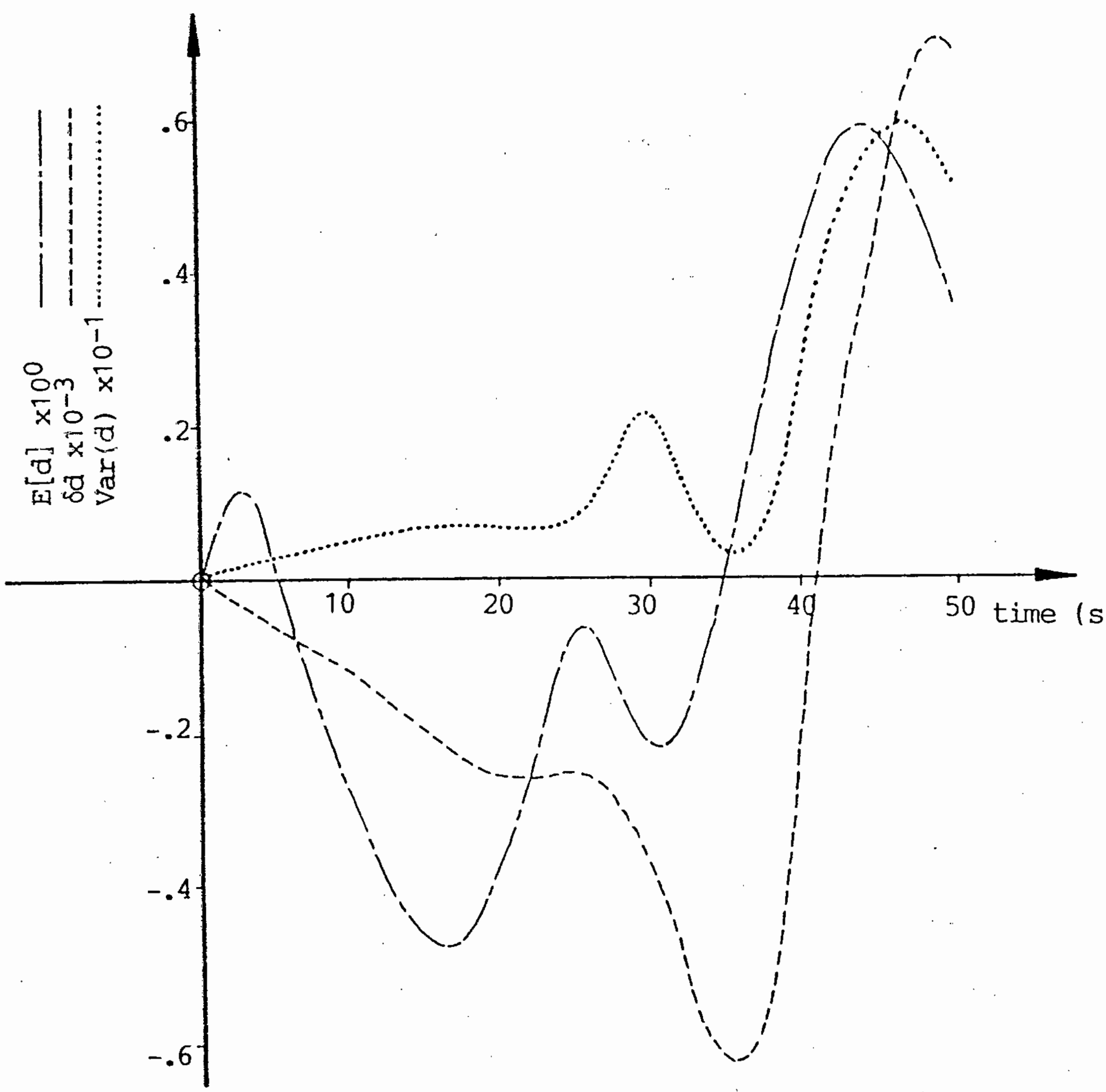

Fig. 8.1 - Typical PFEM results for top-node response characteristics of standard riser

In the marine riser example, the variance appears to grow with time. The results of Liu et al. for the two degree-of-freedom system indicate that there are two components to this growth. Firstly the MC and the HGQ simulations indicate that there is a slight growth of the variance with time. Secondly, the accuracy decay with time that is associated with the PFEM, manifests itself as large oscillations of the second order component of the mean, and hence the variance. The first effect dominates the response variance growth for the first two cycles, after which the second effect dominates. The PFEM is thus fairly accurate for the first two response cycles in the example of Liu et al.

There is some dependence of the magnitude of the second-order component of the mean on the initial deterministic conditions; however, this dependence appears to be problem dependent, and limited to the initial portions of the analysis.

The Probabalistic Finite Element Method (PFEM), developed by Liu et al. [16,17], has been formulated for the analysis of the riser model with uncertain hydrodynamic coefficients, C_d and C_m. It has been shown that the PFEM's application is limited by coefficient of variation (cov) bounds for the random parameters, C_d and C_m. For a typical riser, the C_d's cov is restricted to less than 95%, and the C_m's cov to less than 1%. The avialable literature gives cov's of 38% for C_d, and 25% for C_m, however the data in the literature is scarce.

The PFEM Is more applicable to the analysis of mooring cables, which have drag dominated loading. With the C_m cov values available in the literature (the data is scarce), of 25%, the diameter of the cable is limited to about 5 mm. For cov values of approximately 10%, diameters of about 30 mm may be modelled. Therefore, if more accurate data is available for a specific site, the PFEM might be applicable to the analysis of the uncertainties associated with mooring cables.

The PFEM, in its present form, is thus limited in its applicability to the modelling of the effect of the hydrodynamic coefficient uncertainties on marine risers. Other uncertainties in the model, such as stiffness uncertainties, may be modelled with the PFEM. The PFEM is also limited in its present form in that the accuracy dacays rapidly with time. More developmental work is required for the method to be applicable to this type of problem, or other techniques such as Monte-Carlo simulation may be employed.

10. REFERENCES

1) D.R. Stephens, D.P. McConnell, "Offshore pipeline design codes compared for loads, stress limits", Oil and Gas J., July 15, 1985, pp. 128-132

2) D.R. Stephens, D.P. McConnell, "Pipeline design codes compared graphically", Oil and Gas J., July 29, 1985, pp. 139-144

3) M.M. Bernitsas, C.J. Hoff, J.E. Kokarakis, "Nonlinear Inverse Perturbation in Structural Dynamics Redesign of Risers", J. of Energy Resources Technol., Vol. 107, June, 1985, pp. 256-263

4) M.M. Bernitsas, J.E. Kokarakis, "Buckling of Risers in Tension due to Internal Pressure: Nonmovable Boundaries", J. of Energy Resources Technol., Vol. 105, Sept., 1983, pp. 277-281

5) M.M. Bernitsas, J.E. Kokarakis, A. Imron, "Large deformation three-dimensional static analysis of deep water marine risers", Appl. Ocean Research, Vol. 7, No. 4, 1985, pp. 178-187

6) M.M. Bernitsas, "Riser Top Tension and Riser Buckling Loads", Comput. Meths. for Off-shore Struct., ASME AMD Vol. 37, pp. 101-109, November 1980

7) P.G. Bergan, Mollestad, N. Sandsmark, "Non-linear static and dynamic response analysis for floating offshore structures", Engrg. Comput., Vol. 2, March, 1985, pp. 13-20

8) J.S. Chung, A.K. Whitney, W.A. Loden, "Nonlinear Transient Motion of Deep Ocean Mining Pipe", J. of Energy Resources Technol., Vol. 103, March, 1981, pp. 2-10

9) C.A. Felippa, J.S. Chung, "Nonlinear Static Analysis of Deep Ocean Mining Pipe - Part 1: Modeling and Formulation", J. of Energy Resources Technol., Vol. 103, March, 1981, pp. 10-15

10) J.S. Chung, C.A. Felippa, "Nonlinear Static Analysis of Deep Ocean Mining Pipe - Part 2: Numerical Studies", J. of Energy Resources Technol., Vol. 103, March, 1981, pp. 16-25

11) J.S. Chung, A.K. Whitney, "Axial Stretching Oscillation of an 18,000-Ft Vertical Pipe in the Ocean", J. of Energy Resources Technol., Vol. 105, June, 1983, pp. 195-200

12) C.P. Sparks, J.P. Cabillic, J.-C. Schawann, Longetudinal Resonant Behavior of Very Deep Water Risers", J. of Energy Resources Technol., Vol. 105, Sept., 1983, pp. 282-289

13) C.P. Sparks "the Influence of Tension, Pressure and weight om Pipe riser Deformations and Stresses", J. of Energy Resources Technol., Vol. 106, March, 1984, pp. 46-54

14) C.P. Sparks, "Mechanical Behavior of Marine Risers Mode of Influence of Principal Parameters", J. of Energy Resources Technol., Vol. 102, Dec., 1980, pp. 214-222

15) J.F. McNamara, H.D. Hibbitt, "Numerical Analysis of Flexible Pipes and Risers in Offshore Applications", Proposed paper for presentation at the 1986 OMAE Speciality Symposium on "Offshore and Artic Frontiers" at ETCE, New Orleans, LA, Feb. 23-27, 1986

16) W.K. Liu, T. Belytschko, A. Mani, "Probabilistic Finite Elements for Nonlinear Structural Dynamics", Comput. Meths. in Appl. Mech. and Engrg., Vol. 56, 1986, pp. 61-81

17) W.K. Liu, T. Belytschko, A. Mani, "Random Field Finite Elements", Int. J. for Numer. Meths. in Engrg., Vol. 23, 1986, pp. 1831-1845

18) J.F. McNamara, M. Lane, "Practical Modeling for Articulated Risers and Loading Columns", J. of Energy Resources Technol., Vol. 106, Dec., 1984, pp. 444-450

19) S. Chakrabarti, D. Cotter, "Hydrodynamic Coefficients of a Mooring Tower", J. of Energy Resources Technol., Vol. 106, June, 1984, pp. 183-190

20) C.L. Kirk, "Dynamic response of marine risers by single wave and spectral analysis methods", Appl. Ocean Research, Vol. 7, No. 1, 1985, pp. 2-13

21) R.D. Young, J.R. Long, J.R. Fowler, "Marine riser design is simplified", Oil and Gas J., May 2, 1983, pp. 129-145

22) M.H. Patel, S. Sarohia, K.F. Ng, "Finite-element analysis of the marine riser", Engrg. Struct., Vol. 6, July, 1984, pp. 175-184

23) P-T.D. Spanos, "ARMA Algorithms for Ocean Wave Modeling", J. of Energy Resources Technol., Vol. 105, Sept., 1983, pp. 300-309

24) P-T.D. Spanos, T.W. Chen, "Vibrations of Marine Riser Systems", J. of Energy Resources Technol., Vol. 102, Dec., 1980, pp. 203-213

25) P-T.D. Spanos, M. ASCE, T.W. Chen, "Random Response To Flow-Induced Forces", J. of the Engrg. Mech. Div., Vol. 107, No. EM6, 1981, pp. 1173-1190

26) K.G. Nolte, F.H Hsu, "Maxima for a Vectorial Parameter From a Random-Multidirectional Source", J. of Energy Resources Technol., Vol. 107, June, 1985, pp. 238-243

27) M.E. McCormick, Ocean Engineers Wave Mechanics, John Wiley and Sons, New York, 1973

28) D.W. Dareing, T. Huang, "Marine Riser Vibration Response Determined by Modal Analysis", J. of Energy Resources Technol., Vol. 101, Sept., 1979, pp. 159-166

29) ABAQUS Examples Manual, Version 4-5, revised Nov. 1085, Hibbitt, Karlsson and Sorensen Inc.

30) T. Huang, S. Chucheepsakul, "Large Displacement Analysis of a Marine Riser", J. of Energy Resources Technol., Vol. 107, March, 1985, pp. 54-59

31) T. Huang, D.W. Dareing, W.T. Beran, "Bending of Tubular Bundles attatched to Marine Risers", J. of Energy Resources Technol., Vol. 102, March, 1982, pp. 24-30

32) B.J. Natvig, "A Large Angle - Large displacement Analysis Method for Marine Risers", Comput. Meths. for Off-shore Struct. ASME AMD Vol. 37, pp. 111-125 November, 1980

33) N.N. Panicker, I.R. Yancey, "Deepwater Production Riser", J. of Petrolium Technol., Aug., 1984, pp. 1392-1400

34) R.P. Nordgren, "Dynamic Analysis of Marine Risers With Vortex Excitation", J. of Energy Resources Technol., Vol. 104, March, 1982, pp. 14-19

35) P.G. Wybro, K.B. Davies, "The Dorada Field Production Risers", J. of Petrolium Technol., Dec., 1983, pp. 2947-2957

36) E.B. Denison, M.M. Kolpak, D.L. Garret, "A Comprehensive Approach to Deepwater Marine Riser Management", J. of Petrolium Technol., May, 1985, 835-842

37) W.R. Wolfram, R.H. Gunderson, "Structural Design of Production Risers and Offshore Production Terminals", Offshore Technol. Conf., 1979, pp. 1569-1576

38) D.B. McIver, T.S. Lunn, "Improvements to Frequency-Domain Riser Programs", Offshore Technol. Conf., 1983, pp. 395-403

39) J.M.T. Thompson, A.R. Bokaian, R. Ghaffari, Subharmonic and Chaotic Motions of Compliant Offshore Sructures and Articulated Mooring Towers", J. of Energy Resources Technol., Vol. 106, June, 1984, pp. 191-298

40) R. Nielsen, J.W. Pendered, "Some Aspects of Marine Pipeline Analysis", Numerical Methods in Offshore Engineering, pp. 555-569, Wiley-Interscience, April, 1978

41) T.H. Dawson, In-Line Forces on Vertical Cylinders in Deepwater Waves", J. of Energy Resources Technol., Vol. 107, March, 1985, pp. 18-23

42) S. Kao, "An Assessment of Linear Spectral Analysis Method for offshore Structures via Random Sea Simulation", J. of Energy Resources Technol., Vol. 104, March, 1982, pp. 39-46

43) M. Kato, T. Aba, M. Tamiya, T. Kumakiri, "Drag Foeces on Oscillating Cylinders in a Uniform Flow", J. of Energy Resources Technol., Vol. 107, March, 1985, pp. 12-17

44) Y.C. Kim, M.S. Triantafyllou, "The Nonlinear Dynamics of Long, Slender Cylinders", J. of Energy Resources Technol., Vol. 106, June, 1984, pp. 250-256

45) A.C. Walker, P. Davies, "A Design Basis for the J-Tube Method of Riser Installation", J. of Energy Resources Technol., Vol. 105, Sept., 1983, pp. 263-270

46) ABAQUS User Manual, Version 4-5, revised Nov. 1085, Hibbitt, Karlsson and Sorensen Inc.

47) S.K. Chakrabarti, R.E. Frampton, "Review of riser analysis techniques", Appl. Ocean Research, Vol. 4, No. 2, 1982, pp. 79-90

48) S. Shyam Sunder, J.J. Conner, "Sensitivity analysis for steel jacket offshore platforms", Appl. Ocean Research, Vol. 3, No. 1, 1981, pp. 13-26

49) J.E. Hall, A.J. Healey, "Dynamics of Suspended Marine Pipelines", J. of Energy Resources Technol., Vol. 102, June, 1980, pp. 112-119

50) T. Sarpkaya, "Vortex-Induced Oscillations", J. of Appl. Mech., Vol. 46, June, 1979, pp. 241-258

51) F. Rajabi, M.F. Zedan, A. Mangiavacchi, "Vortex Shedding Induced Dynamic Responce of Marine Risers", J. of Energy Resources Technol., Vol. 106, June, 1984, pp. 215-221

52) M.J. Every, R. King, O.M. Griffin, "Hydrodynamic Loads on Flexible Marine Strucyures due to Vortex Shedding", J. of Energy Resources Technol., Vol. 104, Dec., 1982, pp. 330-336

53) O.M. Griffin, S.E. Ramberg, "Some Recent Studies of Vortex Shedding With Application to Marine Tubulars and Risers", J. of Energy Resources Technol., Vol. 104, March, 1982, pp. 2-13

54) R.K. Jain, C.L. Kirk, "Dynamic Response of a Double Articulated Offshore Loading Structure to Noncolinear Waves and Current", J. of Energy Resources Technol., Vol. 103, March, 1981, pp. 40-47

55) N. Hogben, B.L. Miller, J.N. Searle, G. Ward, "Estimation of fluid loading on offshore structures", Proc. Instn. Civ. Engrs., Vol. 63(2), 1977, pp. 515-562

56) T.E. Horton, M.J. Feifarek, "The Inertial Pressure Concept for Determining the Wave Forces on Submerged Bodies", J. of Energy Resources Technol., Vol. 104, March, 1982, pp. 46-52

57) J.S. Chung, "Hydrodynamic Forces on a Marine Riser: A Velocity-Potential Method", J. of Energy Resources Technol., Vol. 104, March, 1982, pp. 52-57

58) R. Sigbjörnsson, "Stochastic theory of wave loading processes", Engrg. Struct., Vol. 1, Jan., 1979, pp. 58-64

59) N. Spidsöe, R. Sigbjörnsson, "On the reliability of standard wave spectra in structural response analysis", Engrg. Struct., Vol. 2, April, 1980, pp. 123-135

60) A,N. Williams, "Nonlinear Inertia Forces on Slender Cylindrical members", J. of Energy Resources Technol., Vol. 106, June, 1984, pp. 222-225

61) A. Sanchez-Archilla, "Long-Term Analysis of Wave Climate Usine Short-Term Techniques", J. of Energy Resources Technol., Vol. 106, June, 1984, pp. 228-233

62) C.T. Stansberg, "Statistical Analysis of Slow-Drift Responses", J. of Energy Resources Technol., Vol. 105, Sept., 1983, pp. 310-317

63) Y.-C. Li, J.B. Herbich, "Wavelength and Celerity for Interacting Waves and Currents", J. of Energy Resources Technol., Vol. 106, June, 1984, pp. 226-227

64) N.M. Patrikalakis, C. Chryssostomidis, "Vortex-Induced Response of a Flexible Cylinder in a Constant Current", J. of Energy Resources Technol., Vol. 107, June, 1985, pp. 244-249

65) T. Overik, G. Moe, E. Hjort-Hansen, "Flow-Induced Motions of Multiple Risers", J. of Energy Resources Technol., Vol. 105, March, 1983, pp. 83-89

66) T. Overik, G. Moe, "Added Mass and In-Line Steady Drag Coefficient of Multuple Risers", J. of Energy Resources Technol., Vol. 107, March, 1985, pp. 2-11

67) Z. Demirbilek, T. Halvorsen, "Hydrodynamic Forces on Multitube Production Risers Exposed to Currents and Waves", J. of Energy Resources Technol., Vol. 107, June, 1985, pp. 226-234

68) B.E. Bennett, G.P. Wilhelm, "Analysis of Production Riser Systems", Offshore Technol. Conf., 1979, pp. 1577-1583

69) R.E. Hobbs, "Solutions for Small Slope Pipeline Lifting Problems", J. of Energy Resources Technol., Vol. 106, March, 1984, pp. 63-64

70) G. Davies, Computational aspects of marine cables, M.Sc. thesis, University of Cape Town, To be submitted 1988.

71) D.L. Garrett, "Dynamic Analysis of Slender Rods", J. of Energy Resources Technol., Vol 104, Dec 1982, pp. 302-306

72) R .D. Cook, Concepts and Applications of Finite Element Analysis, Second Ed., John Wiley and Sons, New York, 1981

73) J.H. Vugts, D.J. Hayes, "Dynamic analysis of fixed offshore structures: a review of some basic aspects of the problem", Engrg. Struct., Vol. 1, April, 1979, pp. 114-120

74) J.F. McNamara, "Solution Schemes for Problems of Nonlinear Structural Dynamics", J. of Pressure Vessel Technol., May, 1974, pp. 96-102

75) T.J.R. Hughes, "Transient Algorithms and Stability", Computational Methods for Transient Analysis. Vol. 1: Computational Methods in Mechanics , Ed. T. Belytschko, T. R. Hughes, Elsevier Science Publishing Co, Netherlands, 1984

76) A.H-S. Ang, W.H. Tang, Probability Concepts in Engineering, Vol. 1 - Basic Principles, John Wiley and Sons, New York, 1975

77) A.H-S. Ang, W.H. Tang, Probability Concepts in Engineering, Vol. 2 - Decision, Risk and Reliability, John Wiley and Sons, New York, 1984

78) R.A. Ibrahim, "Structural dynamics with parameter uncertainties", Appl. Mech. Review, Vol. 40, March, 1987, pp. 310-328

79) M. Grigoriu, M. ASCE, B. Alibe, "Response of Offshore Structures to Random Waves" J. of Engrg. Mech., Vol. 112, No. 8, 1986, pp. 729-744

80) R. Burrows, Quasistaic response of offshore structures using probabilistic methods", Appl. Math. Modelling, Vol. 1, Sept. 1977, pp. 325-332

81) J.W. Leonard, H. Tuah, "Nonlinear deterministic and stochastic response of cable systems with large bodies under hydrodynamic loads", Engrg. Stuct., Vol. 8, April, 1986, pp. 93-106

82) I. Konuk, "Application of an Adaptive Numerical technique to 3-D Pipeline Problems With Strong Nonlinearities", J. of Energy Resources Technol., Vol. 104, March, 1982, pp. 58-62

83) R.D. Young, J.R. Fowler, E.A. Fisher, R.R. Luke, "Dynamic Analysis as an Aid to the Design of Marine Risers", J. of Pressure Vessel Technol., Vol. 100, May, 1978, pp. 200-205

84) K.C. Park, "An Improved Stiffly Stable Method for Direct Integration of Nonlinear Strucyural Dynamic Equations", J. of Appl. Mech., June, 1975, pp. 464-470

85) D.K. Faddeev, V.N. Faddeeva, Computational Methods in Linear Algebra, W. H. Freeman and Co., San Fransisco, 1963

86) H.D. Hibbitt, "Some Practical Issues in Nonlinear Structural Analysis with Finite Element Methods", Seminar draft, 1985

87) B.I. Irons, S.A. Ahmed, Techniques in Finite Elements, Ellis Horwood, Chichester, 1980

88) B. Noble, Applied Linear Algebra, Prentice-Hall, New Jersey, 1969

89) K-J. Bathe, E.L. Wilson, Numerical methods in finite element analysis, Prentice-Hall, New Jersey, 1976, 528p.

90) G.W. Haggenmacher, R.S. Lahey, "Practical aspects of the finite element method", Finite Elements in the Commercial Environment, Vol. 1, Ed. J Robinson, Robinson and Associates, Dorset, 1978

91) J.B. Zugg, The Analysis of Offshore Pipelines During Laying Operations, B.Sc. Thesis, Dept. Civil Eng., University of Cape Town, 1986

92) H.C. Martin, G.F. Carey, Introduction to Finite Element Analysis - Theory and Applications, McGraw-Hill, New York, 1973

93) G.Strang, G.J. Fix, An Analysis of the Finite Element Method, Prentice-Hall, New Jersey, 1973

94) R.H. MacNeal, "Higher order versus lower order elements; economics and accuracy", Finite Elements in the Commercial Environment, Vol. 1, Ed. J Robinson, Robinson and Associates, Dorset, 1978

95) G.F. Carey, J.T. Oden, Finite Elements - A Second Course, Vol. 2, Prentice-Hall, New Jersey, 1983, 301p.

96) R.D. Henshell, "On Hybrid Finite Elements", The Mathemetics of Finite Elements and Applications, Ed. J.R. Whiteman, Academic Press, London, 1973

97) Status of ABAQUS version 4-5 as of March 24 1087, Hibbitt, Karlsson and Sorensen Inc.

98) E. Hinton, D.R.J. Owen, An Introduction to Finite Element Computations, Pineridge Press, Swansea, 1979

99) I.E. Brown, Dynamic Analysis of Plane Frames, B.Sc. Thesis, Dept. Civil Eng., University of Cape Town, 1986

100) D.E. Newland, An Introduction to Random Vibrations and Spectral Analysis, Second Edition, Longman, Bath, 1984

101) ABAQUS Theory Manual, Version 4-5, revised Nov. 1085, Hibbitt, Karlsson and Sorensen Inc.

102) G.C. Hart, J.D. Collins, "The Treatment of Randomness in Finite Element Modeling", Society of Automotive Engineers, Oct. 1970, pp. 2509-2520

103) P. Burger of Hibbitt, Karlsson and Sorensen Inc., personal interview, May 1987

10) T.J.R. Hughes, "Transient Algorithms and Stability", Computational Methods for Transient Analysis. Vol. 1: Computational Methods in Mechanics , Ed. T. Belytschko, T. R. Hughes, Elsevier Science Publishing Co, Netherlands, 1984

11) R.A. Ibrahim, "Structural dynamics with parameter uncertainties", Appl. Mech. Review, Vol. 40, March, 1987, pp. 310-328

12) B.I. Irons, S.A. Ahmed, Techniques in Finite Elements, Ellis Horwood, Chichester, 1980

13) M.E. McCormick, Ocean Engineers Wave Mechanics, John Wiley and Sons. New York, 1973

14) J.F. McNamara, "Solution Schemes for Problems of Nonlinear Structural Dynamics", J. of Pressure Vessel Technol., May, 1974, pp. 96-102

15) D.E. Newland, An Introduction to Random Vibrations and Spectral Analysis, Second Edition, Longman, Bath, 1984

16) B. Noble, Applied Linear Algebra, Prentice-Hall, New Jersey, 1969

APPENDIX A: SUMMARY OF ABAQUS' CAPABILITIES - with reference to marine riser problems [29,46,99]

The version of ABAQUS used in this study is 4-5-169. ABAQUS is updated periodically

This appendix should be read in conjunction with the text in sections 1-5, in order to place the appendix into perspective, and to avoid repetition.

A1 General procedures

ABAQUS is a large, commercially available, finite element program, developed by Hibbitt, Karlsson and Sorensen, Inc.. ABAQUS provides for the analysis of both linear and non-linear problems. The following general procedures are available:

i) Stress analysis procedures.
ii) Static stress analysis.
iii) Dynamic analysis.
iv) Heat transfer.
v) Element removal and replacement.
vi) Coupled diffusion/stress - soil consolidation.
vii) Eigenvalue buckling prediction.
viii) Coupled heat transfer/stress analysis.
ix) Natural frequency extraction.
x) Modal dynamic analysis.

A2 Stress analysis procedures

A broad class of stress analysis problems can be solved with the program. The "step" concept employed by ABAQUS allows for flexible problem solving. A single analysis may be broken up into static and dynamic portions, which is useful in the case of the marine riser, where the static equilibrium is used as the initial position for the dynamic analysis.

ABAQUS can handle three types of nonlinearities: material, geometric and boundary. The marine riser class of problem is prone to two main sources of nonlinearities: that of large displacements and rotations, and the hydrodynamic drag.

A3 Static stress analysis

Static analysis is used when inertia effects can be neglected. The program uses Newton's method for the solution of the nonlinear equilibrium equations generated by this class of problem. The solution is obtained as a series of increments, with iteration within each increment to obtain equilibrium.

ABAQUS provides for user or automatic control of the solution stepping. The automatic option is versatile, and is usually chosen. The program checks the convergence rate, and adjusts the step increments accordingly.

A4 Dynamic analysis

For problems where inertia is of importance, the program provides direct integration of the equations of motion by the Hilber-Hughes-Taylor operator. A parameter, α, in the operator, is used to introduce artificial damping, which is useful in the marine riser type of problem, where higher-order spurious modes must be filtered out. An automatic time stepping option is available.

A5 Element library

The element library is intended to provide a complete geometric modelling capability; thus any combination of elements may be used to make up the model. All elements use numerical integration, allowing complete generality in material behaviour. Standard truss, beam, shell, plane stress, solid stress and heat transfer elements are available, as well as specialised pipe elements that allow for internal pressure, and elbow elements that allow for warping.

A5.1 Beam elements

Beam elements are the most commonly used type in marine riser problems. Two- and three-dimensional linear, quadratic and cubic beam elements are available. Hybrid versions of the beams are also available. The quadratic and cubic elements use simplified Cosserat theory, which includes shear deformation, but not warping effects. The Cosserat beams behave like "shear" or Timoshenko beams when short, but as they become more slender the transverse shear stiffness acts as a penalty function, constraining the cross-section to remain normal to the axis, and the beam behaves more like an Euler beam. The linear beams are formulated using Euler theory.

The beams allow for a large variety of loadings, including centrifugal, Coriolis, buoyancy, drag, uniform and non-uniform force per unit length, and concentrated forces. Pipe beams are available which are similar to the ordinary beams, but allow for the inclusion of internal pressures.

Axial stiffness, AE, and bending stiffness, EI, may be defined seperately if desired.

A6 Material library

The material library is intended to provide comprehensive coverage of both linear and nonlinear, isotropic and anisotropic material models. Material properties may be entered as a function of one or several variables, for different orientations. Provision is made for the modelling of elastic-plastic material behaviour, friction, and surface contact.

A7 Model definition

ABAQUS provides for a large range of procedures. The modelling of contact problems is possible, including friction, foundation, rigid surface, slide lines, dashpot, spring and gap effects. Plastic effects may be included. Complete control of the boundary and initial conditions, as well as the application of multi-point constraints is possible. A restart facility is available, so that an analysis may be broken and restarted at a later stage.

ABAQUS has facilities for modelling offshore structures. The *AQUA and *WAVE options facilitate the modelling of waves, currents, and the hydrodynamic forces acting on the structure. Stokes' and linear wave theories are available. Morison's equation is used to apply the inertial and the nonlinear drag hydrodynamic forces. Relative velocities and accelerations are used in the formulations.

A8 History definition

The analysis history definition consists of a prescription of the variation of of the external parameters, such as loads, boundary specifications and model changes, to which the response of the system is required, and specifying the desired output. The history is defined in "steps".

A9 Print/Plot description and User Subroutines

The user has full control over the program output, including element and nodal ouputs, energy outputs, and plot definitions.

The user subroutines allow for user costomised control of the boundary conditions, the loading, the multi-point constraints, the material properties, and the initial stress state.

APPENDIX B: DERIVATION OF THE GOVERNING SYSTEM OF EQUATIONS

The geometrically linearised system of equations that are used in the formulation of the small displacement, horizontal, planar model, developed in section 6 are listed as equations 6.1 to 6.4 in section 6. The derivation of these equations follows the procedures of Chakrabarti et al. [47].

Consider the elemental free body diagram of the riser as shown in figure B.1.

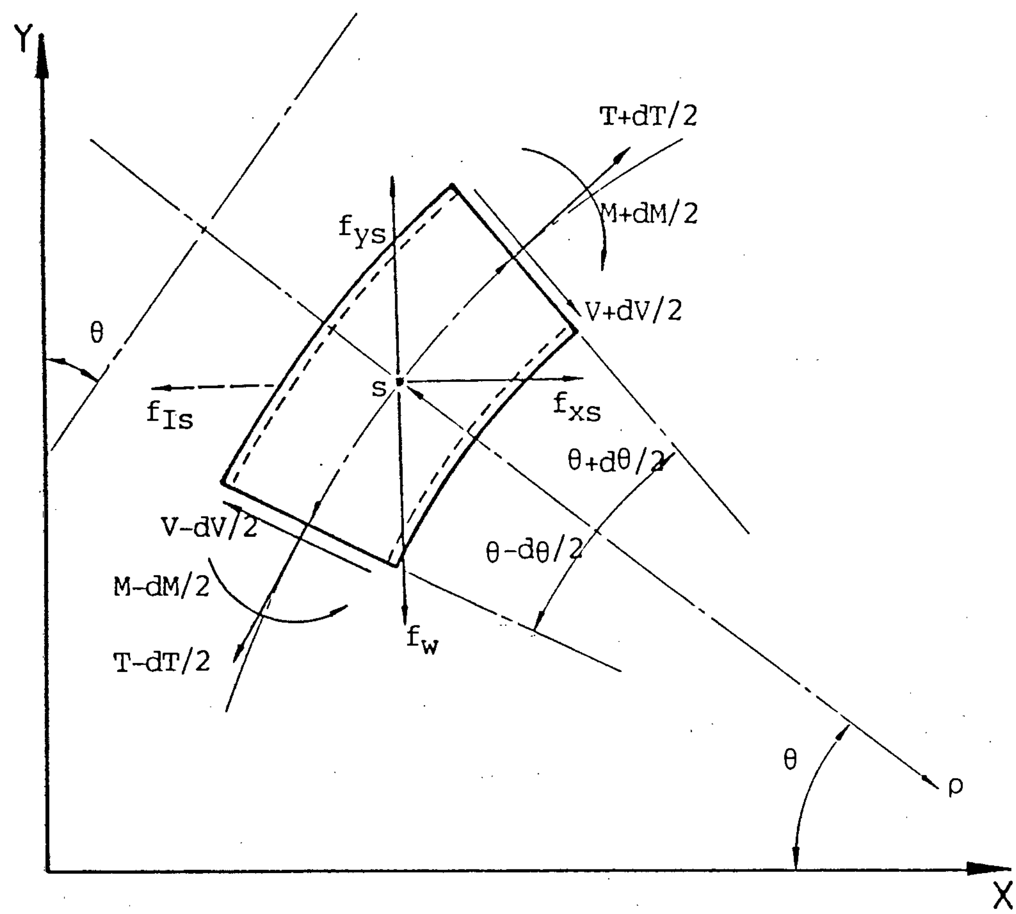

fig. B.1 - Elemental free body diagram of riser [Chakrabarti et al., 47]

Bernitsas [6] derives the governing equations for a large displacement three-dimensional riser model.

The following assumptions are made for a small displacement model:

a) The length of the segment is so small that

$$\cos \delta\Theta \approx 1 \quad \text{and} \quad \sin \delta\Theta \approx \delta\Theta \quad \text{.................(B.1)}$$

b) Small deflection beam theory is applicable, so that

$$\sin \Theta \approx \delta x/\delta s \quad \text{and} \quad \cos \Theta \approx \delta y/\delta s \quad \text{............(B.2)}$$

c) Angle of deflection, Θ, is so small that

$$\delta s \approx \delta y \ , \quad \cos \Theta \approx 1 \quad \text{and} \quad \sin \Theta \approx \Theta \approx \delta x/\delta y$$

and

$$\delta\Theta/\delta y \approx \delta^2 x/\delta y^2 \quad \text{..............................(B.3)}$$

Summing forces in the x direction, and summing the moments, gives the following relationships:

Horizontal force equilibrium:

$$\delta/\delta y\ (T\ \delta x/\delta y) + \delta V/\delta y + f_{xs} - m_x\ \delta^2 x/\delta t_2 = 0 \quad \text{...(B.4)}$$

Moment equation:

$$\delta M/\delta y + V = 0 \quad \text{....................................(B.5)}$$

where for pure bending, the moment, M, can be related to curvature:

$$M = EI/r = EI\ \delta\Theta/\delta s = EI\ \delta^2 x/\delta y^2 \quad \text{............(B.6)}$$

The statically equivalent horizontal load due to the external and internal fluid pressures is shown by Chakrabarti et al. to be:

$$f_{xp} = (A_o p_o - A_i p_i)\, \delta^2 x/\delta y^2 - (A_o \mu_o - A_i \mu_i)\, \delta x/\delta y \quad .(B.7)$$

The external forces acting on the riser is f_x, as defined in equation 6.2, section 6.

Combining equations B.4, B.5 and B.7, and the external horizontal forces gives the governing system of equations, as defined by equation 6.1, section 6.

APPENDIX C: RESONANT EXCITATION OF RESPONSE SENSITIVITIES

Consider the general case of a single degree-of-freedom system, where the mass, damping and stiffness matrices, and forcing vector are all a function of the random parameter, b:

$$M\ a + C\ v + K\ d = f \quad \text{.................................(C1)}$$

$$M\ (\delta a/\delta b) + C\ (\delta v/\delta b) + K\ (\delta d/\delta b) = \\ = \delta f/\delta b - a\ (\delta M/\delta b) - v\ (\delta C/\delta b) - d\ (\delta K/\delta b) \quad \text{......(C2)}$$

The damped natural frequencies of the system described in equation C1 and those described in equation C2 are the same. The excitation in equation C2 involves d, v and a and is, therefore, a resonant excitation. Thus approximations for d(t), such as:

$$d(b_o+\delta b,t) \approx d(b_o,t) + (\delta d/\delta b)_{b=b_o}\ \delta b + \\ + \tfrac{1}{2}(\delta^2 d/\delta b^2)_{b=b_o}\ \delta b \quad \text{.....................(C3)}$$

at b_o, for any small interval δb, are only valid for a short duration and the accuracy deteriorates rapidly thereafter.

Since the PFEM equations 7.10 and 7.11 use the first and second order response sensitivities, they are valid for a short duration only. Liu et al. [16] state that a similar phenominon is also observed in the transient response of nonlinear structures. Liu et al. explain that this might be due to a multiplying effect of the time, t, on the interval δb in the second and third terms in equation C3, which results in the deteriorating accuracy.